# A HYBRID DEEP LEARNING BASED MODEL USING METAHEURISTIC APPROACH FOR THE DETECTION OF BRAIN CANCER

Thesis Submitted for the Award of the Degree of

## DOCTOR OF PHILOSOPHY IN

## **COMPUTER SCIENCE and ENGINEERING**

By Mohit Prakram Registration Number: 42200068

Supervised By
Dr. Kirti Rawal (20248)
Electronics and Electrical Engineering (Professor)
Lovely Professional University, Phagwara



LOVELY PROFESSIONAL UNIVERSITY PUNJAB 2025

## **DECLARATION**

I hereby declare that the presented work in the thesis entitled "A Hybrid Deep Learning Based Model Using Metaheuristic Approach for the Detection of Brain Cancer" in fulfillment of the degree of **Doctor of Philosophy** (**Ph.D.**) is the outcome of research work carried out by me under the supervision of Dr. Kirti Rawal, working as a professor in the School of Electronics and Electrical Engineering of Lovely Professional University, Punjab, India. In keeping with the general practice of reporting scientific observations, due acknowledgements have been made whenever work described here has been based on the findings of other investigators. This work has not been submitted in part or in full to any other university or institute for the award of any degree.

#### (Signature of Scholar)

Name of the scholar:

Registration No.:

Department/school:

Lovely Professional University,

Punjab, India

## **CERTIFICATE**

This is to certify that the work reported in the Ph.D. thesis entitled "A Hybrid Deep Learning Based Model Using Metaheuristic Approach for the Detection of Brain Cancer" submitted in fulfillment of the requirement for the award of the degree of **Doctor of Philosophy (Ph.D.)** in Computer Science and Engineering is a research work carried out by Mohit Prakram, 42200068, is a bonafide record of his/her original work carried out under my supervision, and that no part of the thesis has been submitted for any other degree, diploma, or equivalent course.

## (Signature of Supervisor)

Name of supervisor:

Designation:

Department/school:

University:

**ACKNOWLEDGEMENT** 

I would like to express my sincere gratitude to my supervisor, Dr. Kirti Rawal, Professor,

School of Electronics and Electrical Engineering, Lovely Professional University, Punjab,

India, for her invaluable guidance, feedback, and support throughout my research. Her

critical questions and comments pushed me to sharpen my thinking and brought greater

depth to this work. Her extensive knowledge and experience were instrumental in

completing this research.

In addition, sincere thanks to all the faculty members and non-teaching staff of the School

of Computer Science and Engineering, Lovely Professional University, Punjab, for availing

me all the necessary facilities and cooperation for this work.

I am also very grateful to my wife, **Parul Prakram**, for providing her continuous support

and showing confidence in me, I also want to acknowledge my brother Dr. Manu Prakram

for his continuous and never ending support and my daughters Diva and Eva, who have

been my constant driving force for completing this work.

I find it hard to express my gratitude to the Almighty in words for bestowing upon me his

deepest blessings and providing me with the most wonderful opportunity in the form of the

life of a human being and for the warmth and kindness he has shown me by giving me life's

best.

At last, I wish to express my heartiest thanks to my parents, friends and family members

for their support, love, and inspiration.

(MOHIT PRAKRAM)

Date:

iv

## **ABSTRACT**

Traditionally, the identification of brain tumors has depended on the manual analysis of medical imaging techniques, including Magnetic Resonance Imaging (MRI), Computed Tomography (CT), and Positron Emission Tomography (PET) scans. Radiologists examine these pictures to detect anomalies, pinpoint tumor locations, and evaluate their dimensions and advancement. Nonetheless, manual diagnosis is labor-intensive, susceptible to human error, and significantly reliant on the proficiency of radiologists, rendering it less efficient for extensive or real-time clinical applications. An accumulation or abnormal multiplication of brain cells is called a brain tumor, which can be benign or malignant. Brain tumors are classified by their anatomical site, cellular composition, and primary or secondary status, but early detection is essential for optimizing treatment efficacy, improving patient prognosis, and reducing health risks. The early identification of human brain tumors is essential for improving patient survival and outcomes. This study requires a physical analysis of the MRI brain tumor images. Consequently, there is a must for automated methodologies to enhance tumor diagnosis accuracy. Nonetheless, assessing form, volume, margins, tumor identification, dimensions, segmentation, and classification continues to pose difficulties. This thesis proposes a hybrid deep learning-based model using a metaheuristic approach for the detection and classification of brain cancer, with a focus on identifying tumors at an early stage. Early detection is essential to improve survival rates and ensure timely medical intervention. The research is divided into two major phases. In the first phase, a comparative analysis is conducted to determine the most effective hybrid segmentation approach for extracting tumor regions from MRI images. Six models, including Fuzzy C-means (FCM)-based, K-meansbased, FCM with Particle Swarm Optimization (PSO)-based, K-means with PSO-based, FCM with Moth Flame Optimization (MFO)-based, and K-means with MFO-based segmentation, are evaluated using the MRI Benchmark dataset. Results demonstrate that the K-means with MFObased segmentation model outperforms others in terms of accuracy, sensitivity, F-measure, and computational efficiency, achieving a segmentation accuracy exceeding 99.6%.

In the second phase, the segmented output is used for classification through a Hybrid Brain Tumor Analysis (BTA) model that combines MFO and Convolutional Neural Network (CNN) techniques.

MFO-based segmentation is selected as the final segmentation approach for BTA model training. A novel feature extraction and selection mechanism is employed using MFO for optimal feature pattern extraction, followed by CNN-based classification. The proposed BTA model classifies brain tumors into three classes—meningioma, glioma, and pituitary—achieving improved classification accuracy by integrating MFO with CNN. Performance evaluation shows a 3.22% improvement in overall accuracy, with precision, recall, and F-measure increasing by 4.07%, 2.46%, and 3.25%, respectively, compared to existing models. This research demonstrates that the proposed hybrid approach significantly enhances the accuracy and efficiency of both segmentation and classification, making it a promising tool for early brain cancer detection and classification in clinical applications.

# TABLE OF CONTENTS

DECLARATION	ii
CERTIFICATE	iii
ACKNOWLEDGEMENT	iv
ABSTRACT	v
LIST OF FIGURES.	xi
LIST OF TABLES.	xiii
LIST OF ABBREVIATIONS	xvii
CHAPTER 1 INTRODUCTION	1
1.1 BACKGROUND	2
1.2 INTRODUCTION TO BRAIN TUMOR	3
1.2.1 Brain Tumors in the World	8
1.2.2 Brain Tumor Treatment	9
1.2.2.1 Traditional Methods of Brain Tumor Detection	9
1.2.2.2 Latest Methods of Brain Tumor Detection	10
1.3 INTRODUCTION TO MEDICAL IMAGING	10
1.4 TECHNIQUES OF MEDICAL IMAGE IMAGING	11
1.5 BRAIN TUMOR SEGMENTATION	17
1.6 VARIOUS TYPES OF BRAIN TUMOR SEGMENTATION	18
1.6.1 Segmentation based on Discontinuities	19
1.6.2 Region-based Segmentation	21
1.6.3 Clustering-Based Segmentation	22

	1.7	BR	AIN TUMOR SEGMENTATION AND CLASSIFICATION	27
	1.7	7.1	Problems related to Brain Tumor Segmentation and Classification	28
	1.7	7.2	Application of Brain Tumor Segmentation and Classification	29
	1.7	7.3	Challenges in Brain Tumor Segmentation and Classification	29
	1.8	MC	TIVATION ABOUT BRAIN TUMOR-RELATED WORK	30
	1.9	SIC	SNIFICATION OF BRAIN TUMOR-RELATED WORK	31
	1.10	R	ESEARCH GOALS & SCOPE	31
	1.11	N	MEDICAL IMAGES DATASETS	32
	1.12	C	CONTRIBUTION OF THESIS	34
	1.13	S	TRUCTURE OF THE THESIS	35
CF	HAPT	ER 2	2 LITERATURE REVIEW	37
	2.1	RE	VIEW OF LITERATURE	37
	2.2	LIT	ERATURE SUMMARY (TABULAR FORM)	42
	2.3	RE	SEARCH GAP IDENTIFICATION	47
CF	HAPT	ER 3	RESEARCH PROBLEM & OBJECTIVES	49
	3.1	PR	OBLEM FORMULATION	49
	3.2	RE	SEARCH OBJECTIVES	53
CF	IAPT	ER 4	RESEARCH METHODOLOGY	54
	4.1	FR.	AMEWORK OF BRAIN TUMOR SEGMENTATION	56
	4.1	.1	FCM-based ROT Segmentation	59
	4.1	.2	K-means-based ROT Segmentation	61
	4.1	3	FCM with PSO-based ROT Segmentation	63
	4.1	.4	K-means with PSO-based ROT Segmentation	64
	4 1	5	FCM with MFO-based ROT Segmentation:	65

4.1.6	K-means with MFO-based ROT Segmentation	67
4.2 FR	AMEWORK OF BRAIN TUMOR CLASSIFICATION	69
4.2.1	MRI Pre-processing	71
4.2.2	K-means with MFO-based BTR Segmentation	74
4.2.3	Feature Extraction from BTR	77
4.2.4	MFO-based Feature Selection	77
4.2.5	CNN-based BTA Model Training	79
CHAPTER	5 EXPERIMENTAL SETUP	82
5.1 IN	FORMATION ABOUT USED TOOLS	82
5.2 LA	ANGUAGE USED FOR IMPLEMENTATION	83
5.3 US	SED DATASET	84
5.4 PL	ACE OF WORK	85
5.4.1	Work Done	85
CHAPTER	6 RESULTS & DISCUSSIONS	86
6.1 PE	RFORMANCE MEASUREMENT PARAMETERS	86
6.1.1	Precision Rate	86
6.1.2	Sensitivity or Recall Rate	87
6.1.3	F-measure of H-mean	87
6.1.4	Accuracy Rate	87
6.1.5	Error Rate	87
6.1.6	Matthews Correlation Coefficient (MCC)	87
6.1.7	Dice Coefficient (DC)	88
6.1.8	Jaccard Coefficient (JC)	88
6.1.9	Execution Time	88

6.2	RESULTS FOR TUMOR SEGMENTATION FRAMEWORK	89
6.3	RESULTS FOR TUMOR CLASSIFICATION FRAMEWORK	96
6.4	Comparative Analysis of SOTA Deep Learning Models for Brain Tumor Detection	105
	CNN-MFO vs. MobileNetV2	105
	CNN-MFO vs. EfficientNet V2-B20	106
	CNN-MFO vs. VGG16, ResNet50, InceptionV3, DenseNet121, and GoogleNet	107
CHAP'	TER 7 CONCLUSION & FUTURE SCOPE	112
7.1	CONCLUSIONS	112
7.2	LIMITATIONS	113
7.3	FUTURE SCOPE	115
REFEI	RENCES	117

# LIST OF FIGURES

Figure 1.1: Basic Medical Image Segmentations	2
Figure 1.2: Brain Tumor	4
Figure 1.3: Parts of Brain	5
Figure 1.4: Human Brain Tumour	6
Figure 1.5: Healthy and Brain with Tumour	9
Figure 1.6: ACS-based Pie-chart (a) new cases and (b) deaths in 2020 due to brain tumor	9
Figure 1.7: Different Types of Medical Imaging Approaches	12
Figure 1.8: X-Ray Sample Images	13
Figure 1.9: CT Scan Sample Images	14
Figure 1.10: MRI Sample Images	15
Figure 1.11: PET Sample Images	18
Figure 1.12: Brain Tumor Image Segmentation Approaches	20
Figure 1.13: Example of Cluster	25
Figure 1.14: Clustered Data	26
Figure 1.15: Sample of Brain MRI Images with Types from Dataset	34
Figure 1.16: Latest Swarm-based Algorithms	35
Figure 2.1: Top methods using the BraTS Dataset	42
Figure 2.2: Efficiency Unsupervised Clustering-based Approaches for Medical Images	45
Figure 2.3: Clustering Faces Pixel Mixing Problems	46
Figure 4.1: Flowchart of Proposed Work	55
Figure 4.2: Architecture of Proposed Comparative Model	57

Figure 4.3: (a) Original MRI (b) Grey (c) Color (d) Mask Image of ROT (e) Segmented I	ROT Mask
and (f) Segmented ROT using K-means with MFO with Maximum Accuracy	66
Figure 4.4: Sample of Brain MRI Images with Types from Dataset	67
Figure 4.5: Flowchart of Proposed BTA Model	69
Figure 4.6: Sample of Brain MRI Images with Types from Dataset	70
Figure 4.7: Pre-processing on Sample MRI	71
Figure 4.8: Accuracy (%) Comparison of Proposed Comparative System	75
Figure 4.9: Architecture of Proposed BTA-Net	78
Figure 6.1: Accuracy (%) Comparison of Proposed Comparative System	91
Figure 6.2: Precision, Recall, F-measure, and Time Complexity Comparison of Comparative	Proposed 93
Figure 6.3: Models Comparison with Existing Work	94
Figure 6.4: Quantitative Performance of BTA Model using BTA-Net	97
Figure 6.5: BTA Model Training Accuracy	98
Figure 6.6: BTA Model Training Performance in terms of Cross-Entropy	99
Figure 6.7: BTA Model Training Confusion Matrix	100
Figure 6.8: BTA Model ROC Analysis	101
Figure 6.9: Evaluation of the BTA Model in Relation to Current Research	102
Figure 6.10: CNN-MFO vs MobileNetV2	105
Figure 6.11: CNN-MFO vs EfficientNet V2-B20	105
Figure 6.12: CNN-MFO vs Other SOTA Models	106

# LIST OF TABLES

Table 2.1 Literature Review	43
Table 3.1 Comparison of Segmentation Techniques for Problem Analysis	50
Table 4.1 Brain Tumour Segmentation Comparison	68
Table 5.1 Experimental Setup for Proposed Model Simulation	81
<b>Table 5.2 Dataset for Proposed Model Simulation</b>	83
<b>Table 6.1 Evaluation Parameters for Proposed Brain Cancer Detection Model</b>	87
Table 6.2 Efficiency Comparison of Proposed Comparative System	89
Table 6.3 Contrast with Already Exists Works	94
Table 6.4 Dataset Division for BTA Model	95
Table 6.5 Quantitative Performance of BTA Model	96
Table 6.6 Comparison with State-of-the-Art-Methods	102
Table 6.7 Comparison of SOTA Models for Brain Tumor Detection (MRI)	107

# LIST OF ALGORITHMS

Algorithm 1	48
Algorithm 2	50
Algorithm 3	54
Algorithm 4	56
Algorithm 5	62
Algorithm 6	64
Algorithm 7	67
Algorithm 8	68

# LIST OF SYMBOLS

Symbol	Meaning
+	Addition or Positive Sign
-	Subtraction or Negative Sign
×	Multiplication
÷	Division
=	Equals
<b>≠</b>	Not Equal To
≈	Approximately Equal To
>	Greater Than
<	Less Than
≥	Greater Than or Equal To
≤	Less Than or Equal To
%	Percent
0	Degree (Angle or Temperature)
$\sqrt{}$	Square Root
Σ	Summation
$\infty$	Infinity
ſ	Integral
π	Pi (3.14159)
α	Alpha (Angle or Coefficient)
β	Beta (Coefficient or Angle)
γ	Gamma (Angle or Coefficient)
δ	Delta (Change or Difference)
Δ	Delta (Uppercase, Change, or Difference)
μ	Mu (Mean in Statistics or Micro in Measurements)
Σ	Sigma (Summation, Uppercase)
σ	Sigma (Standard Deviation, Lowercase)

Ω	Omega (Ohm, Unit of Electrical Resistance)
θ	Theta (Angle)
λ	Lambda (Wavelength, Eigenvalues)
Ψ	Psi (Used in Quantum Mechanics)
ð	Partial Derivative
$\oplus$	Direct Sum
$\otimes$	Tensor Product
⇒	Implies
$\Leftrightarrow$	If and Only If
<b>:</b> .	Therefore
÷	Because
$\cap$	Intersection (Set Theory)
U	Union (Set Theory)
⊆	Subset
C	Proper Subset
⊇	Superset
⊃	Proper Superset
Ø	Empty Set
*	Aleph (Cardinality of Infinite Sets, Set Theory)
$\forall$	For All
3	There Exists
€	Element Of
∉	Not an Element Of
=	Identical To

## LIST OF ABBREVIATIONS

**Abbreviation** Full Form

**CT** : Computed Tomography

MRI : Magnetic Resonance Imaging

**ROI** : Region Area of Interest

**CAD** : Computer-Aided Diagnosis

**ABTA** : American Brain Tumor Association

**ACS** : American Cancer Society

**AI** : Artificial Intelligence

**GIS** : Geographic Information Systems

**RF** : Radio frequency

**DWI** : Diffusion-Weighted Imaging

**fMRI** : Functional MRI

**MRA** : Magnetic Resonance Angiography

MRS : Magnetic Resonance Spectroscopy

**PET** : Positron Emission Tomography

**LoG** : Laplacian of Gaussian

**FCM**: Fuzzy C-Means

**CNNs** : Convolutional Neural Networks

**BraTS**: Brain Tumor Segmentation

**MFO** : Moth-Flame Optimization

**BTR** : Brain Tumour Region

**BTA** : Brain Tumor Analysis

**PSO** : Particle Swarm Optimization

**ABC** : Artificial Bee Colony

**FFA** : Firefly Algorithm

**CSA** : Cuckoo Search Algorithm

MCC : Matthews Correlation Coefficient

**XAI** : Explainable AI

**ARK-PSO**: Adaptive Regularized Kernel-based PSO with FCM

MAG-Net : Multi-task Attention Guided Network

**GA** : Genetic Algorithm

**DWT** : Discrete Wavelet Transform

**RBS-MVO**: Randomly Updated Beetle Swarm and Multi-Verse Optimisation

**ET** : Enhancing Tumor

**WT** : Whole Tumor

TC : Tumor Core

**ANNs** : Artificial Neural Networks

## LIST OF PUBLICATIONS

#### **JOURNAL PUBLICATIONS**

- 1. Prakram, M., Rawal, K., Prakram, M., & Sharma, P. (2025). AN OPTIMIZED MRI-BASED BRAIN TUMOR SEGMENTATION: A COMPARATIVE STUDY OF IMPROVED CLUSTERING MECHANISMS. *Palestine Journal of Mathematics*, 14
- 2. Mohit Prakram, Kirti Rawal, Arun Singh, Ankur Goyal, Shiv Kant, Shakeel Ahmed, Saiprasad Potharaju, A novel hybrid model for brain tumor analysis with CNN and Moth Flame Optimization, *Informatics in Medicine Unlocked, Volume 57*, 2025, 101671, ISSN 2352-9148, https://doi.org/10.1016/j.imu.2025.101671.

#### **CONFERENCE PUBLICATIONS**

- Prakram, Mohit and Rawal, Kirti and Prakram, Manu, Unsupervised Learning Based Medical Image Segmentation: A Comparative Review of Algorithms with Issues and Challenges (May 5, 2023). Proceedings of the KILBY 100 7th International Conference on Computing Sciences 2023 (ICCS 2023), Available at SSRN: https://ssrn.com/abstract=4835684 or http://dx.doi.org/10.2139/ssrn.4835684
- M. Prakram, K. Rawal and A. Singh, "A System For Detecting Brain Tumors Through the Use of Deep Learning and Image Classification with Improved Accuracy," 2023 6th International Conference on Contemporary Computing and Informatics (IC3I), Gautam Buddha Nagar, India, 2023, pp. 1143-1148, doi: 10.1109/IC3I59117.2023.10397805.

## **CHAPTER 1**

## INTRODUCTION

This chapter provides an overview of a hybrid deep learning approach, enhanced by metaheuristic optimization, for brain tumor segmentation and classification. This work leverages unsupervised clustering and deep learning to automate the detection of brain tumor regions [1-3]. The accuracy of such Computer-Aided Diagnosis (CAD) systems heavily depends on the quality of input images, which are acquired via various medical imaging modalities, including Magnetic Resonance Imaging (MRI) [4]. However, medical images often suffer from noise and uneven illumination, which can complicate analysis [5–7]. Therefore, a pre-processing stage is crucial. Following this, image segmentation—the process of partitioning an image into meaningful regions—is used to extract the Region of Interest (ROI), such as a tumor [8]. One of the best examples of an image processing and computer vision technique is image segmentation. Medical image segmentation is the well-known technique to fragment a picture into smaller, relatively homogenous-featured components, and it allows for the extraction of some important data, such as tumor region. Medical images are used in healthcare since their caliber affects the diagnosis and course of therapy. So that, in medical image-based analysis, segmentation is important since it aims to extract certain features from the images. These images may be used for sophisticated image comprehension. According to science, image segmentation is a fictitious middle-level vision job carried out by neurons located between low-level and high-level cortical regions. Figure 1.1 displays several examples of different types of medical picture segmentations for your perusal.

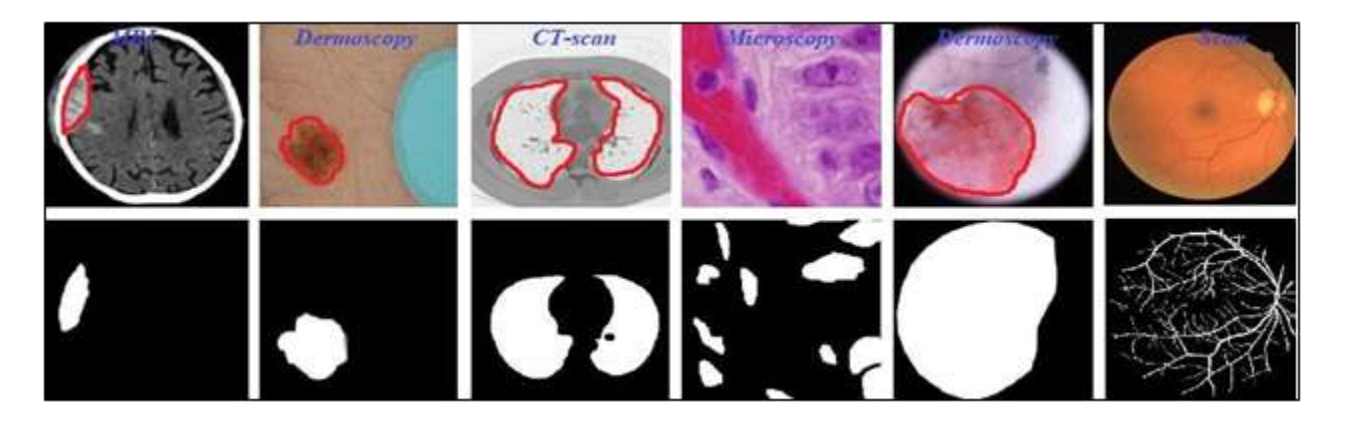


Figure 1.1: Basic Medical Image Segmentations

Figure 1.1 showcases different medical imaging modalities and their respective segmentation results [8]. A collection of original medical images exists in the top row that demonstrates MRI, Dermoscopy, CT-Scan, Microscopy, and Fundus Scans having their areas of concern marked in red. Multiple healthcare-related pictures show brain tumors together with skin lesions alongside lung abnormalities and microscopic cellular components and retinal diseases such as diagnostic elements. The segmental masks in the bottom row use white coloring to mark regions of interest, such as tumors or lesions, against a black background representation. Automated medical image analysis depends on these segmentation masks since they facilitate the accurate localization and extraction of affected areas towards further diagnostic assessment or treatment planning. These segmentation procedures represent fundamental operations within Computer-Aided Diagnosis (CAD) systems that use machine learning and deep learning models to identify medical image abnormalities and their type, as well as to perform precise segmentation. Medical imaging analysis benefits from these techniques that deliver improved diagnostic capabilities as well as diminished human labor needs and standardized, objective results.

## 1.1 BACKGROUND

All human bodies contain multiple complex organs that need proper alignment to preserve total wellness. The brain functions as the overall regulating system of the body while preserving the operations of all body organs. Among the human body's organs, the brain stands as its single most essential element because it controls memory functions and procedures as well as emotions along with sensory perception of vision, smell, taste, and touch and many physiological operations. A severe threat to life exists from any abnormalities in brain operations. Annual brain tumor rates

have risen for all age demographics, according to the American Brain Tumor Association (ABTA) in February 2016, which studied children through young adults from ages 15 to 39. The classification system splits brain tumors into two groups according to their malignant or benign status. These distinct types of tumors differ between malignant formations composed of irregular cells leading to uninhibited growth and benign formations consisting of regular non-cancerous cells. Medical experts and patients view these tumors as critical because their expansion produces symptoms like vision deterioration and long-standing nausea, which create severe medical problems. Brain tumors exist with complex attributes that create major difficulties during both diagnosis procedures and medical treatment [9]. Medical professionals use MRI as an important diagnostic and monitoring method to track tumor development. Manually identifying tumors in combination with MR image noise requires extensive and time-consuming processes because of the complex tumor patterns. Standards of diagnosis depend heavily on detection at an early stage combined with exact tumor locations. MRI scans provide doctors with precise information to monitor tumor growth, which leads to prompt and correct identifications. The diagnostic method starts with image segmentation to extract tumor tissues from brain images. The extensive complexity of medical images, together with abundant data generation, makes hand-based tumor evaluation susceptible to inaccuracies. Medical image analysis and classification require automated systems because threats to traditional manual analysis methods increase daily. When medical professionals collaborate with segmentation algorithms, the accuracy of tumor detection improves significantly because this leads to enhanced treatment results for patients.

## 1.2 INTRODUCTION TO BRAIN TUMOR

Brain tumors stand as one of the most lethal global diseases, producing severe consequences that can result in death when medical treatment is not received. Abnormal cell development inside the brain triggers tumors, which spread because of genetic mutations and environmental elements. Brain tumors classify into two groups as primary brain tumors grow inside brain tissue, yet secondary brain tumors start elsewhere before reaching brain tissue. The classification of tumors depends on their identified severity level [10]. The severity of brain tumors depends on their type since benign tumors stay non-cancerous and create less harm, whereas malignant tumors carry both cancerous characteristics and fast-spreading properties that present life-threatening medical risks. Urgent medical attention must be sought because of malignant tumors' aggressive behaviour.

Proper diagnosis and immediate treatment lead to better patient outcomes since their detection at an early stage determines survival rates.

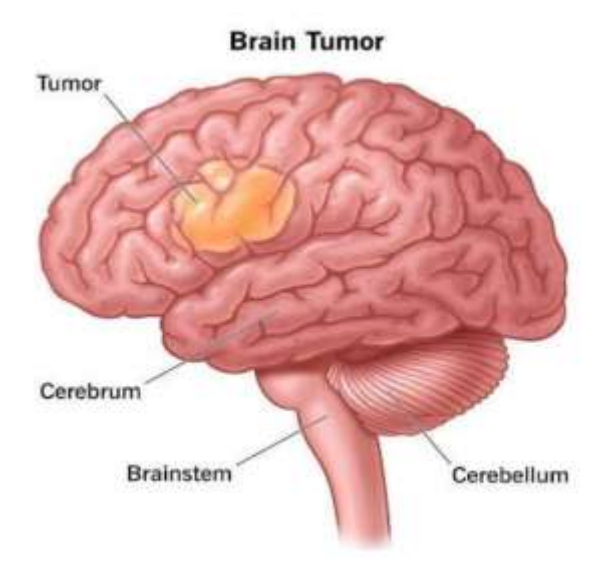


Figure 1.2: Brain Tumor

Figure 1.2 illustrates a brain tumor located in the cerebrum, highlighting key anatomical regions of the human brain. The tumor appears as a yellowish mass, representing abnormal and uncontrolled cell growth within the brain.

- Tumor: An uncontrolled growth of brain cells that may be benign (non-cancerous) or malignant (cancerous), often disrupting normal brain functions by compressing nearby tissues.
- Cerebrum: The largest part of the brain, responsible for reasoning, memory, sensory processing, and voluntary movement.
- Brainstem: The lower section connecting the brain to the spinal cord, regulating vital functions such as breathing, heart rate, and reflexes.
- Cerebellum: Located at the back of the brain, it manages coordination, balance, and fine motor control.

The human brain, weighing about 1.4 kg (3 pounds), governs all bodily activities and mental processes, including intellect, creativity, emotion, and memory [11]. Protected by the skull, it comprises the cerebrum, cerebellum, and brainstem, with the brainstem acting as a relay between

the cerebrum, cerebellum, and spinal cord. The brain continuously receives and transmits information throughout the body [12].

Different brain regions are illustrated in Figure 1.3.

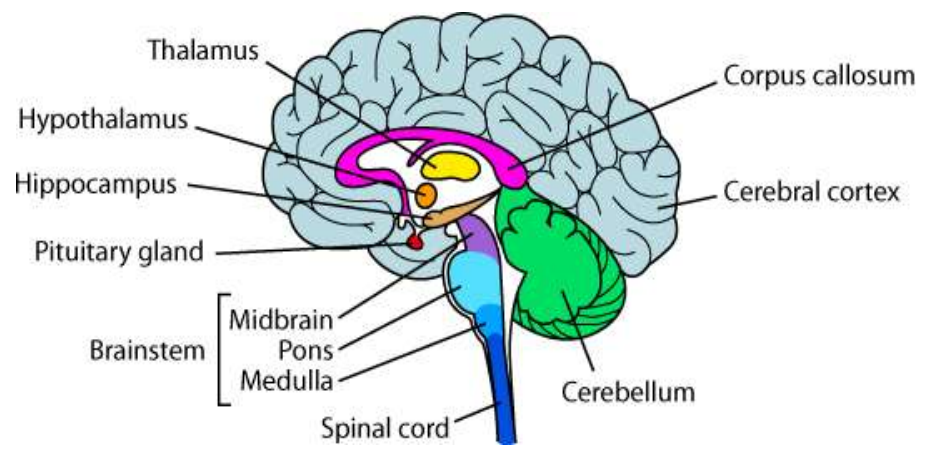


Figure 1.3: Parts of Brain

A brain tumor is a proliferation of abnormal cells within or next to the brain. Brain tumors are a typical proliferations inside the brain that may be classified as either malignant (cancerous) or benign (noncancerous). The impacts on the brain from malignant and benign tumors are analogous and can result in identical issues, contingent upon the tumor type and its location within the brain [13]. Various types of brain tumors exist. Some brain tumors are benign, while others are malignant. Brain tumors may originate in the brain (primary brain tumors) or may metastasize from other regions of the body to the brain (secondary, or metastatic, brain tumors). The region of the brain tumor is given in Figure 1.4.

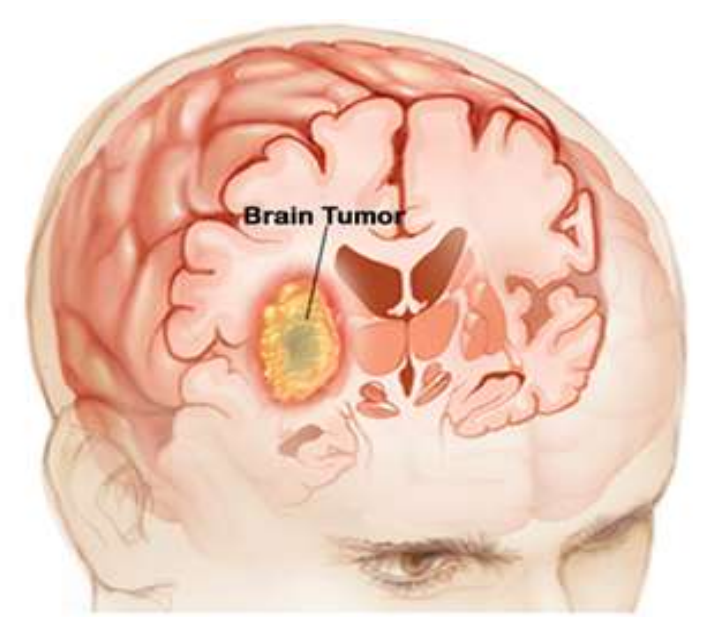


Figure 1.4: Human Brain Tumour

Image segmentation represents a significant challenge in image processing and is extensively utilized across several applications, including sports, biomedical fields, remote sensing satellites, and security measures. A segmentation process splits an image into its individual components or objects. The delineation of tumors from MRI is a significant application of image segmentation [14]. The manual identification of tumors in MRI requires skilled radiologists, a process that is both time-intensive and prone to inaccuracies. The huge volume of patients and scans renders manual detection and segmentation too burdensome. There is a necessity to automate this process, and segmentation techniques are crucial in accomplishing this objective. Advancements in restorative imaging systems enable their application in various medical areas, such as computerassisted pathology diagnosis, surgical planning and guidance, and longitudinal analysis. Both MRI and CT, among all restorative imaging modalities, are frequently employed imaging techniques in neurology and neurosurgery [15]. Segmentation of objects, chiefly anatomical structures and beyond diagnosing pathologies using MRI scans may be essential, as the results often serve as the basis for several applications. Systems for executing segmentation shifts are entirely dependent on specific provisions and picture modalities. Moreover, the segmentation of medical images presents a challenging task, as they generally contain a substantial amount of data and occasionally exhibit artifacts due to the patient's limited acquisition range and the typically poorly defined boundaries of delicate tissues. It is identified by the analysis of medical pictures, such as MRI scans. MRI segmentation has been suggested for numerous clinical studies of diverse complexity. In a clinical

setting, medical image processing is typically synonymous with radiology or "clinical imaging," and the medical professional tasked with analyzing (and occasionally obtaining) the images is a radiologist. Managing brain tumors presents distinct challenges that complicate their categorization. The population of tumor types may be endless, exhibiting a variety of shapes and sizes. It may form at any range, exhibiting varying picture intensities. Certain factors may distort the surrounding structures or contribute to edema, altering the characteristics of the pictures associated with the tumors [16]. Furthermore, the availability of some MRI procurement norms yields a varied abundance of data regarding the brain. Each image often emphasizes a particular area of the tumor. The automatic segmentation utilizing previous models, which alternately employ prior information, may face challenges during execution. The inadequate segmentation of the brain's internal structures arises from the assertion that significant energy should also be considered for drugs targeting tumors. It mitigates human errors while enhancing surgical or radio restorative procedures. Oversaw the economic aspects related to tumors. In brain oncology, it is also appealing to introduce a representative human brain model that can integrate tumor data derived from MRI and CT information, including localization, type, shape, functional positioning, and interactions with other brain structures. Despite various efforts to enhance the therapeutic imaging community, precise segmentation and characterization of anomalies remain challenging tasks [17]. Existing strategies clear out significant space for expanded automation and, furthermore, material accuracy. In the human body, when abnormal cells are generated in an uncontrolled way, they convert into brain tumors, and these are categorized into two types named as

- ❖ *Benign:* It is a noncancerous type of brain tumor, and the formation is so slow that it is less aggressive. This type of tumor does not spread to other regions of the brain or other parts of the human body.
- ❖ *Malignant:* It is a cancerous type of brain tumor and not always easy to differentiate from surrounding normal tissues in the brain. So, the extraction or segmentation of these types of tumors is not easy without damaging the surrounding tissues of the human brain.

The American Cancer Society (ACS) reports that malignant brain tumor cases grew worldwide during the previous several decades [18]. For improved brain tumor curability, researchers need to concentrate on diagnosing malignancies during early-stage or benign-stage development by

utilizing CAD systems. Medical professionals in both research and clinical practice now focus intensely on automated brain tumor detection instruments because they help reduce diagnostic errors while minimizing false positive results and minimizing the time it takes for automatic MRI-based diagnostic models [19]. Doctors can use four different imaging methods to detect brain tumors: PET (Positron Emission Tomography) scans, angiography, MRI scans, and CT scans. The primary data source for this research consists of MRI scan images, which serve to evaluate tumor segmentation techniques with proposed advanced clustering-based methods [20].

The non-invasiveness of MRI scan data, along with its extensive use in medical practices, makes it the selection choice for this study. The high spatial resolution capability of MRI scans combined with excellent soft tissue contrast delivers necessary tumor-related information about size together with shape and positioning specifics inside the brain. Doctors need this information to establish precise diagnoses along with planning treatment protocols at the beginning of the disease [21]. MRI imaging holds a widespread preference for medical image analysis because it delivers advantageous characteristics for both tumor segmentation and classification tasks. The brain tumor image set in Figure 1.5 shows the simple ability to differentiate between normal brain tissue and areas affected by tumors.

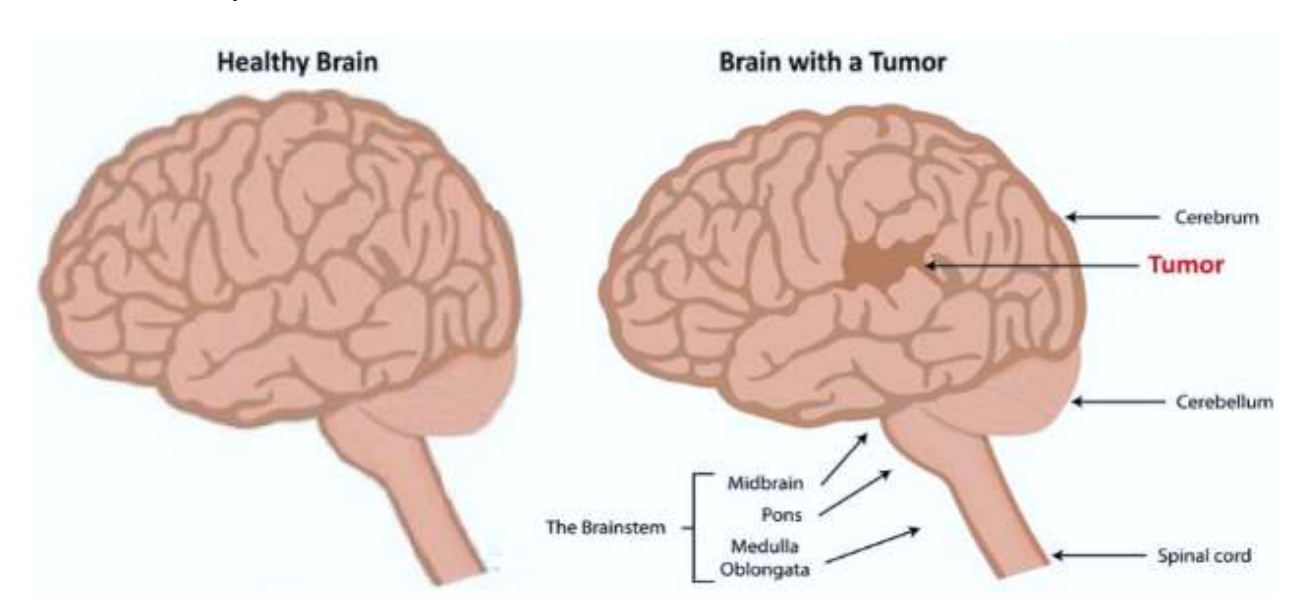


Figure 1.5: Healthy and Brain with Tumour

#### 1.2.1 Brain Tumors in the World

Brain tumors continue to develop into a leading mortality factor since both national and international statistics demonstrate increasing death rates. For 2023, brain tumors caused the

deaths of 18,760 people per year based on statistics from the ACS. Each year 17,200 individuals encounter death because of malignant brain tumors, which demonstrates the seriousness of the condition [22]. Physicians report 50,000 fresh cases of brain tumors annually throughout Indian medical facilities. The critical requirement for childhood brain tumor diagnosis and treatment becomes evident because 20% of brain cancer occurrences occur in pediatric patients.

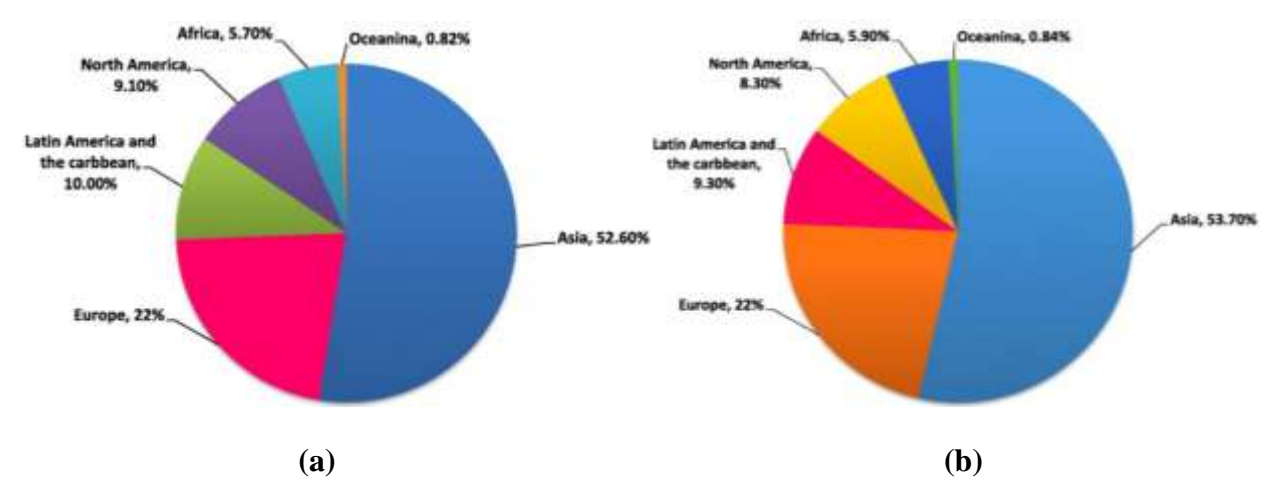


Figure 1.6: ACS-based Pie-chart (a) new cases and (b) deaths in 2020 due to brain tumor

Each year the total number of brain tumor diagnoses amounts to 5 to 10 instances per 100,000 people, and these instances are increasing annually. These statistics emphasize the growing number of brain tumors and demonstrate the critical necessity of advanced medical research and early diagnosis and effective treatments for dealing with this dangerous condition.

#### 1.2.2 Brain Tumor Treatment

The choice of treatments for brain tumors depends on particular tumor variables alongside patient health status and tumor characteristics, including its type, size, location, and level of malignancy. Standard treatments for brain tumors incorporate different therapeutic approaches between surgery and radiation therapy and chemotherapeutic administration and targeted treatment and immunological interventions. Multiple treatments are commonly combined to enhance their combined effectiveness when treating brain tumors.

#### 1.2.2.1 Traditional Methods of Brain Tumor Detection

Brain tumor treatment and cure become achievable when the condition receives proper early detection. The cure rates for brain tumors remain extremely low because patients often obtain diagnoses too late, especially in cases of malignant tumors. The imaging procedures create brain

image data for analysis that reveals tumor position. Human operators are usually responsible for brain tumor detection, yet this method proves both prolonged and error-prone while being labor-intensive. The procedure of manual tumor identification necessitates a major commitment of time and personnel work and extends medical diagnosis delays that consequently deteriorate patient health [23]. The accuracy of human-based categorization methods tends to be imprecise; thus, patients are at higher risk of missed diagnoses or medical oversight. The patient's life remains at risk when detection or identification mistakes or treatment errors occur, even at a minor level. Brain tumor treatment requires quick diagnosis, so the reduction of detection duration and prevention of human mistakes become essential for accurate identification. The reliability of manual detection varies to such an extent that automated machine/deep learning and Artificial Intelligence (AI) models step in to boost accuracy and efficiency and reduce diagnostic delays.

## 1.2.2.2 Latest Methods of Brain Tumor Detection

Today machines alongside AI bring continuous discussions across the world. Medical detection and diagnosis of brain tumors obtain speed and efficiency through advanced technology integration while achieving higher precision rates. The automated diagnosis method leads to efficient diagnosis procedures while producing fewer mistakes. The newest technologies enable machines to examine two times more test samples in the same time period than when relying on manual testing methods. The AI-powered software examines MRI and CT scan images to track tumors along with pinpointing their specific placements to help medical experts make proper patient care decisions. Laboratory treatment of identified tumors becomes possible after identification when those tumors become ready for segmentation or slicing for removal or treatment needs. Advanced precision through these measures leads directly to increased procedural success metrics. Brain tumor segmentation requires high accuracy alongside efficient execution of tasks [24]. The use of machine-based technologies represents the preferred approach for tumor detection because these systems lead to better process efficiency and improved patient survival outcomes.

## 1.3 INTRODUCTION TO MEDICAL IMAGING

Digital image processing is a rapidly developing technology domain crucial for medical imaging [25]. In this context, Magnetic Resonance Imaging (MRI) serves as a vital tool, enabling the creation of detailed visual representations of human body structures to detect and analyze various

conditions [26]. The primary challenge in analyzing these scans is image segmentation, which involves partitioning the image to isolate meaningful regions for analysis. While MRI technology is a cornerstone of medical diagnosis, its images often contain significant noise and low contrast, complicating the segmentation process. This research focuses on developing robust segmentation techniques for MRI scans to enhance tumor detection precision and classification speed. Different types of medical imaging approaches are shown in Figure 1.7.

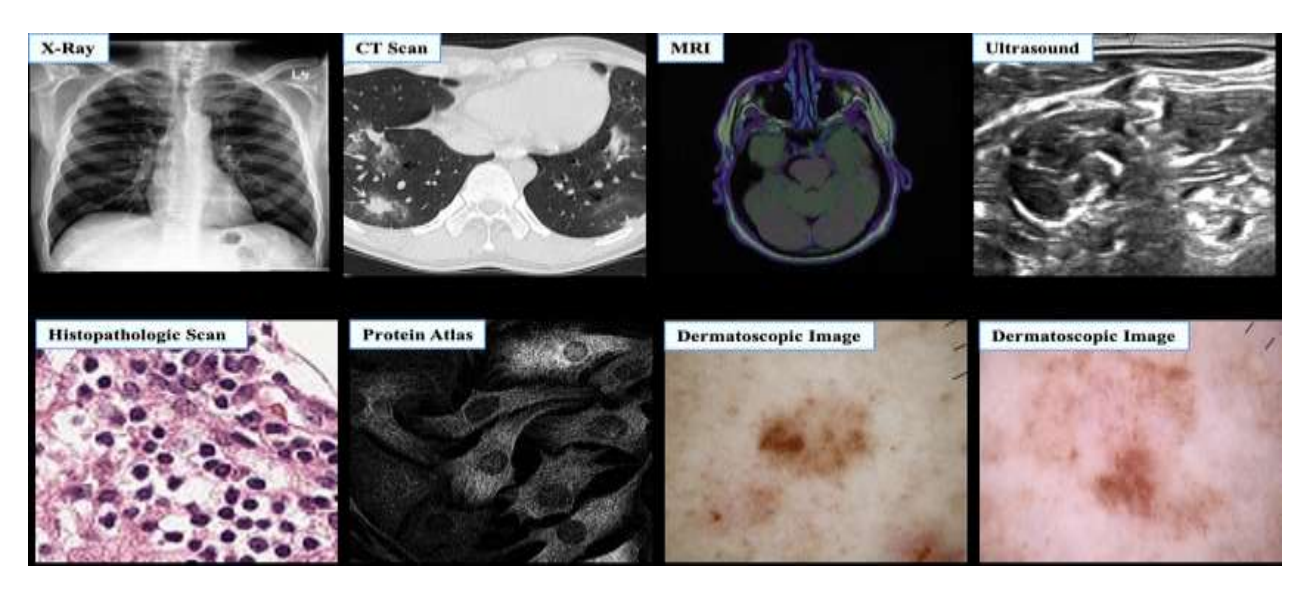


Figure 1.7: Different Types of Medical Imaging Approaches

## 1.4 TECHNIQUES OF MEDICAL IMAGE IMAGING

Several medical imaging techniques are used for diagnosing pathological diseases, including X-ray, Computed Tomography (CT), Positron Emission Tomography (PET), and Magnetic Resonance Imaging (MRI).

**X-ray Imaging:** Uses electromagnetic radiation to visualize bone structures, making it useful for detecting fractures. Doctors use X-ray imaging for essential medical detection of bone fractures and pulmonary tuberculosis, as well as other conditions [27]. The sample of X-ray images are shown in Figure 1.8.



Figure 1.8: X-Ray Sample Images

**CT Imaging:** Employs specialized X-rays to create cross-sectional images, providing detailed views of bones, organs, and tissues. The sample of CT scan images are shown in Figure 1.9.

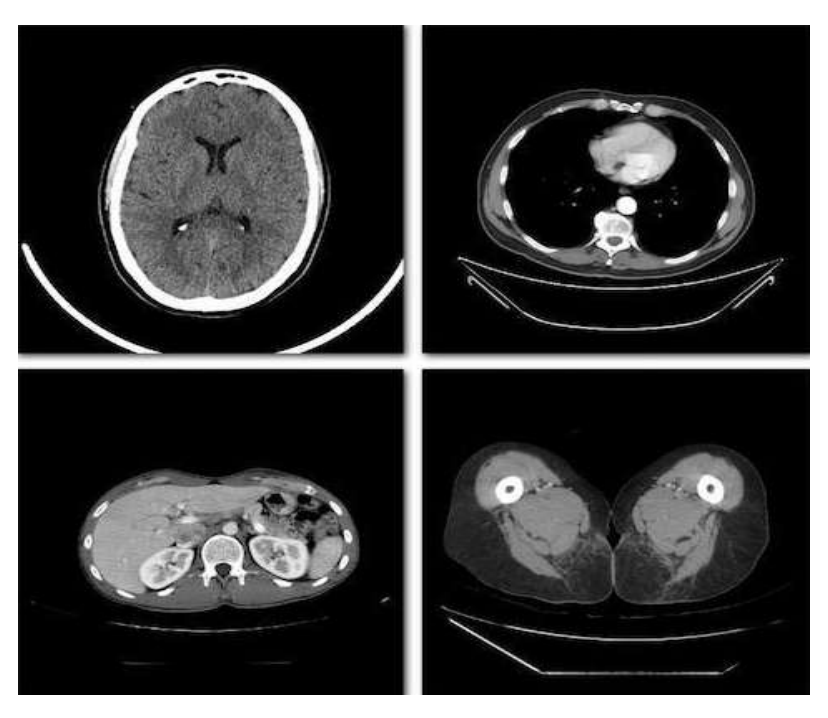


Figure 1.9: CT Scan Sample Images

## **Primary uses of CT Scan Imaging:**

- **I.** Detailed examination of internal structures becomes possible by this technology, which shows images from different horizontal sections.
- **II.** CT imaging enables doctors to identify and measure the condition of bones along with their injuries, including scoliosis.
- **III.** The imaging technique detects both conditions of the lungs and liver as well as monitoring body masses.
- **IV.** CT imaging functions as a navigation system to help doctors plan subsequent medical operations and biopsy procedures as well as render therapy procedures.

**MR Imaging:** A non-invasive technique that uses magnetic fields and radio waves to produce highly detailed images of the body, as shown in Figure 1.10. The procedure of MRI creates pictures of bodily tissues using magnetic fields and radiofrequency waves while eliminating the requirement of using ionizing radiation [28].

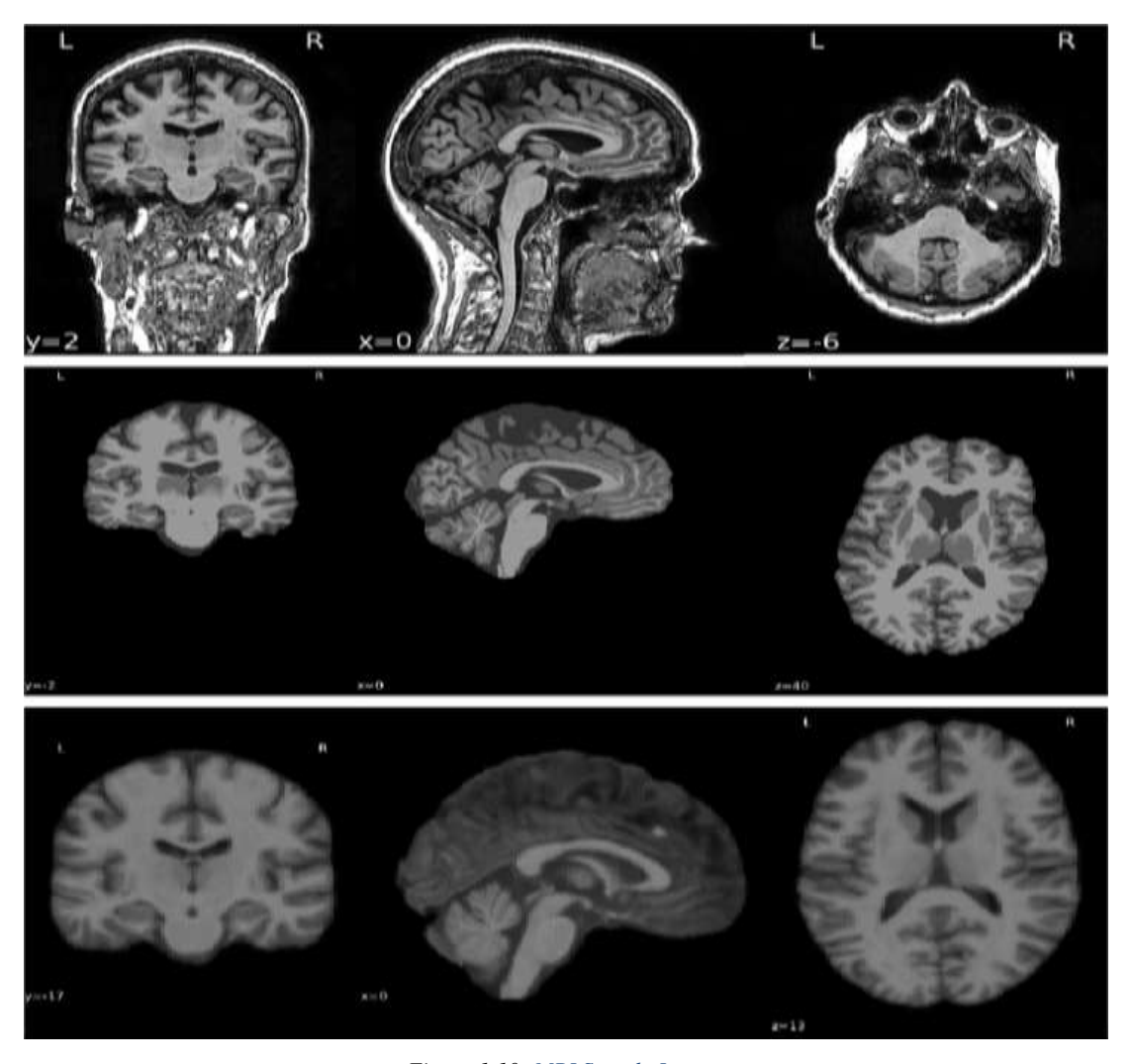


Figure 1.10: MRI Sample Images

**Working principles of MRI:** The operating principle of MRI scans enables detection of hydrogen atoms present in the human body through an abundance of water and fat molecules. The three core elements of the process form a sequence:

- **1.** A high-powered magnet positions patients for alignment so all body hydrogen nuclei (protons) face along the magnetic field direction.
- 2. The protons receive brief bursts of Radiofrequency (RF) pulses through this process, which makes them deviate from their existing alignment state. After pulse application ends, the protons restore their natural state by softly returning and generating signals at the same time.
- **3.** The emitted signals travel to detectors, which send signals to a computer for analysis purposes until detailed body image representations form. Through signal production from

different tissue types such as muscles, organs, and fat, the diagnostic technique achieves contrast-based imaging of soft tissues.

**Types of MRI Images:** MRI can be used to produce different types of images, each suited for specific diagnostic purposes. Some of the commonly used MRI techniques include

T1-Weighted Images: The primary function of T1-weighted images consists of anatomical assessment while also providing detailed opposition between tissues and clear bone marrow and fat visibility.

T2-Weighted Images: Studies show the high-water content areas in these pictures make them suitable for identifying inflammation and edema alongside tumors and pathological diseases. The brain assessment through MRI scans relies heavily on T2-weighted imaging because it shows fluid accumulation areas well.

Diffusion-Weighted Imaging (DWI): The specific MRI examinations measure water particle motions inside body tissues. The medical community relies on DWI to examine stroke patients because restricted diffusion reveals areas of brain tissue affected by ischemia.

Functional MRI (fMRI): The methodology of fMRI determines brain activity patterns through blood flow variations. MRI constitutes an essential technology for studying brain processes as well as cognition and emotions together with sensory functions.

Magnetic Resonance Angiography (MRA): MRA technology functions as a diagnostic tool which illustrates blood vessels so doctors can detect vascular conditions such as aneurysms and arterial blockages.

Magnetic Resonance Spectroscopy (MRS): The chemical composition of tissues can be evaluated through the advanced application of MRS, which expands the capabilities of MRI. The capability of this procedure proves crucial in brain disorder and tumor studies because it detects alterations in brain metabolism.

#### **Advantages in MRI Technology:**

1. MRI uses no radiation during imaging, thus establishing its safer position relative to X-rays and CT scans, particularly for scenarios requiring frequent imaging. The ability to identify different types of soft tissues makes MRI a powerful tool that enhances its capability for brain, organ, and muscle assessments.

2. Multiple MRI images in axial, sagittal, and coronal planes can be obtained without shifting patients to achieve thorough anatomical evaluation. Modern MRI techniques use fMRI as well as MRS to produce functional and metabolic data, which extends MRI functionality beyond structural imaging capabilities.

#### **Key uses of MRI:**

- **I.** This technique detects abnormal tissue growths in the brain as well as brain tumors and strokes.
- **II.** The MRI technique allows physicians to obtain complete images of both sensitive brain structures and muscles along with ligaments as well as other soft tissues, which normal X-ray and CT scan technology cannot detect.
- **III.** MRI generates clearer visualization of tissues based on its ability to create better details in comparison to CT images.
- **IV.** The imaging process within MRI operates without utilizing radiation, which minimizes health dangers for patients.
- V. MRI technology enables doctors to identify heart problems together with detecting both cardiac structure anomalies and blood circulation issues.
- **VI.** The advanced imaging technology of MRI provides detailed pictures to health professionals within a risk-free diagnostic context.

Positron Emission Tomography (PET): A nuclear medicine technique that visualizes metabolic activity, which is useful for detecting cellular-level changes in diseases. As a diagnostic tool, PET functions to detect cellular activity modifications leading to medical condition analysis. The medical staff intravenously delivers the radiotracer substance, which concentrates in the scanned body parts during imaging procedures. The tracer substance detects active chemical areas to aid disease detection [29]. The areas in question display either heat (high intensity) or cool (low intensity) characteristics on image scans. PET scans become more effective when used together with MRI or CT scanners because this combination produces detailed body assessments for improved medical diagnostics, and the sample images of PET are shown in Figure 1.11.

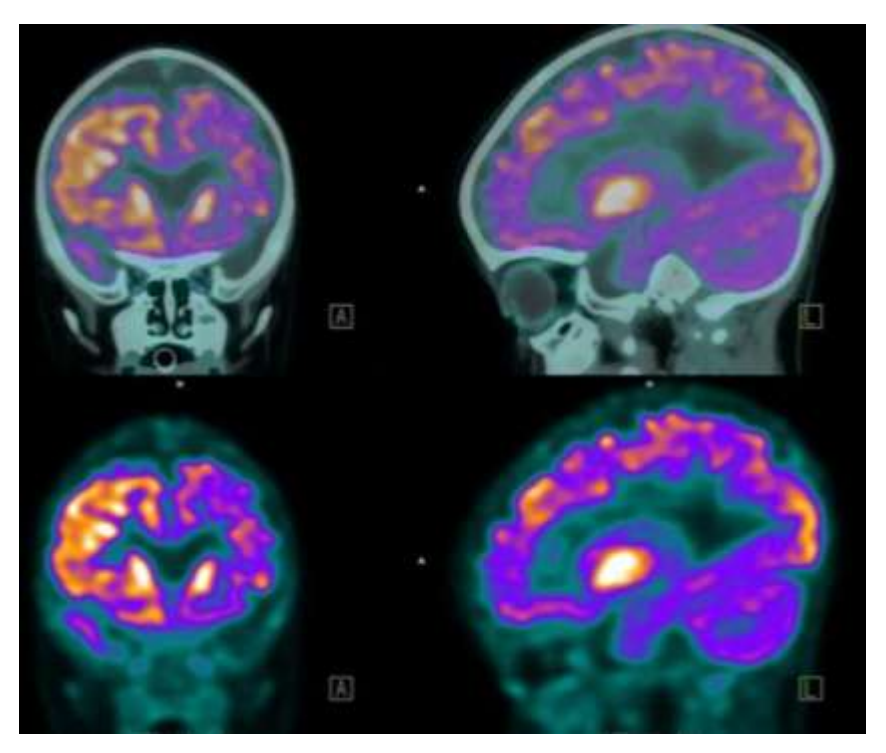


Figure 1.11: PET Sample Images

## **Key Benefits of PET Scans:**

- I. The functional capability of organs becomes visible in PET scans even though MRI and CT machines generate structural information.
- II. Diagnosis receives increased accuracy through the combination of PET with CT scanning technology.
- **III.** The diagnostic method stands out because it produces minimum discomfort, thus offering patients a favorable approach.

## 1.5 BRAIN TUMOR SEGMENTATION

Medical imaging professionals use brain tumor segmentation to automatically find and mark tumors in MRI scans because this operation serves as a crucial diagnostic and therapeutic planning process. The diagnostic and therapeutic assessment, along with disease monitoring, benefits from this method [30]. The segmentation process for brain tumors proves difficult because tumors often show diverse shapes combined with several sizes and intensities spread throughout various brain locations. There are some challenges in Brain Tumor Segmentation are as:

• Tumors exist in diverse dimensions throughout the entire brain space because they take irregular forms of different sizes.

- Segmentation becomes more complicated because MRI images display irregular contrast throughout their area.
- Learning becomes more challenging when tumors occupy just a minor section of the image because of class imbalance.
- The presence of artifacts and noise in MRI scans makes them affect the accuracy of segmentation results.
- Processes based on Deep Learning Models Need Access to Extensive Labelled Datasets for their Training Development.

Basically, brain tumors are classified into two main categories:

- **A. Benign Tumors** Non-cancerous growths that do not invade nearby tissues.
- **B.** Malignant Tumors Cancerous tumors that spread and grow aggressively.

Some common types include:

- **1.** Gliomas (e.g., Glioblastoma Multiforme GBM)
- 2. Meningioma's
- 3. Pituitary Tumors
- 4. Metastatic Brain Tumors

#### 1.6 VARIOUS TYPES OF BRAIN TUMOR SEGMENTATION

Medical image segmentation and their analysis function as an essential tool across diagnosis practices and surgery operations as well as computer vision-based systems encompassing biomedical image processing applications. The main function of image segmentation involves dividing images into separate regions that display homogenous properties under defined criteria. The initial component of computer vision systems and decision-making operations heavily depends on segmentation due to its crucial requirement of precise execution. The field of medical image segmentation together with soft computing techniques has experienced significant improvements throughout multiple years of development. Accurate diagnosis requires radiologists to use images with well-defined segmented regions because these segmented areas enable identification of brain tumor abnormalities between benign and malignant groups. Medical image segmentation requires different techniques because they need adaptation to handle distinct clinical

problems [31-34]. The implementation of these techniques meets three major barriers because of choosing stable algorithms, determining robust performance indicators, and consistently finding the application-specific region of interest. In an MRI tumor detection task, the Region of Interest (ROI) is the tumor, but in eye image examination, the ROI becomes the iris. A consistent and reliable result across all scenarios remains impossible through any single segmentation method, which demands developers create or update advanced segmentation methods for improved performance and ROI-specific adaptability [35]. Several approaches are used by the researchers for segmenting brain tumors from medical images, including:

- 1. Segmentation based on Discontinuities
- 2. Region-based Segmentation
- 3. Clustering-Based Segmentation

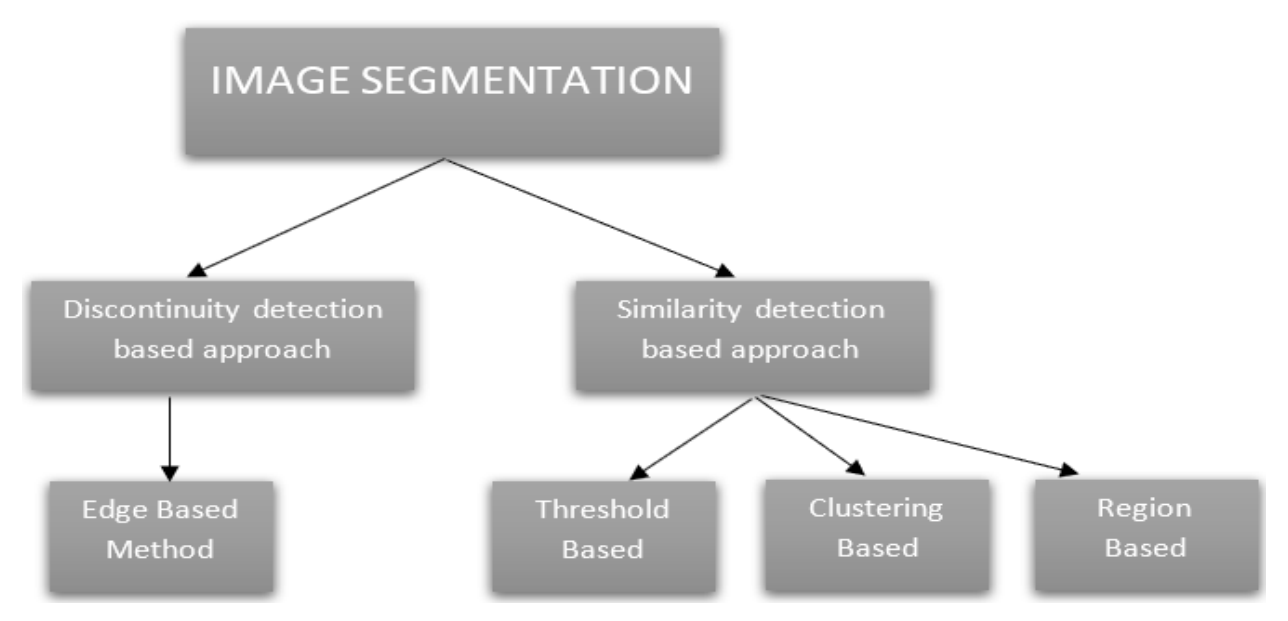


Figure 1.12: Brain Tumor Image Segmentation Approaches

#### 1.6.1 Segmentation based on Discontinuities

Image segmentation happens through sudden changes in the detection of intensity values within images according to this method. Three classifications exist under this method, including Point Detection and Line Detection and Edge Detection.

**Point Detection:** The identification of intense components that appear frequently throughout an image constitutes the core concept of point detection. Image processing occurs through the usage

of a high-pass filter in the form of a mask that operates by convolving it with the image for the purpose of point intensity change detection using equation 1.

$$R = \sum_{p=1}^{k} Z_p \times f_p \tag{1}$$

Where  $Z_p$  is the grey level of the pixel and  $f_p$  is the mask coefficient at location p. The point in the image is detected at the location on which the mask is centered if  $|R| \ge T$ , where T is a non-negative threshold.

**Line Detection:** The detection of lines depends on previously defined masks that search for orientation-specific linear elements. Four different types of line detection masks exist to identify elements along horizontal, vertical, and two diagonal +45° and -45° directions. Every pixel with a higher absolute value of Ri compared to Rj for all values of j except i indicates a likelihood of line association in the direction of the selected mask. A signal peak occurs when the system selects the mask that yields the maximum response value.

**Edge Detection:** The outline of objects present in images is defined by edges during image processing operations. When a substantial immediate alteration occurs in gray-level intensity between adjacent image regions, then an edge becomes evident. The process of edge detection removes unneeded information while keeping only essential structural information about objects. The two fundamental categories of edge detection operators exist.

- Gradient operators are tools that evaluate first-order image derivatives, which include the Sobel operator, Prewitt Operator and Roberts Operator.
  - 1. Sobel Operator
  - 2. Prewitt Operator
  - 3. Robert's Operator
- Gaussian operators calculate image second-order derivatives through the following methods:
  - 1. Canny Edge Detector
  - 2. Laplacian of Gaussian (LoG)
  - 3. Marr-Hildreth Operator

### 1.6.2 Region-based Segmentation

The main objective of segmentation operations consists in partitioning an image into several distinct areas. The technique executes its operations based on the comparative patterns inside the image. The process of region-based segmentation creates uniform regions out of areas that share common features. The approach includes three subcategories.

**Region Growing:** It provides a method that unites smaller sub-regions into larger ones using defined criteria. The technique identifies first seed points before growing regions by including neighboring pixels that possess comparable characteristics. The process continues running until the applied rule condition remains valid; otherwise, the process ends. If seed points follow a rule to connect with neighboring pixels sharing similar attributes, the result becomes a consolidated segmented area.

**Region Splitting:** Image segmentation through region splitting produces divisions of an image using fixed criteria. The technique starts by treating the whole image at the top level because of its top-down methodology. A region has no modification if it matches all the predetermined requirements. The region undergoes further splitting into sub-regions when it fails to match the defined condition. Repetitive application of this method continues until every segment matches the assigned segmentation requirement.

**Region Split and Merge:** The method starts by splitting an image into regions through predetermined rules. The merged areas from segmentation produce the final results. A quadtree data structure serves as the common implementation method for carrying out this technique, through which the parent node shows the full image while child nodes display subdivided areas. The merging operation consolidates areas with identical features to heighten the performance of segmentation procedures.

**Threshold-Based Segmentation:** Thresholding stands as a basic segmentation approach that separates objects from the background by using a threshold value (T). The quality of segmentation results depends on what algorithm is used for thresholding. Users need to scan a histogram to find

the most suitable threshold value so objects appear uniformly bright yet separate from background content.

- A single fixed value of threshold T applies identically throughout every section of the complete image in global thresholding. Objects use the same region when pixels maintain intensity worth higher than T, although pixels below T get assigned to a separate region.
- The threshold value T uses local neighborhood information to determine its setting through this method rather than using universal thresholding for pixel analysis. This makes it valuable for images with multidimensional intensity patterns and diverse illumination.

The segmentation methods serve primary roles in image processing systems and help detect targets while classifying them effectively.

## 1.6.3 Clustering-Based Segmentation

The independent operation of clustering algorithms differs from classification algorithms where clusters are not predefined. The algorithms find excellent applications in detecting hidden patterns within data sets through heuristic methods. Such methods break images into groups that contain pixels that possess comparable features [36]. The fundamental clustering properties allow data elements to join groups where components inside share more similarities than elements from separate clusters.

K-means Clustering Algorithm: The K-means algorithm represents an unsupervised learning method that serves as one of the basic clustering deployment strategies. The algorithm establishes a predetermined number of clusters that reorganize the specified image data. The clustering process starts with K centroid selection made at random to represent the initial cluster centers. The image pixels receive their assignment to the nearest centroids by calculating their distance to these centroids [37-39]. The clustering concludes when all image pixels obtain their correct cluster assignment and new centroid positions are computed from the determined cluster centers. The operational sequence continues until the centroids transform into fixed positions that no longer move. K-means clustering is a type of unsupervised learning algorithm used for unlabeled data (i.e., data without predefined categories or groups). The objective of this computation is to come across bundles in the used data, with the number of get-togethers spoken to by the variable K. The

count works iteratively to dole out each data point to one of K social affairs subject to the features that are given. Data spotlights are gathered subject to feature equivalence. The delayed consequences of the K-means clustering estimation are:

- ❖ The centroids of the K bundles, which can be used to name new data
- ❖ Labels for the planning data (each datum call attention to what is doled out to a singular gathering)

K-means is one of the most straightforward unsupervised learning algorithms that addresses the significant clustering problem. The algorithm provides a straightforward approach to partition a given dataset into a predetermined number of clusters (k), which is defined beforehand. The fundamental concept is to delineate k centroids, each corresponding to a distinct cluster. These centroids should be established in a strategic manner, considering various regional factors that provide diverse outcomes. Therefore, the optimal decision is to position them as far apart as reasonably possible. The corresponding phase involves assigning each guide to a designated educational cluster and linking it to the subsequent centroid [39-44]. As soon as no points are pending, the fundamental progress is completed, and an initial assembly phase is concluded. We must now identify k new centroids as the barycenter of the clusters resulting from the previous expansion. Ultimately, these numerical targets limit a certain function, in this case, a squared error function. The objective task

$$J = \sum_{j=1}^{k} \sum_{i=1}^{n} ||X_i^{j} - C_j||^2$$
 (2)

Where  $||X_i|^j - C_j||^2$  is a picked separation measure between an information point  $X_i^j$  and the bunch focus  $C_j$ , is a pointer of the parting of the n info focuses from their individual group focuses. The computation is made out of the associated advances:

- 1 Spot K centers into the space spoken to by the things that are being gathered. These centers speak to beginning get-together centroids.
- 2 Dole out everything to the social affair that has the closest centroid.
- 3 At the point when the sum total of what things have been designated, recalculate the spots of the K centroids.
- 4 Rehash Steps 2 and 3 until the centroids never again move. This makes a unit of the articles into social affairs from which the estimation to be restricted can be resolved.

Although the algorithm is guaranteed to converge, the k-means algorithm does not necessarily find the optimal solution, which would be the global objective function minimum. The algorithm is also sensitive to the initial, randomly selected cluster centers. The k-means computation can be kept running on various events to lessen this effect. K-means is a direct count that has been changed in accordance with various issue zones. As we are going to see, it is a better-than-average probability for extension to work with fleecy component vectors [45].

**A Model:** Suppose that we have n test incorporate vectors x1, x2, ..., xn, all from a comparative class, and we know that they fall into k diminished bundles, k < n. Allow mi to be the mean of the vectors in gathering I. In case the packs are especially detached, we can use a base division classifier to disengage them. That is, we may say that x is in bundle I if || x - mi || is the base of completely the k divisions. This suggests the following method for finding the k-means:

Construct preliminary guesses for the means:  $\mathbf{m}_1$ ,  $\mathbf{m}_2$ ...  $\mathbf{m}_k$ Awaiting, there are no changes in the value of any mean

Utilize the approximate means to categorize the samples into different clusters

For  $\mathbf{i} \Box 1$  to all  $\mathbf{k}$  values

Substitute  $\mathbf{m}_i$  with the mean of each sample for created cluster  $\mathbf{i}$ End

Here is an illustration presentation to show how the values mean  $\mathbf{m}_1$  and  $\mathbf{m}_2$  transfer into the centers of two different clusters.

End—Algorithm

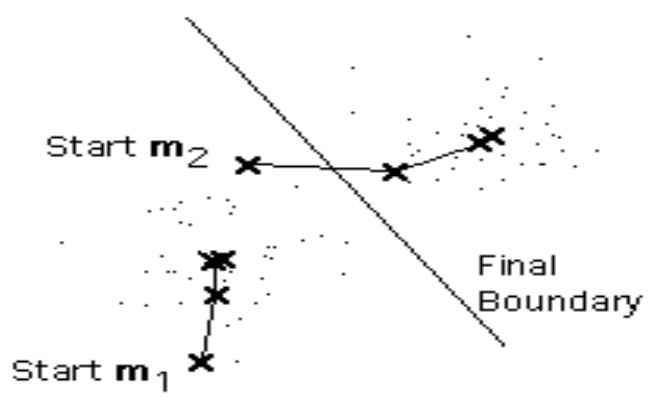


Figure 1.13: Example of Cluster

**Observations:** This is an elementary rendition of the k-means approach. It tends to be perceived as an avaricious computation for parceling the n tests into k bunches with the intention of limiting the whole of the squared partings to the collection focuses. It has a small number of weaknesses:

- The method to instate the means was not designated. One well-known tactic to commence is to arbitrarily pick k of the examples.
- The results delivered count on the primary qualities for the means, and it every now and again happens that problematic parcels are discovered. The standard arrangement is to attempt various diverse commencement phases.
- O It is able to come about that the planning of tests nearest to mi is empty, with the goal that mi can't be reinvigorated. This is an inconvenience that needs to be taken care of in an execution, nevertheless one that we shall overlook.
- $\circ$  The results count on the measurement used to gauge  $\| x mi \|$ . A well-known plan is to normalize each factor by its standard deviation; nevertheless, this isn't regularly striking.
- o The consequences count on the assessment of k.

This last issue is particularly badly designed, since we consistently get no opportunity to acquire of significant what number of packs exist. In the model showed up more than a comparable count associated with comparable data conveys going with 3-means clustering. Is it ideal or progressively lamentable over the 2-means clustering?

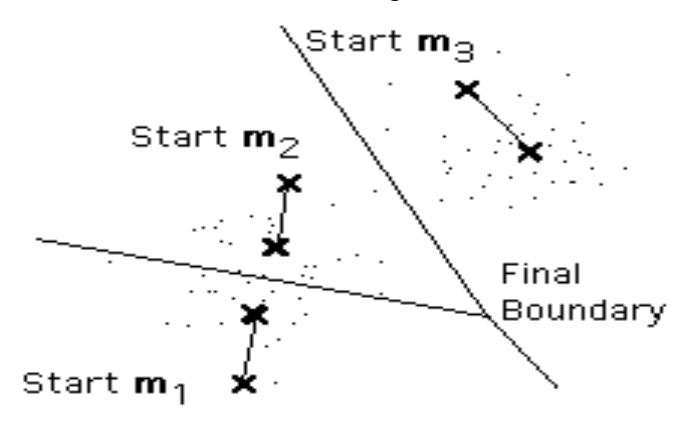


Figure 1.14: Clustered Data

Unfortunately, there is no general theoretical solution for finding the ideal number of clusters for a given dataset [46]. A basic procedure is to distinguish the concerns of various runs and distinguish k classes and pick the greatest one as per a given measure, yet users had better be cautious on the grounds that growing k brings around smaller blunder size esteems by definition, yet additionally an expanding risk of overfitting.

**Fuzzy C-Means (FCM) Clustering Algorithm:** It differs from K-means because it enables pixels to join multiple clusters simultaneously, so their membership amounts change according to varying

criteria. The soft clustering technique balances flexibility well in situations where multiple data points share common features and need this type of analysis. The selection of initial centroids remains a highly sensitive step within FCM, and the number of clusters must be determined at the point of initialization [47-54]. The sensitivity requires users to carefully adjust parameters for optimal results when using this method.

Major advantages of the algorithm of image segmentation:

- Content-based image retrieval.
- Video surveillance.
- Used for locating objects and boundaries of line curves, images, and so on.
- Essential in computer-aided diagnosis systems of various applications.
- It divides the images into the specified description.
- Better in data storing, communication, and image gaining.
- It is versatile, robust, accurate, and efficient techniques present to segment the regions.

Applications of image segmentation algorithms

- Machine vision.
- Content-based image retrieval.
- Object detection.
- Tumor detection and segmentation.
- Mass detection.
- Segmented body tissues/organs in medical application.
- Task recognition.
- Traffic control system.
- Video surveillance.
- Segmentation and texture analysis.

### 1.7 BRAIN TUMOR SEGMENTATION AND CLASSIFICATION

Healthcare specialists who work with medical imaging must perform brain tumor segmentation along with classification tasks for exact diagnosis and treatment planning. Medical imaging personnel need to separate tumor regions in MRI or CT scans before categorizing tumors as gliomas, meningiomas, or pituitary tumors. Neuroimaging practices now achieve better brain tumor segmentation through the combination of U-Net and traditional segmentation processes such as thresholding and region-growing alongside K-Means and Fuzzy C-Means clustering along with modern CNNs and DeepLabV3+ deep learning models. The classification system integrates background and deep learning methods employing SVM and Random Forest together with CNNs that deploy VGG16 and ResNet via transfer learning techniques. The development of the field progresses forward while it encounters multiple enduring drawbacks, which stem from tumor variety alongside weak MRI contrasts along with unbalanced class distributions and insufficient available data. AI-related segmentation and classification research will integrate privacy-protected training via federated learning while adding both explainable AI techniques and 3D volumetric analysis and multi-modal imaging fusion outlooks for future work. Technological advancements will boost automation levels for tumor identification systems, thereby allowing radiologists to make decisions backed by clear evidence.

Brain tumor segmentation and classification refers to the process of automatically identifying and distinguishing different types of brain tumors within a medical image, typically an MRI scan, by separating the tumor tissue from healthy brain tissue, allowing for accurate diagnosis and treatment planning; this is usually achieved using computer vision techniques, particularly deep learning algorithms, to analyze the image and classify the tumor based on its characteristics like size, location, and appearance. Key points about brain tumor segmentation and classification:

• **Image modality:** MRI is the most commonly used imaging modality for brain tumor analysis due to its high soft tissue contrast.

#### Segmentation process:

• Identifying tumor boundaries: The algorithm identifies the pixels or voxels that belong to the tumor region, effectively outlining the tumor's edges.

• Pixel classification: Each pixel within the image is assigned a label indicating whether it belongs to the tumor, healthy brain tissue, or other relevant structures.

### • Classification process:

- Tumor type identification: Once the tumor is segmented, the system analyzes its features (like texture, intensity, and shape) to classify it into different types of brain tumors, such as glioma, meningioma, or pituitary adenoma.
- Grading: Some systems can further classify tumors based on their aggressiveness (grade), like low-grade or high-grade gliomas.

## Common techniques used for brain tumor segmentation and classification:

- Deep learning models: Convolutional Neural Networks (CNNs) like U-Net are widely used for segmentation due to their ability to learn complex features from medical images.
- Atlas-based methods: Utilizing a predefined brain atlas to register the patient's image and identify tumor regions based on anatomical landmarks.
- Feature extraction techniques: Analyzing texture features within the tumor region.

### 1.7.1 Problems related to Brain Tumor Segmentation and Classification

Various difficulties affect both the accuracy and reliability of automated systems used for brain tumor segmentation and classification. The problem of high tumor variability concerning shape and size along with location results in poor model generalization across different brain tumor cases. The poor contrast and noisiness present in MRI scans make tumor borders difficult to discern, thus causing mistakes during segmentation and classification. The occurrence of class imbalance creates a major problem because uncommon tumor types become skewed towards prevalent diagnosis categories in deep learning models' predictions. Difficult training of models exists because manual radiologist annotations require extensive time investment and cost money. The distinction between benign and malignant growths becomes difficult because tumors present characteristics that duplicate normal brain tissue structures. The performance of models suffers when they become sensitive to initial conditions and model hyperparameters, particularly when using clustering-based or deep learning techniques. Medical professionals must have transparent processes for diagnosis since deep learning models do not provide understandable decision-making

mechanisms. Resolving these difficulties demands sophisticated AI methods together with enhanced accessibility to data as well as strong validation protocols to improve brain tumor segmentation and classification systems' accuracy and reliability levels.

## 1.7.2 Application of Brain Tumor Segmentation and Classification

Brain tumor segmentation and classification have numerous critical applications in the medical field, significantly improving diagnosis, treatment planning, and patient outcomes. Automated segmentation helps radiologists precisely identify and delineate tumor regions in MRI and CT scans, reducing manual effort and enhancing diagnostic accuracy. Classification models assist in differentiating tumor types, such as gliomas, meningioma's, and pituitary tumors, enabling oncologists to tailor personalized treatment plans, including surgery, radiation, or chemotherapy. These techniques are also valuable for tumor progression monitoring, allowing doctors to track growth, recurrence, and response to treatment over time [58]. In surgical planning, accurate tumor segmentation helps neurosurgeons determine the safest approach for tumor removal while minimizing damage to surrounding healthy brain tissue. Additionally, AI-driven brain tumor analysis contributes to radiogenomics, which links imaging features with genetic mutations, aiding in precision medicine. It is also used in telemedicine and remote diagnostics, providing automated tumor detection in resource-limited settings where expert radiologists may not be available. Furthermore, clinical research and drug development benefit from these advancements, enabling large-scale tumor analysis for developing new therapeutic strategies [59]. As deep learning and AI technologies evolve, brain tumor segmentation and classification will continue to revolutionize neuro-oncology, improving early detection, treatment efficacy, and overall care.

### 1.7.3 Challenges in Brain Tumor Segmentation and Classification

Brain tumor segmentation and classification face several challenges that impact the accuracy and reliability of automated systems. The high variability in tumor shape, size, and location makes it difficult to develop generalized models that perform consistently across different patients. Low contrast and noise in MRI scans further complicate the distinction between tumor and healthy tissue, leading to potential misclassification. Class imbalance is another significant issue, as certain tumor types are rarer, causing bias in machine learning models. The lack of large, well-annotated medical datasets limits the training and validation of deep learning models, making robust generalization difficult. Additionally, tumors often exhibit overlapping features with normal brain

structures, making precise segmentation challenging. The sensitivity of clustering-based and deep learning models to hyperparameter tuning and initialization also affects segmentation accuracy. Furthermore, the black-box nature of deep learning models raises concerns about interpretability and trustworthiness in clinical applications [60]. Overcoming these challenges requires advanced AI techniques, better dataset availability, improved explainability in deep models, and efficient real-time processing methods to ensure accurate, reliable, and clinically useful tumor segmentation and classification. Challenges in brain tumor segmentation and classification:

- Variability in tumor appearance: Brain tumors can have irregular shapes, blurry boundaries, and diverse intensity patterns, making accurate segmentation difficult.
- Multimodal image analysis: Utilizing different MRI sequences (T1, T2, and FLAIR) can improve accuracy but requires complex integration.
- Inter-observer variability: Different radiologists may interpret tumor boundaries differently.

### 1.8 MOTIVATION ABOUT BRAIN TUMOR-RELATED WORK

For the detection and treatment of cancer, image-based tumor segmentation and classification has a number of potential advantages, including:

**Enhanced accuracy:** Tumor properties, including size, shape, and location, may be precisely identified and quantified with the use of image-based tumor segmentation and classification systems. This may result in diagnoses and treatments that are more specialized and exact.

**Time-saving:** Automating the process of tumor identification and analysis using image-based tumor segmentation and classification techniques may speed up the procedure and lighten the burden of medical personnel.

**Non-invasive:** Image-based tumor segmentation and classification algorithms do not need biopsies or surgical procedures since they are non-invasive. This may lessen the pain experienced by patients and the danger of consequences from invasive operations.

**Better monitoring:** Image-based tumor segmentation and classification techniques may be used to track tumor development and response to therapy over time, assisting medical personnel in modifying treatment strategies as necessary.

**Improved results:** Image-based tumor segmentation and classification techniques may assist medical personnel in making more knowledgeable treatment choices, improving patient outcomes.

**Accessible:** Image-based tumor segmentation and classification techniques may be used in a variety of locations, including underdeveloped and rural regions where access to expert medical personnel may be restricted [61].

Generally speaking, image-based tumor segmentation and classification have the potential to greatly enhance cancer diagnosis, therapy, and follow-up, resulting in improved patient outcomes.

## 1.9 SIGNIFICATION OF BRAIN TUMOR-RELATED WORK

Brain Tumour Segmentation and categorization of brain tumors are essential in medical imaging and healthcare, markedly enhancing the accuracy, efficiency, and efficacy of brain tumor diagnosis and treatment planning. Accurate segmentation aids in delineating tumor margins, quantifying tumor dimensions, and monitoring its evolution over time, hence facilitating informed decision-making by radiologists and neurosurgeons. Automated classification facilitates the differentiation of various tumor forms, including gliomas, meningiomas, and pituitary tumors, which is crucial for tailored treatment approaches such as surgery, chemotherapy, or radiation therapy. Advanced AI-driven segmentation decreases manual labor, reduces human errors, and facilitates early diagnosis, resulting in enhanced patient survival rates. Moreover, precise classification aids in prognostic prediction and enhances medical research by offering critical insights into tumor behavior. The amalgamation of deep learning and machine learning models in segmentation and classification has transformed brain tumor analysis, providing expedited, more dependable, and economical diagnostic methods. Consequently, these improvements substantially boost healthcare systems, ultimately increasing patient outcomes and quality of life.

#### 1.10 RESEARCH GOALS & SCOPE

The research goals in brain tumor segmentation and classification focus on developing accurate, efficient, and interpretable AI-driven solutions to assist in early diagnosis and treatment planning. The primary objectives include improving segmentation accuracy by leveraging unsupervised learning architectures such as K-means and FCM to accurately delineate tumor boundaries in MRI

and CT scans. Another key goal is enhancing tumor classification models using machine/deep learning and deep learning techniques, such as CNNs and transfer learning, to differentiate between tumor types like gliomas, meningiomas, and pituitary tumors. Researchers also aim to address challenges such as class imbalance, noise in medical images, and variability in tumor morphology by incorporating data augmentation, synthetic dataset generation, and multi-modal imaging fusion (MRI, PET, and CT). Additionally, improving explainability and interpretability in AI-based models is essential to ensure that automated systems can provide clinically reliable and transparent diagnoses [62-67].

The scope of brain tumor segmentation and classification research extends to multiple domains, including radiology, neurology, medical image processing, and artificial intelligence. It encompasses advancements in automated segmentation, feature extraction, and classification techniques, integrating both handcrafted and deep learning-based approaches. Furthermore, the research is applicable in CAD systems, surgical planning, and personalized medicine, ultimately aiding healthcare professionals in early detection, treatment response monitoring, and prognosis prediction. The integration of federated learning and cloud-based AI models expands the scope by enabling real-time and scalable tumor analysis across multiple hospitals while ensuring patient data privacy [68]. Future research directions involve refining real-time segmentation models, 3D volumetric analysis, and AI-driven decision support systems, making brain tumor diagnosis more accessible, reliable, and efficient.

## 1.11 MEDICAL IMAGES DATASETS

There are several datasets available for image-based tumor segmentation and classification. Here are a few examples:

The Brain Tumor Segmentation (BraTS) dataset contains the following information: This is a very popular dataset for the segmentation of brain tumors, and it contains magnetic resonance imaging (MRI) images of brain tumors. The collection contains pictures of patients suffering from a wide variety of brain cancers, including glioblastoma and meningioma. On the official website of the BRATS Challenge, which can be found at

https://www.med.upenn.edu/cbica/braintumors2020/data.html, the BRATS (Brain Tumor Segmentation) dataset is available for download.

**Kaggle Data Set:** provides brain MRI images for Brain Tumor Detection. The data set can be downloaded via <a href="https://www.kaggle.com/datasets/navoneel/brain-mri-images-for-brain-tumor-detection">https://www.kaggle.com/datasets/navoneel/brain-mri-images-for-brain-tumor-detection</a>

**Figshare Data Set:** Figshare is an online open access repository where researchers can preserve and share their research outputs, including figures, datasets, images, and videos. The data set can be downloaded via <a href="https://figshare.com/articles/dataset/brain\_tumor\_dataset/1512427">https://figshare.com/articles/dataset/brain\_tumor\_dataset/1512427</a>

Some sample data of the used dataset is shown in Figure 1.15.

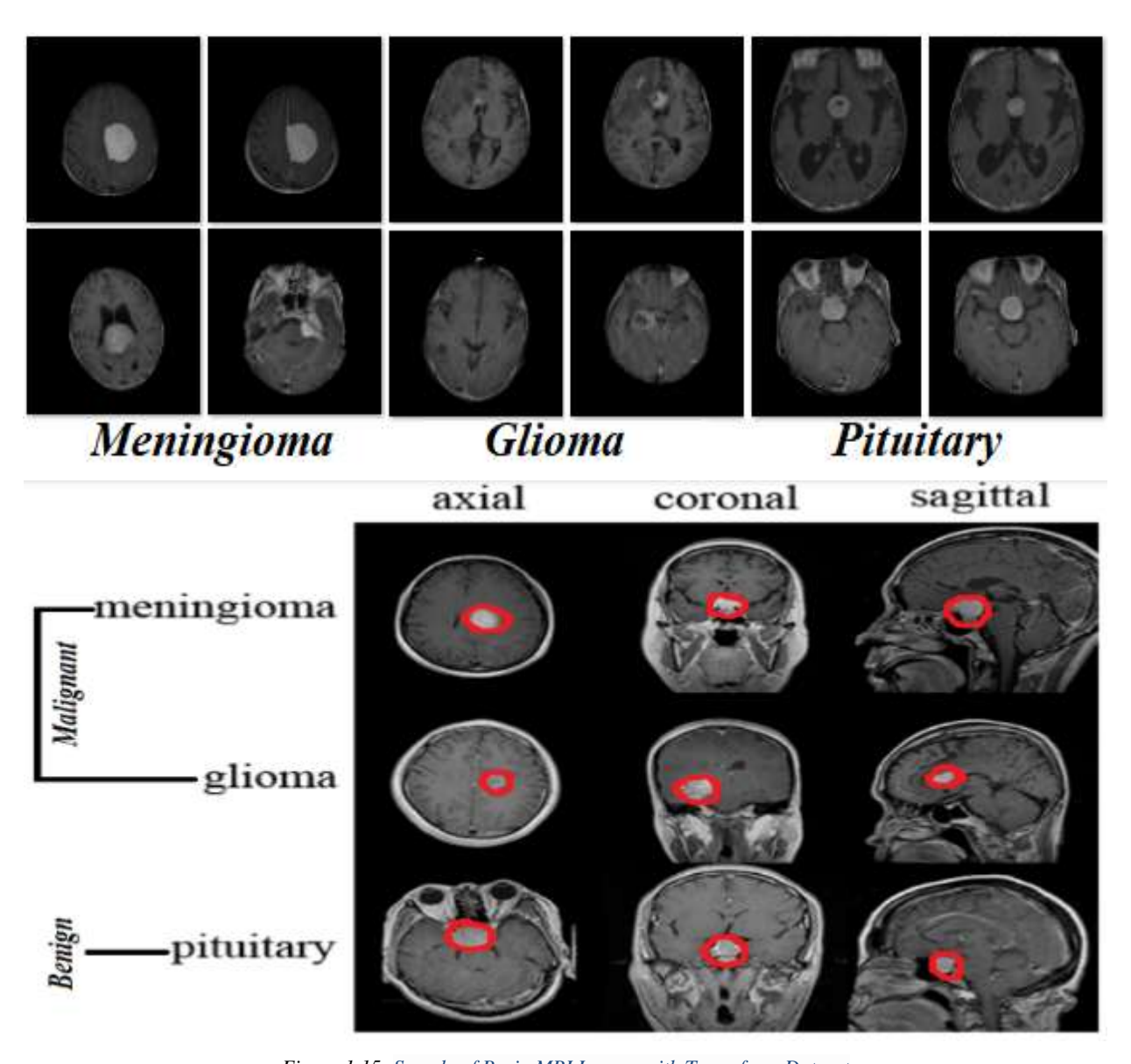


Figure 1.15: Sample of Brain MRI Images with Types from Dataset

## 1.12 CONTRIBUTION OF THESIS

The research demonstrates that early tumor detection is beneficial for preserving human lives, driven by the pressing necessity for advancements in medical imaging technology to enhance the diagnosis and treatment of brain cancers. Brain tumors present significant challenges to healthcare, requiring accurate and effective segmentation methods for adequate analysis due to their complexity and diverse characteristics. Recent medical research has greatly enhanced the understanding of brain tumors, with MRI becoming an essential instrument for their detection. Nevertheless, the segmentation of these tumors continues to be a formidable task, occasionally susceptible to errors and inaccuracies. This study seeks to address these challenges by examining and comparing advanced clustering mechanisms via Moth-Flame Optimization (MFO), a swarmbased technique for precise Brain Tumor Region (BTR) segmentation, and subsequently developing a Hybrid Model for Brain Tumor Analysis (BTA) utilizing Convolutional Neural Networks (CNN) as an innovative deep learning methodology. In prior research, various swarmbased metaheuristic algorithms were compared to identify MFO as the superior technique in conjunction with K-means clustering for segmenting the BTR from MRI [11]. Here, five different models for swarm-based optimization techniques are used that are shown in Figure 1.15, and the names of the algorithms are Particle Swarm Optimization (PSO), Artificial Bee Colony (ABC), Firefly Algorithm (FFA), Cuckoo Search Algorithm (CSA), and Moth-Flame Optimization (MFO), as illustrated in Figure 1.16 [12].

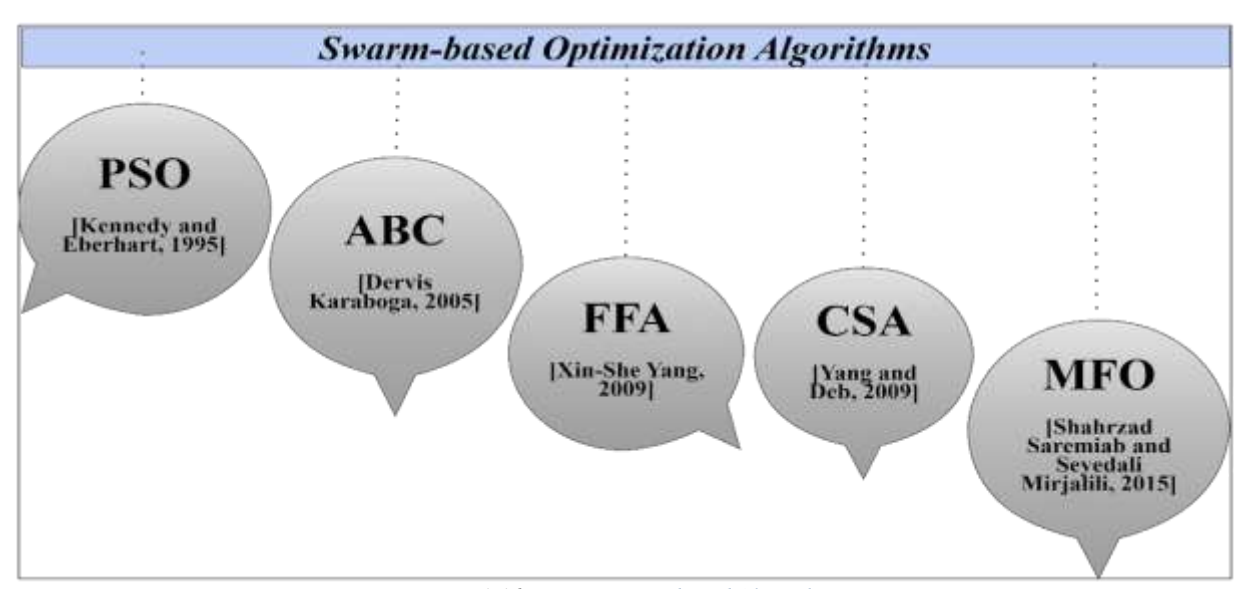


Figure 1.16: Latest Swarm-based Algorithms

The comparative review of existing segmentation methods in prior research is to uncover and refine clustering mechanisms that might substantially improve the accuracy and efficiency of MRI-based brain tumor segmentation. This optimization's potential influence transcends research facilities, extending into clinical environments and providing healthcare practitioners with a more dependable instrument for the early detection and diagnosis of tumors. The pursuit of an enhanced segmentation approach transcends academic interest; it aims to elevate patient outcomes and advance the progression of medical procedures. This study aims to offer useful insights that can transform the approach to the BTA model, promoting breakthroughs that promise more accurate diagnoses, prompt interventions, and enhanced patient care. This project aims to catalyze positive change in neuroimaging and brain tumor detection within the context of essential medical innovation. The major contributions are listed as:

- **1.** To present a short survey on the detection and classification of brain tumors to identify the challenges and issues.
- **2.** Pre-processing methods are employed to enhance the quality of MRI data and improve the clarity of images.
- **3.** To detect and segment the BTR from MRI, K-means with MFO as a swarm-based optimization is used, validate
- **4.** To train and validate the BTA model, CNN with MFO is used as a novel deep learning approach.
- **5.** To find out the BTA model efficiency, performance parameters are calculated and compared with existing works in terms of sensitivity, precision, F1-score, Mathew Correlation Coefficient (MCC), Dice, Jaccard, specificity, accuracy, and time.

## 1.13 STRUCTURE OF THE THESIS

Chapter 2 presents a comprehensive review of the literature related to brain tumor segmentation and classification using various techniques, including clustering methods, deep learning architectures, optimization strategies, and evaluation metrics. The chapter also includes a detailed literature summary in tabular form to provide a comparative analysis of different methodologies. Furthermore, this chapter identifies the research gaps in existing approaches, laying the foundation for the proposed work.

Chapter 3 introduces the problem formulation, derived from an extensive literature survey on brain tumor segmentation and classification. It outlines the key research objectives established based on the identified challenges. Towards the end, the chapter provides a detailed explanation of the proposed clustering and deep learning algorithms that aim to enhance segmentation and classification accuracy.

Chapter 4 describes the research methodology employed in this study, detailing the algorithms and models developed to improve brain tumor segmentation and classification. This chapter elaborates on the techniques used, such as machine learning, convolutional neural networks (CNNs), hybrid clustering approaches, and deep learning-based segmentation models.

Chapter 5 discusses the experimental setup required for implementing the proposed brain tumor segmentation and classification model. It also covers the computational resources, datasets used (e.g., BraTS dataset), pre-processing techniques, and software tools necessary for the research. Towards the end, the chapter highlights the infrastructure and facilities utilized for experimentation and model evaluation.

Chapter 6 presents the experimental results and analysis of the proposed segmentation and classification techniques. This chapter includes a discussion of the performance metrics (such as Dice coefficient, Jaccard index, accuracy, precision, recall, and F1-score) and a comparative analysis with existing state-of-the-art methods. Additionally, it covers the implementation details, hybrid algorithm execution, and insights derived from experimental findings. The chapter concludes by evaluating the proposed methodologies against benchmark datasets and existing literature.

Chapter 7 concludes the thesis by summarizing the key findings and contributions of the research. It also explores potential areas for future work, such as improving segmentation models using 3D deep learning architectures, explainable AI (XAI) techniques, multi-modal image fusion (MRI, PET, CT), and federated learning approaches for privacy-preserving medical image analysis.

This structured approach ensures a comprehensive study on brain tumor segmentation and classification, addressing challenges and proposing innovative solutions to advance medical image processing and AI-driven diagnostics.

## **CHAPTER 2**

## LITERATURE REVIEW

### 2.1 REVIEW OF LITERATURE

This chapter includes multiple scenarios to present a quick assessment of existing work related to brain tumor segmentation and classification techniques. The existing work based on the image classification with the help of a hybrid approach is well illustrated. In this chapter, we will discuss the segmentation of various types of data that are captured from CT scans in medical science. A brief but deep explanation of some of the most significant contemporary clustering emphasizing medical image segmentation as well as classification techniques will be provided. These methods are utilized in the process of segmenting a wide variety of medical pictures.

Chander et al. published an article in Elsevier in 2011 considering the Otsu's method, which was modified in combination with the PSO approach for segmentation of images. Furthermore, the effectiveness had been improved by computing the threshold level, which is evaluated by experimental analysis and is able to adequately address picture segmentation concerns. Also, it was demonstrated that the enhanced segmentation method outperformed other recognized methods [13].

After that, a model was developed in 2013 by *Bandyopadhyay and Paul* employing the K-means clustering-based diagnostic method to segment the BT using MRI images. Furthermore, precision of the segmented images had been improved by the authors by dividing the devised system into two parts. In the first, the registration of an image was discussed, and in the second, the fusion of two registered MRI pictures. The segmentation of tumor areas in MRI is then done using the concept of improved K-means. The design system, however, was restricted by the restrictions of the data pattern and was not suitable for the 3D modelling of medical image segmentation and also ran into the problem of segmentation mixing [14].

In order to address these problems in MIS, **Zhao et al.** in 2014 developed a methodology to address the pixel mixing issue in K-means-based segmentation of medical images. Here, the author

introduces the PSO concept to enhance the effectiveness of using MRI for tumor segmentation. In this case, the initial clusters for the MRI pixels are created using the PSO concept, and the mixing problem is then tried to be solved using fitness. The experimentation revealed the modified K-means technique had been employed considering the K-means for performance metrics such as execution speed and accuracy rate [15].

The same year, a study based on the notion of conventional fuzzy C-means (FCM) for segmenting BTs was published in IJIRCCE. To identify tumors from the MRI, the tumor investigators in this instance also used an advanced K-means [16].

In 2017, *Parasar and Rathod* published a comparison of seeded region growth, watershed, and FCM combined with the swarm-based PSO for the medical image segmentation of ultrasound pictures utilizing the PSO and K-means combination [17].

*Ventateshan and Parthiban* focused on using the K-means with PSO for the segmentation of MRI images with hybrid technique in 2017. The kernel filter was also employed for better results, and it was assessed for its quicker execution time, but accuracy still requires more attention [18].

*Hasan* did research in 2018 using the PSO to autonomously segment brain cancers using MRI data. To achieve segmentation accuracy of about 92%, the authors used the segmentation technique with PSO [19].

In 2018, *Karegowda et al.* suggested a technique based on MRI-based BT-based segmentation. The authors concluded that using PSO is a wise move after further contrasting the K-means, FCM (also a clustering method), and Adaptive Regularized Kernel-based PSO with FCM (ARK-PSO) approaches. According to experimental findings, PSO-based segmentation is more accurate than the conventional techniques such as meta-heuristic techniques [20].

**Arun Kumar et al.** implemented a better automated method for segmenting and identifying BT locations using K-means in 2019. The pre-processing stages are included in which an image is improved in order to accurately forecast a BT [21].

The authors first used the Harvard Whole Brain Atlas dataset for the improvement of MRI brain image; *Hrosik et al.* published an article using the K-means technique in conjunction with FFO in

the same year. The results demonstrated that the hybrid strategy performed more effectively than the others [22].

In 2020, *Chander et al.* built a model to help the process of tumor segmentation from various levels of MRI scans with the assistance of clustering-based methods such as the K-means algorithm and Support Vector Machine, also known as SVM, as a machine learning method. The system's (developed) accuracy rose when compared to the earlier work [23], indicating that the model was successful.

In 2021, *S Gupta et al.* developed a model for brain tumor segmentation and classification utilizing a multi-task attention-guided network as a proposed machine learning approach. This study aims to construct a multi-task attention-guided network (MAG-Net) for the segmentation and classification of tumors using brain MRI data. The authors utilized the publicly accessible dataset referred to as "Figshare." This dataset has three tumor types: meningioma, glioma, and pituitary tumor, presented in coronal, axial, and sagittal views, respectively. The model demonstrated potential in comprehensive experimental trials, surpassing current state-of-the-art models while utilizing the minimal number of training parameters. [24].

AR Khan et al. conducted research in 2021 to develop a model for segmentation of brain tumors using a clustering approach with deep learning for synthetic data. Here, authors generated a hybrid approach with K-means as clustering and a deep learning mechanism for the augmented data classification. The suggested procedure in this research includes three basic stages named as: preprocessing, K-means-based clustering for the brain tumor region segmentation, and benign/malignant tumor classification utilizing MRI data via a fine-tuned VGG19 model as a deep learning approach. Furthermore, the concept of synthetic data augmentation is introduced to increase the volume of data available for training classifiers, hence enhancing classification accuracy. Comprehensive evaluations were conducted to evaluate the proposed technique utilizing the BraTS 2015 benchmark datasets. The results confirm the efficacy of the proposed strategy, which surpassed previously documented state-of-the-art procedures regarding accuracy [25].

In 2021, *T Tazeen & M Sarvagya* had conducted research to design a model for Brain Tumor Segmentation as well as their Classification from the MRI data with the help of Multiple Feature Extraction approach and Convolutional Neural Network (CNN). In order to take preventative

measures against brain tumors, MRI is used for early diagnosis and assessment. Brain tumors can be better diagnosed with the use of MRI because of the information it provides about sensitive human tissue. In this research, we present a technique for detecting and classifying brain tumors utilizing an ensemble of CNNs to extract and classify features [26].

FJ Díaz-Pernas and M Martínez-Zarzuela, In 2021 developed a deep learning model for the segmentation and classification of brain tumors. This paper presents a fully automated model for brain tumor segmentation and classification utilizing multi-scaled Deep CNN. The proposed concept of this model diverges from previous efforts in various ways, notably by analyzing input images at three unique spatial scales through discrete neural networks. This method is inspired by the inherent working of the human visual system. The proposed neural model does not necessitate any preprocessing of input images to eliminate skull or vertebral column segments for the analysis of MRI scans featuring meningioma, glioma, and pituitary tumors across sagittal, coronal, and axial perspectives. The proposed method is evaluated against conventional machine learning and deep learning techniques utilizing a publicly available MRI imaging dataset of 3064 slices from 233 patients. Our methodology surpassed other approaches utilizing the same database by attaining an exceptional accuracy of 0.973 (97.3%) in tumor categorization. [28].

In 2022, *M Arif et al.* had developed a model for brain tumor segmentation and their classification using the concept of Genetic Algorithm (GA)-based U-Net as a deep learning approach. The following steps are used by the authors in this work, a deep learning method for detecting brain tumors: Data is obtained from the REMBRANDT dataset, which contains multi-sequence MRIs of 130 patients; (b) pre-processing is performed by converting to greyscale, skull stripping, and histogram equalization; (c) GA is used for segmentation; (d) discrete wavelet transform (DWT) is used for feature extraction; (e) particle swarm optimization is used for feature selection; and (f) U-Net is used for classification. The suggested model (GA-UNET) has been shown to perform better than existing state-of-the-art models in experiments and achieved 97% accuracy, 98% sensitivity, and 98% specificity [29].

*KA Kumar & R Boda* in 2022 had developed a multi-objective-based beetle swarm and multiverse optimization algorithm for brain tumor segmentation and their classification in randomly updated populations. The purpose of this research work is to use a wide variety of intelligent approaches to create a model that can accurately classify types of brain

tumors. Here, authors used lots of steps like image pre-processing, skull stripping, tumor segmentation, feature extraction, and classification, which are the primary steps in the proposed model. First, a median filter is applied to the image once it has been converted from RGB to grayscale. In addition, Otsu thresholding is used for skull stripping, which involves erasing the extra-meningeal tissue from the head picture. Optimized thresholdbased tumor segmentation using multi-objective randomly updated beetle swarm and multiverse optimization (RBS-MVO) is the key contribution, and it is used to perform tumor segmentation [30]. The literature from 2022 to 2024 reinforces the shift towards deep learning (DL) as the standard for brain tumor detection, with many studies comparing ML and DL approaches [98-101]. Comprehensive surveys from this period confirm that machine learning and AI are central to modern diagnostics [102-103], with bibliometric reviews identifying key trends and research gaps [104]. Recent studies heavily emphasize the efficacy of DL models [105-107], including ensemble approaches [108] and deep analysis of various DL networks [109]. A significant trend is the use of transfer learning, employing pre-trained models to achieve high accuracy [110]. Other novel approaches include integrating DL with techniques like Proper Orthogonal Decomposition [111] or combining deep features with ML classifiers and genetic algorithms for feature selection [112]. Hybrid models, such as those using optimization techniques with DL, also show promise [113-114]. While these recent works report high classification accuracy, a critical observation is that many, like earlier studies, are validated on similar benchmark datasets [115]. This highlights an ongoing need for models that not only perform well but are also proven to generalize across diverse, multi-institutional clinical data, addressing the gap this thesis aims to fill. A results-based summation is explained using the BraTS dataset and is shown in Figure 2.1.

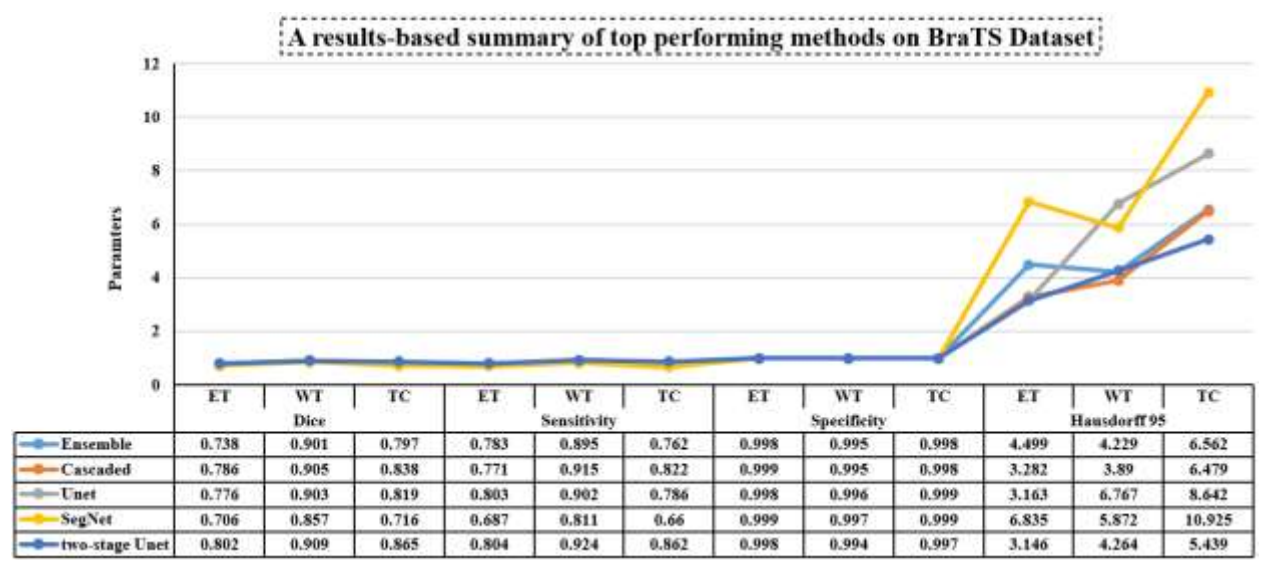


Figure 2.1: Top methods using the BraTS Dataset

In Figure 2.1, three different abbreviations are used: multilevel thresholding (MT), ET (enhancing tumor), WT (whole tumor), and TC (tumor core). In this figure, ensemble techniques have recently been adopted by researchers to obtain cutting-edge performance. The ensemble approaches precisely combine the segmentation findings of many models to increase the robustness of the individual approach, producing better recital than inter-rater agreements. A well-trained and known UNet is used, according to the claim that single UNet-based models continue to provide incredible concert. According to the literature study, segmentation algorithms' accuracy and resilience will be greatly enhanced by analyzing the hyperparameters, which is a pre-processing method. Table 2.1 shows the segmentation of BT using the dataset, and a summary of the BT segmentation-based survey is given.

# 2.2 LITERATURE SUMMARY (TABULAR FORM)

Table 2.1	Literature	Review

References	Proposed Work		<b>Used Techniques</b>	Dataset	S	ummary of Effectiveness
Segmentation of BT						
[13]	MT-based image segmentation	1007	Swarm-based PSO using OTSU method	General	IGF	There is more than 95% accuracy.
[14]	Segmenting the BT from MRI	1007	Clustering using K-means	MRI Data Bank	IGF	There is more than 97% accuracy.

[15]	An improved clustering method for segmentation		Clustering using K-means PSO technique	_	The execution time is 1.5 s.
[16]	Segmenting the BT	IGF	Clustering using K-means FCM clustering	MRI Dataset	The tumour area is detected
[17]	Segmenting the foetus ultrasound image		Clustering using K-means FCM clustering PSO	Foetus Ultrasonic	There is about 93% accuracy.
[18]	MIS	GF GF	FCM clustering Hybridized PSO using kernel filter Segmentation using Quantum PSO	IRIS Dataset	Execution time
[19]	MRI segmentation of BT	of of	Active Contour Swarm-based PSO	MRI Data from Iraqi Centre for Research	Accuracy = 92%
[20]	Segmenting MRI BT images		Clustering using K-means Clustering using FCM PSO-based segmentation Kernel FCM using Adaptive Regularised	_	Computation of Peak Signal- to-Noise Ratio (PSNR), Mean Square Error (MSE), Normalised Cross Correlation (NCC), Structural Similarity Index (SSIM) and Accuracy
[21]	Abnormality in BT	igr	Clustering using K-means Using the ANN	BRATS Dataset	The accuracy is about 94%  The Sensitivity is about 90%  The specificity is about 97%.
[22]	Brain image segmentation	ige ige	Using the OTSU technique Clustering using K-means Segmentation using FFO	Harvard Whole Dataset	Computation of Normalized Root MSE, PSNR, and SSIM

[23]	Detection and Classification of BT	GF	Segmentation using DWT  Clustering using clustering technique and classifier	Harvard University Repository	The accuracy is about 93%.
[24]	Brain tumour segmentation using the concept of DL		Ensemble Cascaded Unet SegNet Two-stage Unet	BRATS Dataset	Computation of Dice, Sensitivity, Specificity , and Hausdorff 95

The following issues are emphasized as downsides after an analysis of the several literature surveys on related work to the segmentation of various medical images:

- The primary mistake in the current or existing unsupervised clustering-based segmentation of an image is the overlapping of image foreground and background due to the problem of pixel mixing.
- The existing swarm-based or clustering-based image segmentation procedure requires more time to perform segmentation in the proper manner, and there may be a significant number of clusters that are unknown.
- According to the discussion in related work, it is evident that large-scale segmentation operations have been plagued by challenges of segmentation of complicated pictures in the scenario of MRI, dermoscopy, CT scans, and microscopic images. This is because image quality and the demand to focus on quality improvements are the primary causes of these problems.
- There are a lot of researchers that run into the problem of pixel mixing because of the frequent changes in pixel value in the neighborhood, but there are still some things that might be improved.
- The quality of the segmentation results is highly dependent on the initialization of the clustering algorithm. Choosing appropriate initial cluster centers can be a challenging task, and incorrect initialization can lead to poor segmentation results.

- Clustering algorithms can suffer from over-segmentation, where the image is divided into too many small regions, or under-segmentation, where the image is not divided into enough regions. Both of these can lead to inaccurate segmentation results.
- Unsupervised clustering-based segmentation can have difficulty with images containing complex objects, such as overlapping or occluded regions, or regions with varying textures or colors. In these cases, more sophisticated segmentation methods may be required.

The effectiveness of segmentation algorithms with and without unsupervised clustering-based approaches is shown in the following Figure 2.2.

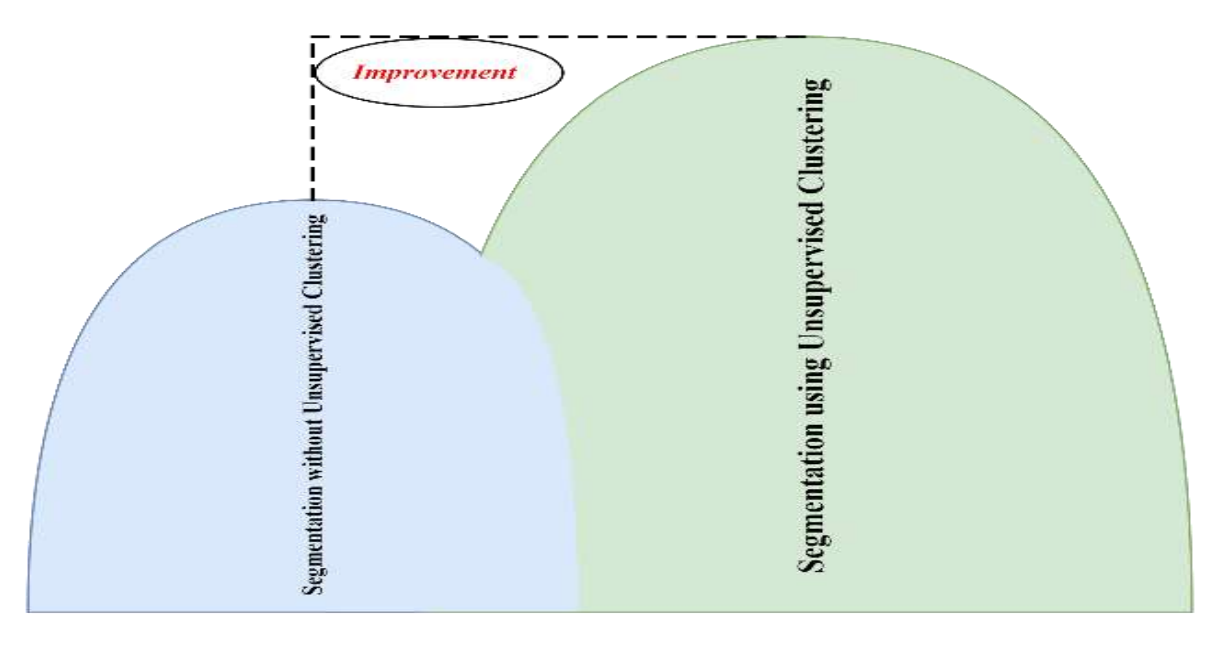


Figure 2.2: Efficiency Unsupervised Clustering-based Approaches for Medical Images

Based on the aforementioned investigation in the related work, came to the conclusion that medical image segmentation is a very complex procedure that requires a number of crucial processes that vary depending on the kind of image data. The technique for segmenting images may split the medical picture into many divisions in accordance with the accessible pixel groups that are organized according to the information about the backdrop and the foreground of the image. We know that the images are made up of different pixel combinations, and based on their intensity value, any segmentation algorithm is performed. Due to such a crucial task, algorithms faced the pixel mixing problem, which is displayed in Figure 2.3.

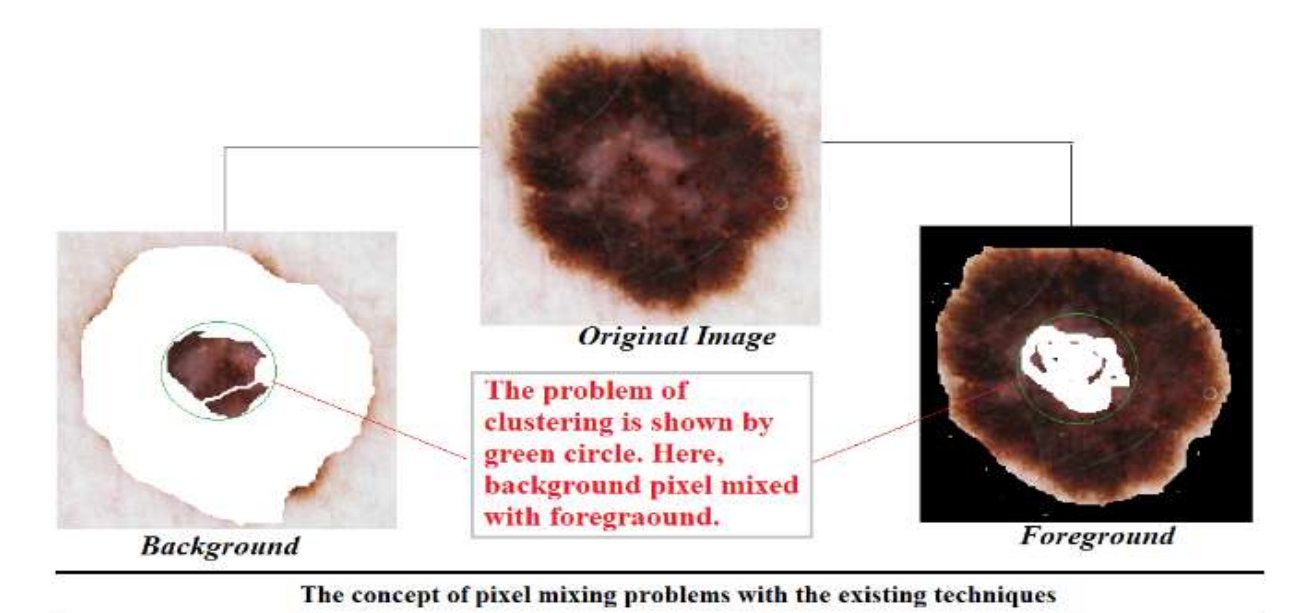


Figure 2.3: Clustering Faces Pixel Mixing Problems

Pixel mixing is a common problem in clustering-based image segmentation. It occurs when pixels with different characteristics, such as color or texture, are clustered together, resulting in the mixing of different regions. This can lead to inaccurate segmentation results, with boundaries between regions becoming blurred or indistinct. Pixel mixing can occur for several reasons during the clustering method, including:

**Inappropriate Distance Metric:** The distance metric used to measure the similarity between pixels can have a significant impact on the clustering results. If the distance metric is not appropriate for the image data, pixels with different characteristics can be clustered together, resulting in pixel mixing.

**Overlapping Regions:** In some cases, regions in an image may overlap, making it difficult to distinguish between them. This can result in pixels from different regions being clustered together, leading to pixel mixing.

**Noise:** Noise in the image data can also contribute to pixel mixing. If the clustering algorithm is not robust to noise, pixels with different characteristics can be clustered together, resulting in inaccurate segmentation.

**Insufficient Number of Clusters:** If the number of clusters used in the clustering algorithm is insufficient, pixels with different characteristics can be clustered together, leading to pixel mixing.

To address pixel mixing in clustering-based image segmentation, several techniques can be used, including:

**Swarm-based hybridization:** Use the concept of swarm-based meta-heuristic approach as well as AI approach to solve such kinds of problems.

**Adaptive Distance Metric:** Using an adaptive distance metric that takes into account the local characteristics of the image can help to overcome pixel mixing.

**Multi-Scale Segmentation:** In this step, performing segmentation at multiple scales can help to separate overlapping regions and reduce pixel mixing.

**Robust Clustering Algorithms:** Using clustering algorithms that are robust to noise and can handle overlapping regions can help to reduce pixel mixing.

**Post-Processing:** Applying some post-processing techniques, such as morphological operations or boundary refinement, can help to improve the accuracy of the segmentation results and reduce pixel mixing.

PSO, ABC, FFA, CSA, and GHA are just a few of the swarm-based optimization algorithms that are available to conduct enhanced medical picture segmentation. Several new approaches are also being developed in this area. However, since they are essentially incompatible with all types of medical imaging, the current conventional procedures are less effective. It is vital to discover an effective combination in order to fix the problem with clustering-based segmentation and boost the effectiveness of the medical diagnostic system.

### 2.3 RESEARCH GAP IDENTIFICATION

After reviewing the research literature already published in the field of medical image segmentation with their classification research, the following points have been identified as interferences drawn and verdicts from the present state of the art. These are depicted below.

1. The fundamental drawback of the current clustering-based segmentation technology is the duplication of foreground and background [14].

- 2. Because of the unknown large number of clusters, the segmentation process takes longer to execute when bio-inspired algorithms are used, which is typical in optimization-based methodologies [24].
- 3. According to the discussion in related work, the difficulties encountered in the segmentation of complicated images in the contexts of MRI, dermoscopy, CT scans, and microscopy are a direct result of poor image quality [25], highlighting the importance of concentrating on enhancing image quality in large-scale segmentation jobs.
- 4. The pixel-mixing problem that researchers encounter [27] is caused by the frequent variations in pixel value that occur in the neighborhood.
- 5. In prior work, contour-based segmentation was utilized, but there was no threshold that was justified, which resulted in segmentation that was prone to mistake [27]. This proposal is capable of being improved, and the definition of the problem justifies doing so in this fashion.
- 6. Although swarm-based optimization is a density-based optimization approach that always requires an enormous amount of data to be processed, it is used for the optimization of the region that has been segmented with an improved fitness function [28]. Thus, validating swarm-based approaches is a crucial next step that has been neglected in the existing literature. Need to test the other swarm-based algorithms, such as Cuckoo, Firefly, and Whale, among others, to make sure that they, too, work correctly at low densities.

## **CHAPTER 3**

# RESEARCH PROBLEM & OBJECTIVES

### 3.1 PROBLEM FORMULATION

From the survey, issues and challenges related to medical image segmentation are discussed, and it is the process of dividing medical images into multiple segments or regions of interest for the purpose of analysis, diagnosis, and treatment planning. However, there are several issues and challenges associated with medical image segmentation, some of which include:

**Limited availability of annotated data:** Medical image segmentation requires large amounts of labeled data for training machine learning models. However, obtaining annotated medical images is a difficult and time-consuming process.

**Complexity of medical images:** Medical images are often complex, with variations in contrast, noise, and image artifacts that make it difficult to accurately segment the images.

**Variability in anatomical structures:** Anatomical structures in medical images can vary significantly between patients, making it challenging to develop a one-size-fits-all segmentation model.

**Integration with clinical workflows:** Medical image segmentation needs to be integrated with clinical workflows to be effective. This requires careful consideration of the clinical context and the specific needs of the healthcare provider.

**Interobserver variability:** Even among medical experts, there can be variability in how medical images are segmented, leading to inconsistencies in diagnoses and treatment plans.

**Scalability:** Medical image segmentation requires large amounts of computational resources, and scaling the process to handle large datasets can be challenging.

**Ethical concerns:** Medical image segmentation can raise ethical concerns related to privacy, data ownership, and the use of sensitive medical information.

Overall, medical image segmentation is a challenging task that requires careful consideration of several factors, including data availability, image complexity, clinical workflows, and ethical considerations. Advances in machine learning and artificial intelligence are helping to address some of these challenges, but continued research is needed to improve the accuracy and scalability of medical image segmentation.

The majority of segmentation techniques for medical images are based on pixel grouping, pixel texture, and pixel color information. According to the most recent study, most segmentation techniques need refinement in order to attain the diagnostic system's efficiency. Most writers weren't concerned with creating an effective system with their choice of ML technique for segmentation. Table 3.1 compares several segmentation approaches based on difficulties and challenges.

Table 3.1 Comparison of Segmentation Techniques for Problem Analysis

Techniques of Medical Image Segmentation	Description of Techniques	Advantages of Techniques	Shortcomings of Techniques
Segmentation-based on the concept of thresholding [13, 22]	Depending on the chosen threshold value, utilize the peak areas of the picture histogram.	<ul> <li>✓ It is an easy process that doesn't need any prior knowledge of pixels.</li> <li>✓ Low computational complexity.</li> </ul>	<ul> <li>✓ Images' spatial features are not taken into account during the process of segmentation.</li> <li>✓ Had issues with neighboring pixel overlap.</li> <li>✓ Cannot guarantee that segmented sets of images are contiguous.</li> </ul>
Segmentation-based on the concept of Edge [39]	The foundation for the operation is the discontinuity in the pixel pattern.	✓ Work better for better quality images.	✓ Segmentation efficiency is affected in the case of noisy images, and output is less accurate.
Segmentation-based on the concept of region [17, 19, 26]	Segmentation is carried out by first identifying homogenous regions and then applying partition.	✓ Work outmost for the particular region in images.	✓ The time complexity of this algorithm is very high with maximum consumption of memory to perform medical image segmentation.
Segmentation-based on the concept of Watershed [17]	Segmentation employs the method of topological interpretation.	✓ Segmentation stability is very high for the boundaries-based scheme	✓ Complexity of the algorithm is very high due to the concept of the gradient calculation.

Segmentation-based on the concept of clustering [14-18, 20- 23, 33, 34, 36, 42]	Classify or create a cluster of an image's pixels into several regions or segments based on the centroid.	<ul> <li>✓ It is an iterative method that takes only a few seconds to segment a picture.</li> <li>✓ Furthermore, they are suited to an irregular picture and provide superior outcomes.</li> </ul>	segmentation performance is worst.  ✓ The number of clusters and their unsupervised position is not fixed due to the
Hybrid-based [17-20, 22, 40-41]	Based on the AI learning process and capable of handling problems related to decision-making.	<ul> <li>✓ There is no need to implement a difficult program.</li> <li>✓ Quicker than most</li> <li>✓ Particular model training is not mandatory</li> </ul>	1 1

The problem of tumor segmentation and classification is an active research area in brain tumors, along with some other medical imaging and machine learning. Some of the common challenges and issues faced by these models include:

**Limited training data:** Tumor segmentation and classification models require large amounts of high-quality training data to learn accurate representations of the tumors. However, obtaining such data is often challenging due to the limited availability of annotated medical images.

**Variability in tumor appearance:** Tumors can have varying shapes, sizes, and appearances, depending on the type of cancer and the stage of the disease. This variability makes it difficult for models to accurately detect and segment tumors.

False positives and false negatives: Tumor segmentation models can sometimes produce false positives (i.e., regions that are identified as tumors but are not actually tumors) or false negatives (i.e., regions that are not identified as tumors but are actually tumors). False positives can lead to unnecessary treatments, while false negatives can result in missed diagnoses and delayed treatments.

**Inter-observer variability:** Medical experts can have different interpretations of medical images, leading to inconsistencies in tumor annotations. This variability can make it challenging to create reliable ground truth annotations for training and evaluating segmentation and classification models.

Generalization to new data: Tumor segmentation and classification models trained on one dataset may not generalize well to new datasets with different characteristics. This issue can be addressed by using transfer learning or domain adaptation techniques to improve the model's ability to generalize to new data.

The purpose of this study is to develop an image-based tumor segmentation and classification system that is dependable and accurate. This system will be able to automatically recognize and classify various types of tumors, as well as their sizes and locations, based on pictures taken from medical scans of tumors. The accurate categorization of malignant pictures requires extensive work that may be accomplished using segmentation. The segmented component is then followed by the process of feature extraction, and then the classification architecture is followed after that. Sadly, the process of segmentation has not garnered a great deal of attention in this particular field. There are a few different segmentation methods that are described in the introductory section; however, these methods come with a number of constraints and difficulties in terms of processing. Furthermore, not every segmentation method is appropriate for each and every kind of picture. The algorithm has to be able to handle a wide variety of tumor types and imaging modalities while yet maintaining a high level of accuracy and reducing the number of false positives and negatives as much as possible. This statement explains the main aspects of the work, including the necessity to handle a range of tumor types and imaging modalities, the potential benefits for cancer diagnosis and therapy, and the precision and dependability required for image-based tumor segmentation and classification. In addition, it highlights how essential accuracy and a low rate of both false positives and negatives are to the efficacy of any method for dividing tumors into their many subtypes and classes. The inability to extract the most useful and relevant feature sets from the pictures or the location of the tumor is the primary contributor to the difficulties encountered by the tumor segmentation and classification system. Cuckoo Search Algorithm (CSA)-based Kmeans clustering is the finest for the segmentation of regions (according to the existing work), which is why there are so many different options available, such as ICA, Genetic Algorithm (GA), Ant Colony Optimization (ACO), and Particle Swarm Optimization (PSO). These can all help to reduce the likelihood of these kinds of issues occurring in the system. As a result of the characteristics of CSA, it is quite simple to exclude undesirable regions from the Region of Interest (ROI). This study effort uses swarm-based K-means clustering to separate the cancerous data and to extract the essential feature from that data. Pattern-based feature extraction using a deep learning algorithm is employed as a classifier. The performance metrics of the suggested job will be calculated at the very end of the system in order to check the work in terms of precision, recall, F-measure, error rate, accuracy, and execution time.

## 3.2 RESEARCH OBJECTIVES

The purpose of this study is to provide an artificial intelligence-based method that has been optimized for the segmentation and classification of brain tumors/cancers derived from MRI images. The following is a list of the objectives that have been established for this work:

- 1. To study and analyze the existing deep learning-based models for detection of brain cancer.
- 2. To preprocess and segment the brain cancer images from the identified dataset.
- 3. To develop a hybrid deep learning-based model using a metaheuristic approach for the detection of brain cancer.
- 4. To test and validate the developed model with the existing models.

# **CHAPTER 4**

# RESEARCH METHODOLOGY

This fragment explains the working strategy used to achieve the mentioned objectives of the model using the concept of deep learning as an artificial intelligence technique for the analysis of brain tumors. The problems of existing work and identified gaps are resolved in this research work by using an optimized segmentation technique to segment the exact region of the brain tumor from the MRI images, and then Artificial Intelligence (AI) is used to train the system based on the extracted feature of the segmented Region of Interest (ROI) of the MRI images. The ensuing stages show the assortment of phases that must be completed:

- **Step 1.**Firstly, design a framework using the concept of Graphical User Interface (GUI) for simulation of a proposed hybrid deep learning-based model using a metaheuristic approach for the detection of brain cancer, and the developed model is an optimized AI-based approach for segmentation and classification of brain tumor MRI images.
- **Step 2.**Upload training and testing images from the dataset of MRI images for the simulation purpose of the developed model.
- **Step 3.** Applying pre-processing to the uploaded MRI images to segment the tumor ROI data from the images by utilizing the concept of an unsupervised clustering-based segmentation approach with swarm-based metaheuristic techniques, and a comparative analysis is done to identify the effective algorithm for the proposed model.
- **Step 4.** Apply the concept of fitness of the meta-heuristic algorithm that is known as the objective function to minimize the unwanted or extraneous area from the ROI data.
- **Step 5.**Develop a code by utilizing the unlabeled pattern-based feature descriptors for feature extraction from the segmented ROI data.
- **Step 6.** Initialize the concept of AI as deep learning for cancer classification purposes in two different phases, namely, **1.** Training and **2.** Testing.
- **Step 7.** After the training of developed system, the testing phase is processed based on the saved trained structure to identify the kind of cancer from the used images.

- **Step 8.** In the testing phase of the model, the test images (which may be cancerous or non-cancerous) are uploaded, and the steps of the methodology from three to five are repeated. In the classification section, the test image feature is matched with the trained deep learning structure, and the result type is returned.
- **Step 9.** After the simulation model efficiency is validated on the basis of the Quantitively Parameters like Precision, Recall, F-Measure, Error Rate, Accuracy and Execution Time and the flowchart of the proposed model is shown in Figure 4.1.

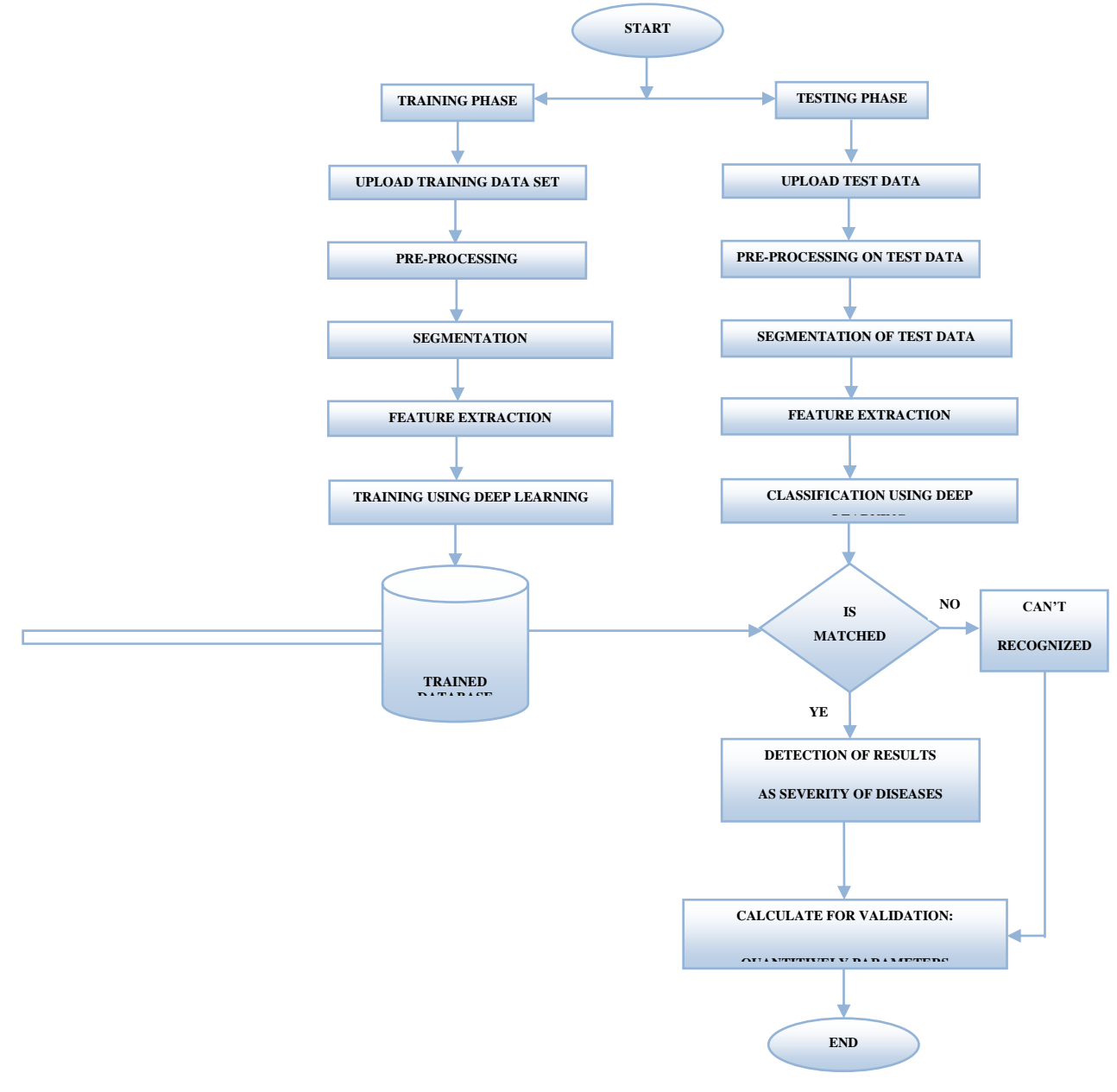


Figure 4.1: Flowchart of Proposed Work

Based on the mentioned flowchart of the proposed model, the entire model is segregated into two different phases; that is why in this research there are two frameworks designed:

- 1. Framework of Brain Tumor Segmentation
- 2. Framework of Brain Tumor Classification

In the below section, both frameworks are explained with the steps used for development and their algorithms.

#### 4.1 FRAMEWORK OF BRAIN TUMOR SEGMENTATION

According to the study, detection of tumors at an early stage is a beneficial way to protect human lives, and the motivation behind undertaking this study is rooted in the critical need for advancements in medical imaging technology to enhance the diagnosis and treatment of brain tumors. Brain tumors pose significant challenges to healthcare, with their complexity and diverse characteristics requiring precise and efficient segmentation techniques for accurate analysis. Current medical research has made remarkable strides in the understanding of brain tumors, and MRI has become a cornerstone in their detection. Nevertheless, the process of dividing these tumors into segments continues to be a difficult undertaking, frequently susceptible to mistakes and imprecisions. This study aims to confront these challenges directly by investigating and contrasting enhanced clustering mechanisms through the application of swarm-based methodologies, including Particle Swarm Optimization (PSO), Artificial Bee Colony (ABC), Firefly Algorithm (FFA), Cuckoo Search Algorithm (CSA), and Moth-Flame Optimization (MFO). While all these swarm-based techniques are adept at optimization, MFO was selected as the primary metaheuristic for this thesis due to its distinct advantages in balancing exploration and exploitation. Unlike PSO, which can sometimes converge prematurely to a local optimum, MFO's mechanism, where moths update their position relative to flames (the best solutions found so far), provides a more robust global search capability. The number of flames is adaptively decreased over iterations, which systematically shifts the algorithm's focus from exploration (searching broadly for new solutions) to exploitation (refining the best-known solutions). This adaptive mechanism is particularly well-suited for the complex and high-dimensional search space of medical image segmentation and feature selection, reducing the risk of pixel mixing and optimizing cluster centroids more effectively than other swarm methods. This research seeks to

uncover and optimize clustering mechanisms by a comparative examination of current segmentation methods, thereby considerably improving the accuracy and efficiency of MRI-based brain tumor segmentation. This optimization's potential influence transcends research facilities, extending into clinical settings and providing healthcare practitioners with a more dependable tool for the early detection and diagnosis of tumors. The pursuit of an enhanced segmentation approach transcends academic interest; it aims to elevate patient outcomes and advance the progression of medical procedures. This project aims to catalyze positive change in neuroimaging and brain tumor detection within the context of essential medical innovation. The major contributions are listed as those that are used in the development of the relative analysis:

- 1. To detect and segment the Region of tumor (ROT) from MRI data, a comparative analysis is performed for Fuzzy C-means (FCM) and K-means with a swarm-based optimization method that is presented in Figure 42.
- 2. To validate and find out the best approach, performance parameters are calculated and compared in terms of Sensitivity, Precision, F1-score, Mathew Correlation Coefficient (MCC), Dice, Jaccard, Specificity, Accuracy, and Time.

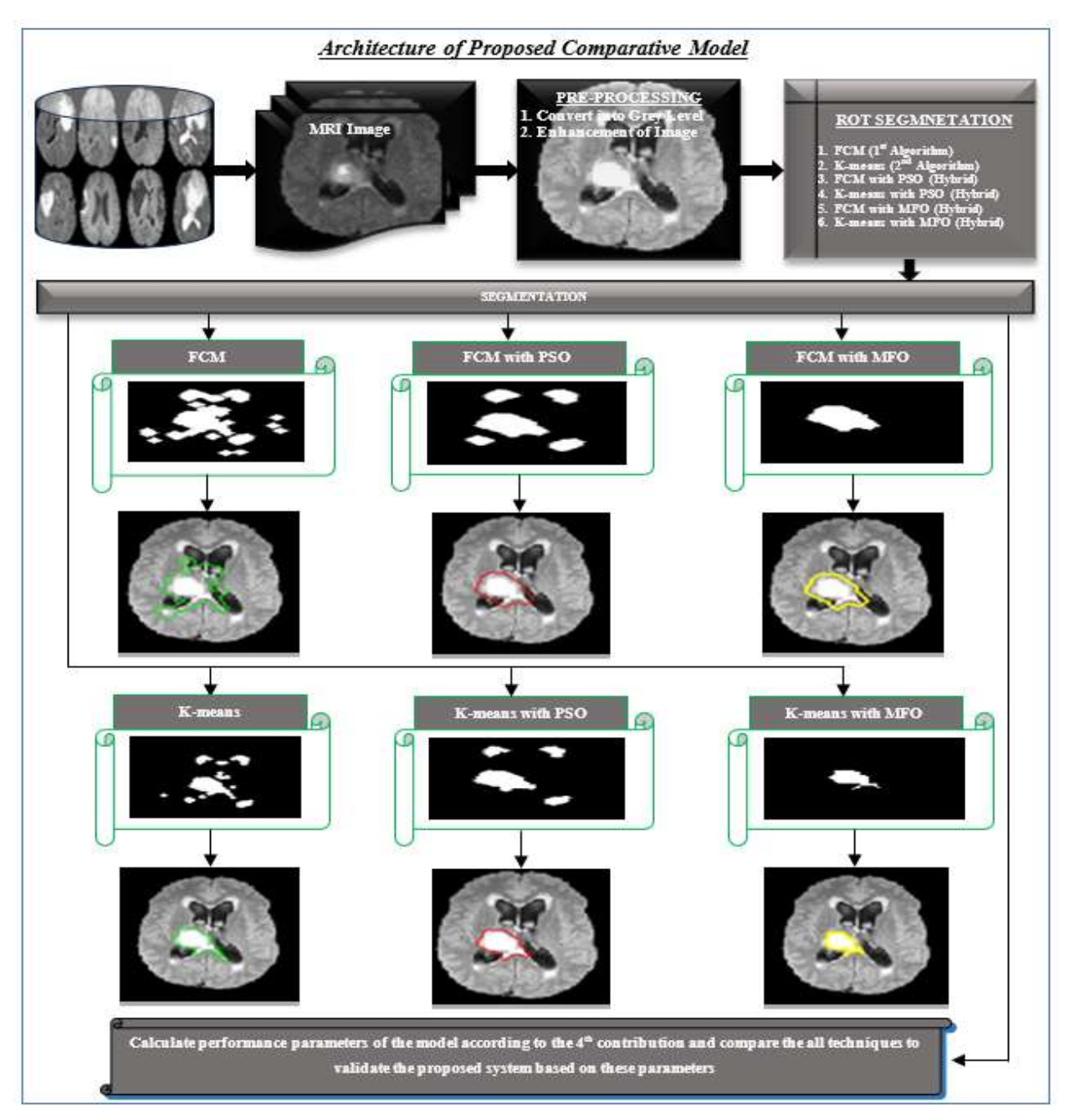


Figure 4.2: Architecture of Proposed Comparative Model

The proposed comparative model's block strategy is depicted in Figure 4.2. Essentially, describe a comparative brain tumor segmentation model using clustering-based methods and their hybridization with swarm-based optimization approaches to improve the efficiency of segmentation techniques. In this study, two distinct scenarios—one using the hybridization of K-means with PSO and MFO and the other involving the hybridization of FCM with PSO and MFO—were used. This section of the thesis describes the proposed comparative system for brain

tumor segmentation from MRI data using different approaches and their hybridization. In this research, we compare classic and enhanced segmentation methods for ROT segmentation from brain MRI data. Here, introduced a comparative scheme using six scenarios:

#### **4.1.1 FCM-based ROT Segmentation**

This suggested system uses FCM for unsupervised clustering-based segmentation of ROT from MRI data. FCM assigns each image pixel to numerous clusters with varying degrees of membership for soft assignments. This soft assignment allows brain tumor segmentation to better depict tissue properties by reflecting medical picture uncertainty and ambiguity. Based on this architecture, FCM creates two parts of an MRI picture: a background and a foreground component, which is the ROT because FCM's capacity to detect tiny gradients and pixel brightness helps it define tumor boundaries. This helps clinicians plan and track treatment by accurately localizing and delineating tumor locations. We apply some pre-processing stages in all six scenarios, starting with MRI image-like color conversion (if needed) using equation 1 and image quality enhancement using algorithm 1 with the help of equations 2 and 3.

$$MRI_{Grevimage} = 0.299 \times I(:,:,1) + 0.587 \times I(:,:,2) + 0.114 \times I(:,:,3)$$
 (1)

Where, MRI Grey image is the grey MRI that is attained after the conversion based on the clipped region of the MRI for quality enhancement. Here, the red component of the image is represented as I(:,:,1), the green as I(:,:,2), and the blue as I(:,:,3). At last, to calculate the usual number of pixels in MRI described by the equation 2, which helps to improve the image quality and makes the tumor portion visible.

$$P_{AVG} = \frac{P_{(region-x\_axis)} \times P_{(region-x\_axis)}}{MRI_{Grey\ image}}$$
 (2)

Equation 2 determines the MRI picture pixel average, where  $P_{(region-x\_axis)}$  represents the number of image pixels along the x-axis in a clipped region of the image ( $P_{CLIP}$ ). The clip limit ( $P_{CL}$ ) of MRI image enhancement is computed using equation 3, and then the procedure is used to enhance the image.

	Algorithm 1: MRI Enhancement
<b>Input:</b> MRI Images □ MRI	

**Output:** Enhanced Data of MRI 

EMRI A. Start MRI Enhancement **B.** Load the MRI **C.** Calculate size of MRI image = [Row, Col., and D] **D.** Set clip limit,  $P_{CL} = P_{CLIP} - P_{AVERAGE}$ E. If D>1 F. MRI R = Red Part of MRIG. MRI\_G = Green Part of MRI H. MRI\_B = Blue Part of MRI I. For I, according to Clip Limit J.  $R = Intensity (MRI_R, P_{CL})$ K.  $G = Intensity (MRI\_G, P_{CL})$ L.  $B = Intensity (MRI_B, P_{CL})$ Μ. End—For N. EMRI Image = cat (3, Red, Green, Blue) O. Else **P.** For I, according to Clip Limit Q. EMRI = Intensity (MRI (I), P<sub>CL</sub>) R. End—For S. End If T. Return: EMRI as an Enhanced MRI image

Here, segregate brain tumors from MRI images as foregrounds after the MRI enhancement process. It contains tumor pixels and excess pixels from the split part's background. The suggested system with the FCM algorithm is

U. End—Algorithm

# Algorithm 2: FCM-based Segmentation Input: Enhanced Data of MRI $\square$ EMRI Output: Background and Foreground of MRI in terms of ROT $\square$ B-MRI and ROT A. Start FCM-based Segmentation B. Initialize a group for segmentation (G = 2)

```
C. EMRI Size = [Row, Col, Plane]
```

**D.** A predetermined number of clusters, C = C1 and C2 // Where C1 for B-MRI and C2 for ROT

**E.** ITR = N is set for iterations.

# F. While I TR $\neq$ N (if max imu m iteration is not ac hieved)

G. For m according to Row

I. If M-Image 
$$[m, n] == C1$$

**J.** B-MRI 
$$[m, n] = EMRI [m, n]$$

**L.** ROT 
$$[m, n] = EMRI [m, n]$$

$$M.$$
 End – If

N. Adjust Centroid C during segmentation using given equation

**O.** 
$$C_{mn} = (\sum_{1}^{n} [C1, C2](\gamma_{G}^{m} * \chi_{G}) / \sum_{1}^{n} C1, C2]\gamma_{G}^{m}$$

P. Repeat and define membership function given equation

$$\mathbf{Q} \cdot [C1, C2] = \sum_{1}^{n} (d_{Gm}^{2}/d_{Gn}^{2})^{1/m-1}]^{-1}$$

R. End – For

S. End – For

T. End – While

U. Return: B-MRI and ROT as a segmented MRI background and foreground

V. End – Algorithm

For the FCM-based segmentation, we use this technique to segment the ROT from MRI images.

#### **4.1.2** K-means-based ROT Segmentation

In the second scenario of the suggested model, employed K-means instead of FCM because it yields superior segmentation results. K-means can segment more appropriate tumor regions from MRI scans, but poor contrast images can cause mix-ups, so it cannot always produce better segmentation results. Since it is an unsupervised clustering method, it can divide input MRI image pixels into numerous clusters based on pixel intensity levels. Large datasets and real-time applications benefit from K-means' computational efficiency over Fuzzy C-means. K-means simplicity permits faster convergence, which is important in clinical settings where speedy decision-making is needed. K-means creates clusters with well-defined borders, improving

segmentation interpretation. This trait is useful for clinical decision-making when tumor and healthy tissue must be distinguished. The suggested algorithm for K-means-based ROT segmentation is written as:

#### **Algorithm 3: K-means-based Segmentation**

**Input:** Enhanced Data of MRI □ EMRI

**Output:** Background and Foreground of MRI in terms of ROT  $\square$  B-MRI and ROT

- A. Start K-means-based Segmentation
- **B.** Initialize a group for segmentation (G = 2)
- **C.** EMRI Size = [Row, Col, Plane]
- **D.** A predetermined number of clusters, C = C1 and C2 // Where C1 for B-MRI and C2 for ROT
- **E.** ITR = N is set for iterations.
- F. While I  $TR \neq N$  (if max imu m iteration is not ac hieved)
- G. For m according to Row
- H. For n according to Col
- I. If EMRI [m, n] == C1
- **J.** B-MRI [m, n] = EMRI [m, n]
- K. Else Default == C2
- **L.** ROT(m, n) = EMRI[m, n]
- M. End If
- N. Adjust Centroid C using their mean
- **O.** C = Average (B-MRI, ROT) using the given equation
- **P.**  $C_{mn} = \sum_{m=1}^{Row} \sum_{n=1}^{Col} \frac{c1_{mn} + mr}{2}$
- Q. End For
- R. End For
- S. End While
- T. Return: B-MRI and ROT as a segmented MRI background and foreground
- U. End Algorithm

The K-means algorithm in the article produced better segmented results than the FCM-based model.

#### **4.1.3** FCM with PSO-based ROT Segmentation

This situation works like FCM; however, it employs PSO as a hybrid segmentation algorithm. PSO is the basic metaheuristic swarm-based strategy that uses fitness to tackle segmentation mix-up. PSO was developed by *Eberhart and Kennedy* for evolutionary image segmentation. The algorithm can traverse over the search space and track coordinates with a fitness solution to solve unsupervised FCM clustering to improve MRI image segmentation. The FCM method utilizing PSO-based ROT segmentation is stated as follows:

#### **Algorithm 4: FCM with PSO-based Segmentation**

**Input:** Enhanced Data of MRI □ EMRI

**Output:** Background and Foreground of MRI in terms of ROT  $\square$  B-MRI and ROT

- A. Start FCM with PSO-based Segmentation
- **B.** Size in terms of T = Size (EMRI)
- **C.** Define fitness function:
- **D.**  $fit(fun) = \{1 \text{ if pixel is less } 0 \text{ otherwise } \}$
- E. For l, according to T
- **F.** fs = EMRI(l)
- **G.**  $ft = \frac{\sum_{i=1}^{Pixels} EMRI(l)}{Length \ of \ EMRI \ Pixels}$
- **H.** fit(fun) = A/c to equation
- I.  $T_{value} = PSO(P,T,LB,UB,N,fit(fun))$
- **J.** Where, Lower Bound (LB), Upper Bound (UB), Number of selection (N)
- K. End-For
- **L.** Set OITR = N // optimization iterations
- M. While  $0 I TR \neq N$  (if not reac hed max iteration)
- **N.** Threshold = Threshold<sub>value</sub>
- **O.** Mask Image = Binary (ROT, Threshold)
- **P.** Boundaries = Find out boundary (Mask Image)
- **Q.** ROT = Boundaries
- R. For k, according to D
- **S.**  $ROT = EMRI \times ROT$

- T. End-For
- U. Return: B-MRI and ROT as a segmented MRI background and foreground
- V. End Algorithm

Better segmented results were obtained using the hybrid segmentation algorithm in the suggested model, which combines FCM and PSO, than using only FCM in the ROT segmentation model.

# 4.1.4 K-means with PSO-based ROT Segmentation

This scenario works like K-means; however, applied PSO to hybridize K-means for segmentation, and the algorithm of K-means with PSO-based ROT segmentation is written as:

# **Algorithm 5: K-means with PSO-based Segmentation**

**Input:** Enhanced Data of MRI □ EMRI

**Output:** Background and Foreground of MRI in terms of ROT 

B-MRI and ROT

- A. Start K-means + PSO-based Segmentation
- **B.** Size in terms of T = Size (EMRI)
- **C.** Define fitness function:
- **D.**  $fit(fun) = \{1 \text{ if pixel is less } 0 \text{ otherwise } \}$
- E. For l, according to T
- $\mathbf{F.} \qquad fs = EMRI(l)$
- **G.**  $ft = \frac{\sum_{i=1}^{Pixels} EMRI(l)}{Length of EMRI Pixels}$
- **H.** fit(fun) = A/c to equation
- I.  $T_{value} = PSO(P,T,LB,UB,N,fit(fun))$
- **J.** Where, Lower Bound (LB), Upper Bound (UB), Number of selection (N)
- K. End For
- **L.** Set OITR = N // optimization iterations
- M. While  $0 I TR \neq N$  (if not reac hed max iteration)
- **N.** Threshold = Threshold<sub>value</sub>
- **O.** Mask Image = Binary (ROT, Threshold)
- **P.** Boundaries = Find out boundary (Mask Image)
- **Q.** ROT = Boundaries

- R. For k, according to D
- **S.**  $ROT = EMRI \times ROT$
- T. End For
- U. Return: B-MRI and ROT as a segmented MRI background and foreground
- V. End Algorithm

Better segmented results were obtained by the hybrid segmentation approach in the suggested system, which combined K-means with PSO, than by either the FCM with PSO-based ROT segmentation model or solely K-means-based ROT segmentation.

#### **4.1.5** FCM with MFO-based ROT Segmentation:

In this scenario, MFO is hybridized with FCM. As justified in Section 4.1, MFO's adaptive exploration and exploitation mechanism is employed here to optimize the clustering process. MFO with an optimal and innovative fitness function solves the FCM separation or pixel mix-up problem during the ROT segmentation. MFO is a swarm-based bio-inspired metaheuristic algorithm inspired by moth (insect) behavior that searches for pixels that mix together during segmentation and separates those pixels using morphological operations. The algorithm of FCM with MFO-based ROT segmentation in the ASBT system is written as:

#### **Algorithm 6: FCM with MFO-based Segmentation**

**Input:** Enhanced Data of MRI □ EMRI

**Output:** Background and Foreground of MRI in terms of ROT  $\square$  B-MRI and ROT

- A. Start FCM + MFO-based Segmentation
- **B.** Apply K-means segmentation on EMRI
- C. To optimized the ROT, MFO is used on FCM output
- **D. Set up basic parameters of MFO:** Population of Moth (P<sub>M</sub>)—Pixel count in EMRI
- **E.** Define position function:

**F.** 
$$v(r) = v_0 \times exp(-distance^m)$$
, if  $m \ge 1$ 

- **G. Where** distance = distance between moth and light
- **H.**  $\mathbf{\nu}_0$  = initial velocity at d=0
- **I.** m = Position of Moth (P<sub>M</sub>)
- **J.** Define novel fitness function:

 $\mathbf{K.} fun(fit) = \{1; if EMRI pixel < \}$ 

Threshold<sub>Pixel</sub> 0;

Otherwise

L. Set, ROT and B-MRI = []

M. For m according to Row

N. For n according to Col

 $\mathbf{O.} \qquad \mathbf{C_{M}} = \mathbf{EMRI} \ (\mathbf{m}, \ \mathbf{n})$ 

**P.**  $M_G = \sum_{1}^{m} \sum_{1}^{n} \frac{EMRI(m,n)}{m \times n}$ 

**Q.** Threshold = MFO (fun (fit),  $C_M$ ,  $M_M$ )

R. End - For

S. End – For

T. If EMRI (Pixels) > Threshold

 $\mathbf{U}$ . ROT = EMRI

V. Else

W. B-MRI = EMRI

X. End - If

**Y.** Set OITR = N // optimization iterations

Z. While 0 I TR  $\neq$  N (if not reac hed max iteration)

**AA.** Mask Image = Binary (ROT, Threshold)

**BB.** Boundaries = Find out boundary (Mask Image)

**CC.** ROT = Boundaries

DD. For k according to D

**EE.** ROT = EMRI  $\times$  ROI

FF. End – For

**GG. Return:** B-MRI and ROT as a segmented MRI background and foreground

HH. End - Algorithm

With the help of the above-mentioned hybrid segmentation algorithm using FCM with MFO-based ROT segmentation, we achieve better results, but the combination with K-means outperforms it, as is shown in the next section of the article.

#### 4.1.6 K-means with MFO-based ROT Segmentation

This is the last scenario of the proposed comparative system and uses K-means with MFO as a hybrid segmentation technique with a novel fitness function defined in equation 8. The algorithm of K-means with MFO-based ROT segmentation is similar to Algorithm 6; here, only the K-means output is used instead of the FCM output. Figure 4.3 displays the segmented result alongside the original pictures, obtained using the aforementioned suggested hybrid algorithm that combines K-means with MFO as an optimization strategy. This method outperforms other cases when it comes to accurately segmenting the tumor region from MRI scans.

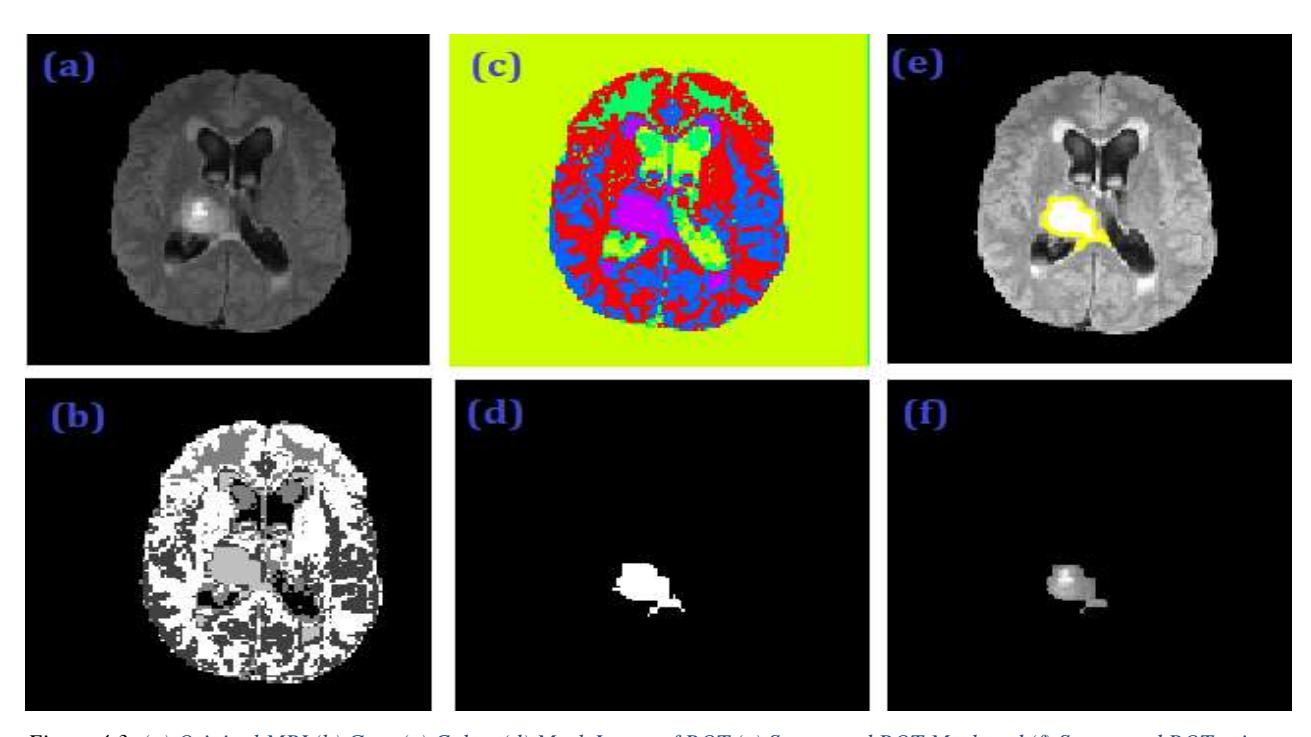


Figure 4.3: (a) Original MRI (b) Grey (c) Color, (d) Mask Image of ROT (e) Segmented ROT Mask and (f) Segmented ROT using K-means with MFO with Maximum Accuracy

Last but not least, the simulation compares the six scenarios described in the study article with respect to the following performance metrics: Accuracy, Sensitivity, F-measure, Precision, MCC, Dice, Jaccard, Specificity, and Time Complexity. In order to evaluate the efficacy of segmentation algorithms in precisely outlining tumor locations, it is essential to evaluate parameters during brain tumor segmentation. There is a distinct function for each of the aforementioned parameters in assessing various parts of the segmentation outcomes. The findings of the experiment and the segmentation of brain tumors utilizing the aforementioned hybrid segmentation approach are

detailed in the following portion of this research article using a few sample MRI images. Figure 4.4 displays the list of sample MRI images that were used from the MRI Benchmark Dataset. The dataset comprises a comprehensive collection of 3064 brain MRI slices, obtained from two distinct hospitals in China: Nanfang Hospital and General Hospital, Tianjin. The scans were gathered between 2005 and 2010. This dataset comprises three distinct types of brain tumors, namely meningioma, glioma, and pituitary tumor. The collection has a total of 708, 1426, and 930 photos for each corresponding tumor type. Essentially, meningioma and glioma are classified as malignant or cancerous, while pituitary tumors are considered benign or non-cancerous. A total of 233 individuals underwent MRI scans, resulting in the acquisition of 1025 sagittal pictures, 994 axial images, and 1045 coronal images.

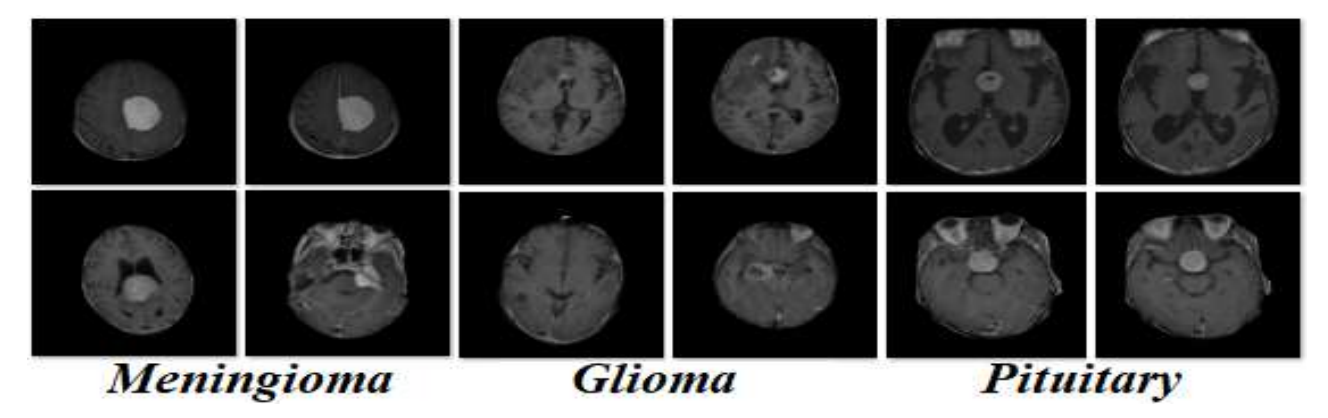
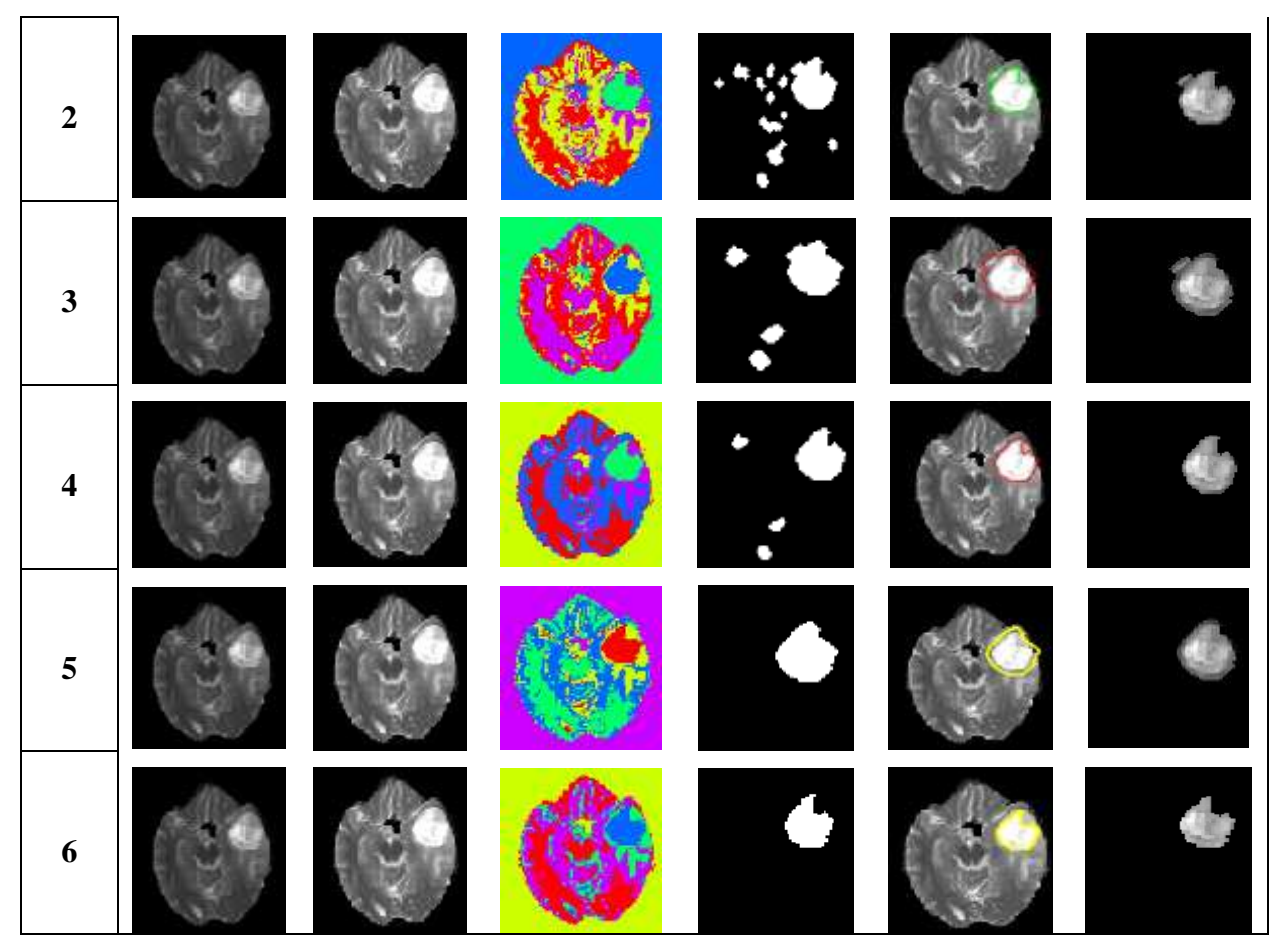


Figure 4.4: Sample of Brain MRI Images with Types from Dataset

The only hope is that by comparing previous studies on ROT segmentation from MRI, we can improve the methods and ultimately get better results when analyzing various proposed approaches. Table 4.1, which includes the source images, describes the simulation results of the suggested comparative models and helps to understand the effects of optimization approaches.

Table 4.1 Brain Tumour Segmentation Comparison

Model	Original MRI	iginal MRI Preprocessed Segmented Images				
	Images	MRI Images	Labelled	Mask	Region	Tumour
1				****		**



The suggested comparison model of brain tumor segmentation employing the hybridization of traditional segmentation approaches with the swarm-based metaheuristic algorithms was tested on the aforementioned dataset of sample MRI images. After the segmentation of the ROT from MRI images, the next section of the model is designed for further processing by utilizing the different steps like feature extraction, feature selection, and then model training and testing of the developed model with the mentioned standard dataset.

#### 4.2 FRAMEWORK OF BRAIN TUMOR CLASSIFICATION

The prior model seeks to address these challenges by examining and comparing advanced clustering techniques via MFO, a swarm-based method, for precise Brain Tumor Region (BTR) segmentation, and subsequently developing a Hybrid Model for Brain Tumor Analysis (BTA) utilizing Convolutional Neural Network (CNN) as an innovative deep learning strategy. In prior research, comparing various swarm-based metaheuristic algorithms identified MFO as the superior strategy in conjunction with K-means clustering for segmenting BTR from MRI images. This

section introduces a hybrid BTA model that employs K-means clustering, MFO, and CNN for brain tumor segmentation and classification into several categories based on the dataset. The primary objective is to identify the BTR from the MRI and classify it as benign or malignant. The proposed BTA model consists of the following key components for simulating and evaluating efficiency: selection of an MRI benchmark dataset, pre-processing of MRI images, hybridization for BTR segmentation, feature extraction, feature selection, and training/classification utilizing CNN. Figure 4.5 displays the flowchart of the proposed BTA model in detailed steps.

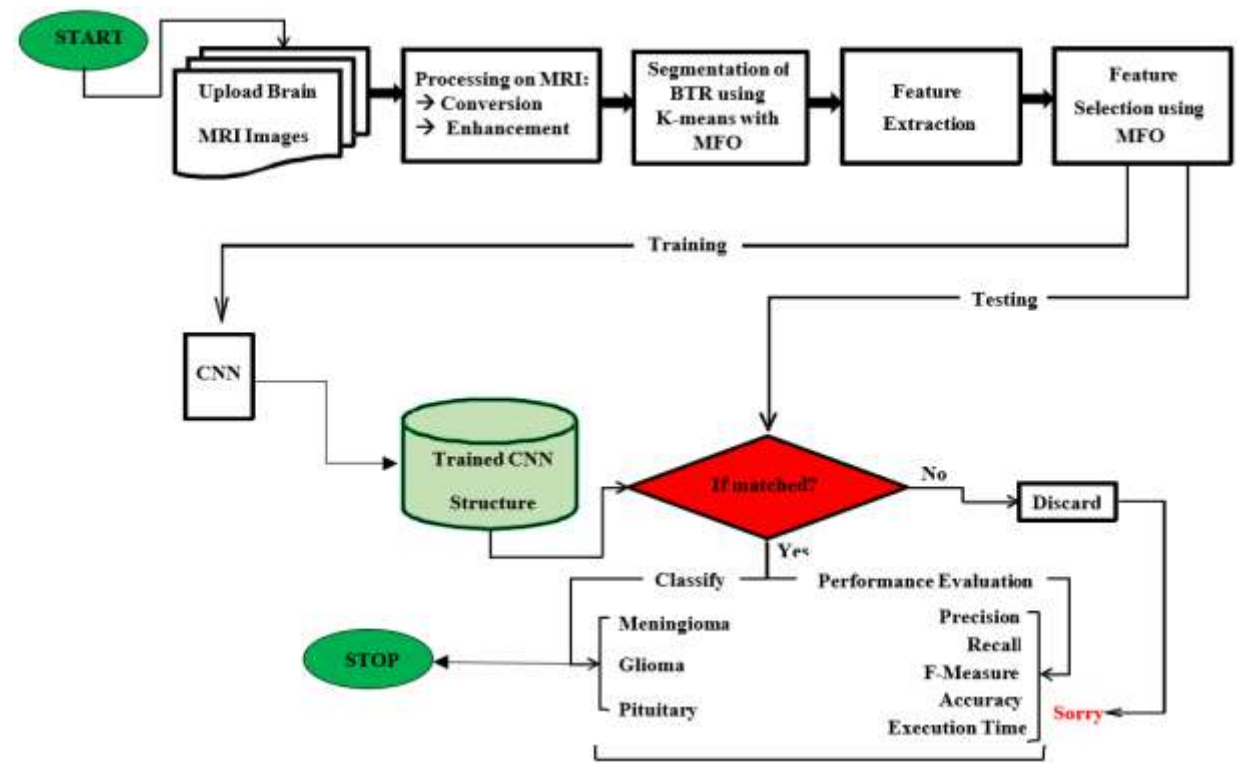


Figure 4.5: Flowchart of Proposed BTA Model

The BTA model flowchart demonstrates that the operational principle of the proposed model consists of four stages: pre-processing, segmentation employing the K-means clustering algorithm enhanced by MFO for superior segmentation of BTR, name-based feature extraction, and feature selection utilizing the MFO method. An additional phase is incorporated, designated as CNN-based BTA model training and tumor classification into the several specified categories shown in Figure 4.6.

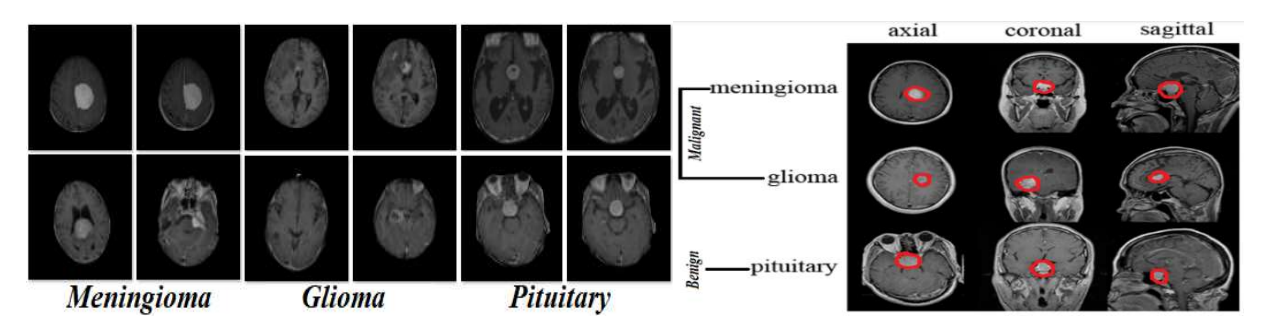


Figure 4.6: Sample of Brain MRI Images with Types from Dataset

The dataset comprises 3,064 brain MRI slices acquired from Nanfang Hospital and General Hospital in Tianjin, China, during the period from 2005 to 2010. This dataset has three categories of brain tumors: meningioma (708 photographs), glioma (1,426 images), and pituitary tumor (930 images). Meningiomas and gliomas are classified as malignant, whereas pituitary tumors are designated as benign. The MRI scans were obtained in three anatomical planes: sagittal (1,025 images), axial (994 images), and coronal (1,045 images), derived from 233 subjects. Figure 4.6 displays samples of several tumor types spanning these planes, with the regions of Interest (ROI) for brain tumors delineated by bold red lines. The figure presents a compilation of sample MRI images sourced from the MRI Benchmark Dataset, which will undergo further processing, commencing with pre-processing in the initial stage.

#### 4.2.1 MRI Pre-processing

The design of the BTA model is a fundamental step undertaken to enhance MRI picture quality for subsequent processing. To improve MRI picture quality, we employ an intensity-based image enhancement approach with constrained adaptation. The concept of limit is employed to establish a range for enhancing the contrast and intensity of each pixel in the image, as delineated by Equation 3.

$$E_{MRI} = (MRI - MRI_{I_L}) \frac{MRI_{I_H} - MRI_{I_L}}{MRI_{I_H} - MRI_{I_L}} + MRI_{I_L}$$
 (3)

Examine an MRI image with a resolution of  $256 \times 256$  pixels, including a total of 'n' pixels. The image's intensity values are restricted within predefined maximum and lowest thresholds, influenced by limited clipping derived from the average pixel intensity. The mean (AVG) pixel count in the MRI image is represented by Equation 4.

$$P_{AVG} = \frac{P_{(region-xaxis)} \times P_{(region-xaxis)}}{GMRI_{Image}}$$
 (4)

Where  $P_{(region-xaxis)}$  signifies the number of pixels along the x-axis in a clipped region ( $P_{CLIP}$ ). The lower and higher intensity values of the MRI image are represented by MRI<sub>IL</sub> and MRI<sub>IH</sub> respectively. The applied pre-processing on the MRI image is illustrated in Figure 4.7.

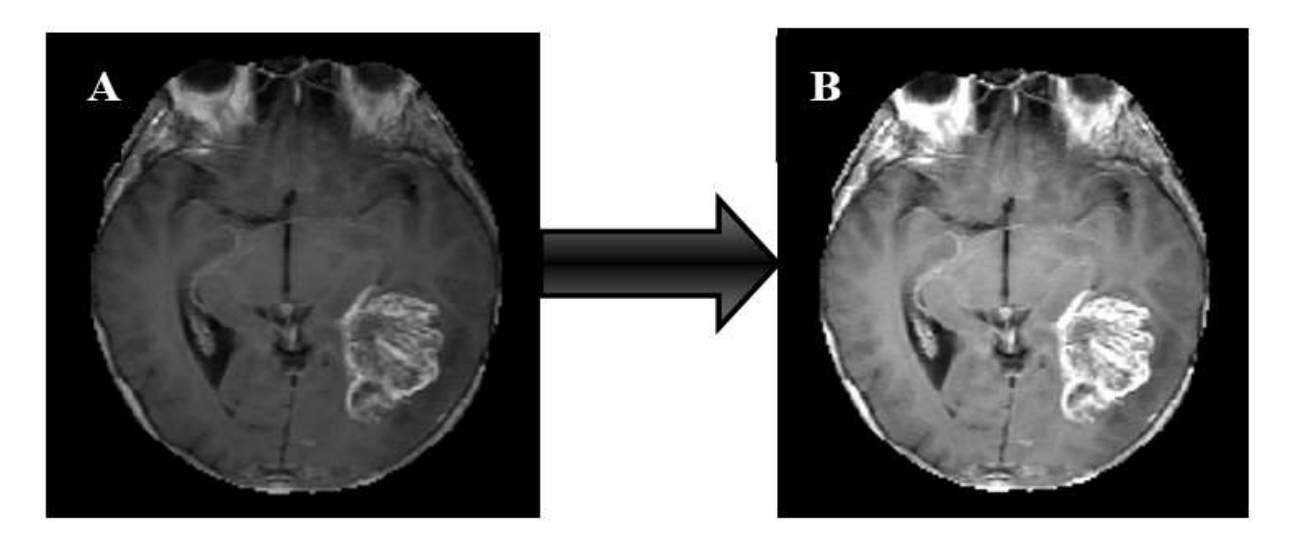


Figure 4.7: Pre-processing on Sample MRI

The graphic seems to depict a processing change in MRI scans, with image A as the original brain MRI and image B as the processed or enhanced version. This is an explanation derived from typical observations in such comparisons:

Image A (Left Side): This displays the unprocessed MRI image, with the tumor location discernible but not dramatically emphasized. The contrast and sharpness may be diminished, complicating the discernment of intricate details.

Image B (Right Side): This depicts the post-processed MRI image, featuring enhancements such as contrast correction, edge highlighting, or segmentation. The tumor site is more distinctly emphasized, possibly facilitating clearer identification and investigation. The pre-processing of MRI images occurs in two steps, with the initial stage involving color conversion as described by equation (3).

$$GMRI_{Image} = 0.299R + 0.587G + 0.114B$$
 (3)

GMRI<sub>Image</sub> refers to the grayscale MRI image acquired after the color conversion using the aforementioned equation, and in the subsequent step, MRI image enhancement is conducted, as

seen in Fig. 6. An intensity-based picture quality improvement is performed after the color conversion process using the restricted clipping idea. Pre-processing enhances the segmentation of tumor regions of interest from MRI images, and the algorithm is written as:

# Algorithm 7: MRI Enhancement

**Input:** MRI Images □ MRI

**Output:** Enhanced Data of MRI □ EMRI

#### V. Start MRI Enhancement

W. Load the MRI

**X.** Calculate size of MRI image = [Row, Col., and D]

**Y.** Set clip limit,  $P_{CL} = P_{CLIP} - P_{AVERAGE}$ 

**Z.** If **D**>1

**AA.**  $MRI_R = Red Part of MRI$ 

**BB.** MRI G = Green Part of MRI

**CC.**  $MRI_B = Blue Part of MRI$ 

DD. For I, according to Clip Limit

**EE.**  $R = Intensity (MRI_R, P_{CL})$ 

**FF.**  $G = Intensity (MRI\_G, P_{CL})$ 

**GG.**  $B = Intensity (MRI_B, P_{CL})$ 

HH. End – For

**II.** EMRI Image = cat (3, Red, Green, Blue)

J.J. Else

KK. For I, according to Clip Limit

**LL.** EMRI = Intensity (MRI (I),  $P_{CL}$ )

MM. End – For

NN. End—If

**OO. Return:** EMRI as an Enhanced MRI image

PP. End – Algorithm

#### 4.2.2 K-means with MFO-based BTR Segmentation

As established in the comparative analysis (Section 4.1), the combination of K-means and MFO yielded the best segmentation performance. Therefore, this hybrid approach is adopted for the classification framework. K-means is used for its computational efficiency and ability to create distinct cluster boundaries , while MFO is applied to optimize the segmentation and overcome issues of suboptimal image contrast. The suggested algorithm for K-means with MFO-based BTR segmentation is written as:

# **Algorithm 8: K-means with MFO-based Segmentation**

**Input:** Enhanced Data of MRI □ EMRI

**Output:** Background and Foreground of MRI in terms of BTR  $\square$  B-MRI and ROT

- V. Start K-means with MFO-based segmentation.
- **W.** Initialize a group for segmentation (G = 2)
- **X.** EMRI Size = [Row, Col, Plane]
- Y. A predetermined number of clusters, C = C1 and C2 // Where C1 for B-MRI and C2 for ROT
- **Z.** ITR = N is set for iterations.

#### AA.While I TR $\neq$ N (if max imu m iteration is not ac hieved)

- **BB.** For m according to Row
- CC. For n according to Col
- DD. If EMRI [m, n] == C1
- **EE.** B-MRI [m, n] = EMRI [m, n]
- FF. Else Default == C2
- **GG.** BTR (m, n) = EMRI[m, n]
- HH. End—If
- **II.** Adjust Centroid C using their mean
- **JJ.** C = Average (B-MRI, BTR) using the given equation

**KK.** 
$$C_{mn} = \sum_{m=1}^{Row} \sum_{n=1}^{Col} \frac{C1_{mn} + mn}{2}$$
(4)

LL. End – For

MM. End – For

#### NN.End - While

**OO.** To optimized the BTR, MFO is used on FCM output

**PP.** Set up basic parameters of MFO: Population of Moth (PM)—Pixel count in EMRI

**QQ.** Define position function:

$$\mathbf{RR.}\nu(r) = \nu_0 \times exp(-distance^m), \quad if \ m \ge 1$$
 (5)

**SS.** Where distance = distance between moth and light

**TT.**  $\nu$ 0 = initial velocity at d=0

UU.m = Position of Moth (PM)

**VV.** Define novel fitness function:

**WW.** 
$$fun(fit) = \{1; if EMRI pixel < \}$$

Threshold<sub>Pixel</sub> 
$$0$$
; Otherwise (6)

**XX.** Set, BTR, and B-MRI = []

#### YY.For m according to Row

#### **ZZ.** For n according to Col

**AAA.** 
$$CM = EMRI(m, n)$$

**BBB.** MG = 
$$\sum_{1}^{m} \sum_{1}^{n} \frac{EMRI(m,n)}{m \times n}$$

**(7)** 

**CCC.** Threshold = MFO (fun (fit), CM, MM)

DDD. End – For

EEE. End - For

FFF. If EMRI (Pixels) > Threshold

**GGG.** BTR = EMRI

HHH. Else

**III.** B-MRI = EMRI

JJJ.End - If

**KKK.** Set OITR = N // optimization iterations

#### LLL. While $0 I TR \neq N$ (if not reac hed max iteration)

**MMM.** Mask Image = Binary (BTR, Threshold)

**NNN.** Boundaries = Find out boundary (Mask Image)

**OOO.** BTR = Boundaries

#### PPP. For k, according to D

**QQQ.** BTR = EMRI  $\times$  BTR

RRR. End-For

SSS. Return: B-MRI and BTR as a segmented MRI background and foreground

TTT. End – Algorithm

The suggested comparison model of brain tumor segmentation employing the hybridization of traditional segmentation approaches with the swarm-based metaheuristic algorithms was tested on the aforementioned dataset of sample MRI images. In the below Figure 4.8, a comparative result is shown that indicates the importance of MFO for the BTR extraction from MRI images with the K-means clustering algorithm.

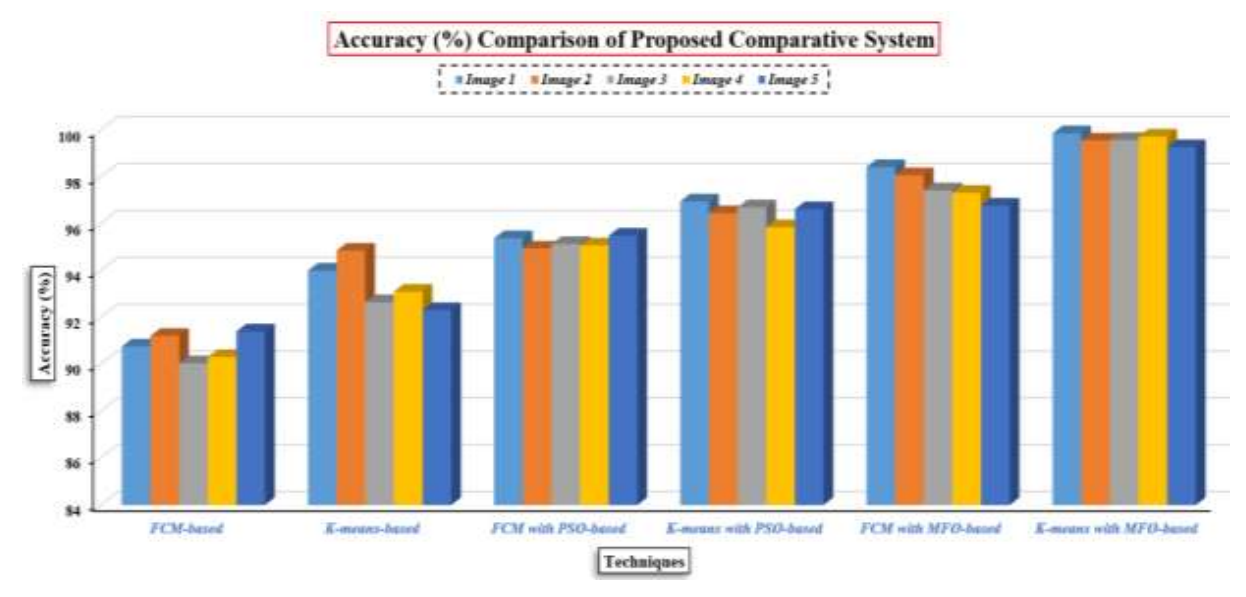


Figure 4.8: Accuracy (%) Comparison of Proposed Comparative System

Figure 4.8 illustrates the accuracies attained by several models in segmenting the precise BTR from the MRI data. The image clearly demonstrates that the accuracy of the K-means model enhanced by MFO far surpasses that of other models, achieving an average accuracy of 99.6% for segmentation based on ground truth data. This is the rationale for employing this idea in conjunction with our suggested BTA model for tumor classification. This study proceeds with a part presenting the results of the proposed model's simulations regarding categorization using feature extraction.

#### 4.2.3 Feature Extraction from BTR

Following BTR segmentation, it is crucial to extract feature patterns from the pixel distribution utilizing a feature descriptor. The name-based descriptor is chosen as the feature extraction method because of its stability and invariance characteristics. It offers a more precise and dependable feature set for the delineated Region of Interest (ROI). The suggested descriptor is a rapid and resilient approach that efficiently extracts local, invariant, and orientation-specific feature sets from the region of interest in medical pictures. The algorithm for the proposed descriptor is described as follows:

# Algorithm 9: Named Feature Extraction Input: BTR □ Brain tumor region from MRI images

Output: F-set □ Feature set from BTR

- A. Start feature extraction
- **B.** [Row, Column, Plane] = Size(BTR)
- C. For M, according to Row
- D. For N, according to Column
- **E.** F-set = ROI [Centroid Extent Area Eccentricity, Orientation, Perimeter Max-Intensity Mean-Intensity Min-Intensity, Contrast, Correlation, Energy, Homogeneity, Mean, Standard-Deviation, Entropy, RMS, Variance, Smoothness, Kurtosis, Skewness, IDM]
- $\mathbf{F}$ .  $\mathbf{End} \mathbf{For}$
- G. End For
- **H. Return:** F-set as a feature pattern of BTR
- I. End Algorithm

Subsequent to the extraction of feature patterns from the BTR, the MFO algorithm is utilized for feature selection. The selection procedure is directed by a fitness function to determine the most pertinent and substantial traits for subsequent analysis.

#### 4.2.4 MFO-based Feature Selection

This phase is crucial for improving the classification accuracy and computational efficiency of the proposed BTA model. The feature set (F-set) extracted in the previous step contains numerous

attributes, many of which may be redundant or irrelevant, leading to the 'curse of dimensionality' and potential model overfitting. To address this, MFO is employed as a feature selection wrapper. Its strong global search capabilities are used to explore the vast combination of features, identifying the optimal subset that maximizes classification accuracy (as defined by the fitness function) while minimizing redundancy. This ensures that only the most discriminative features are passed to the CNN classifier. The procedure for using MFO in feature selection is delineated as follows:

#### **Algorithm 10: MFO-based Feature Selection**

**Input:** F-set □ Feature set from ROI

**Output:** OF-set  $\square$  Optimized feature set from ROI

- A. Start selection
- **B.** Initialize MFOO Parameters:
- $\mathbf{C}$ .  $\mathbf{G}$  Moth population based on the F-set
- **D.** GP Position of Moth
- **E.** OF-set—Optimized feature set
- F. Define fitness function using equation 8
- **G.**  $F(f) = \{1; if F_s * (Gp) \ge F_t = \}$

 $Threshold_{Data} 0$ ;

Otherwise

(8)

- **H.** Where,  $F_s$ : It is selected feature from the F-set
- **I.**  $F_t$ : It is average of the F-set.
- **J.** [Row, Column, Plane] = Size (F-set)
- K. For I according to (Row × Column)
- **L.** Fs = F-set(I)
- **M.** Ft =  $\frac{\sum_{i=1}^{R} F-set(I)}{Row \times Column}$
- **N.**  $Fit(fun) = Fit Fun (F_s, F_t)$
- O. OF-set (I) = MFO (Fit (fun), Set up of MFO)
- P. End-For
- Q. If OF-set = 1, then

- **R.** OF-set = Select feature form F-set
- S. Else
- **T.** OF-set = Null (Irrelevant features)
- U. End-If
- V. Return: OF-set as an optimized feature set
- W. End Algorithm

The MFO-based feature selection method determines an appropriate set of attributes pertinent to brain tumor classifications, such as meningioma, glioma, and pituitary tumors. After determining the optimal feature set, a CNN is employed as a classifier to train the model. Similarly, the CNN is employed for the accurate classification of tumor kinds.

#### 4.2.5 CNN-based BTA Model Training

This is the final stage of the procedure, in which a CNN serves as a deep learning classifier to train the BTA model for three tumor classifications: meningioma, glioma, and pituitary. The enhanced feature set functions as the input for the CNN, together with labels indicating the corresponding tumor types. This section provides a detailed explanation of the recommended training and classification approach utilizing CNN, which significantly enhances the brain tumor classification accuracy of the proposed BTA model. The CNN architecture, designated as BTA-Net, is seen in Figure 4.9.

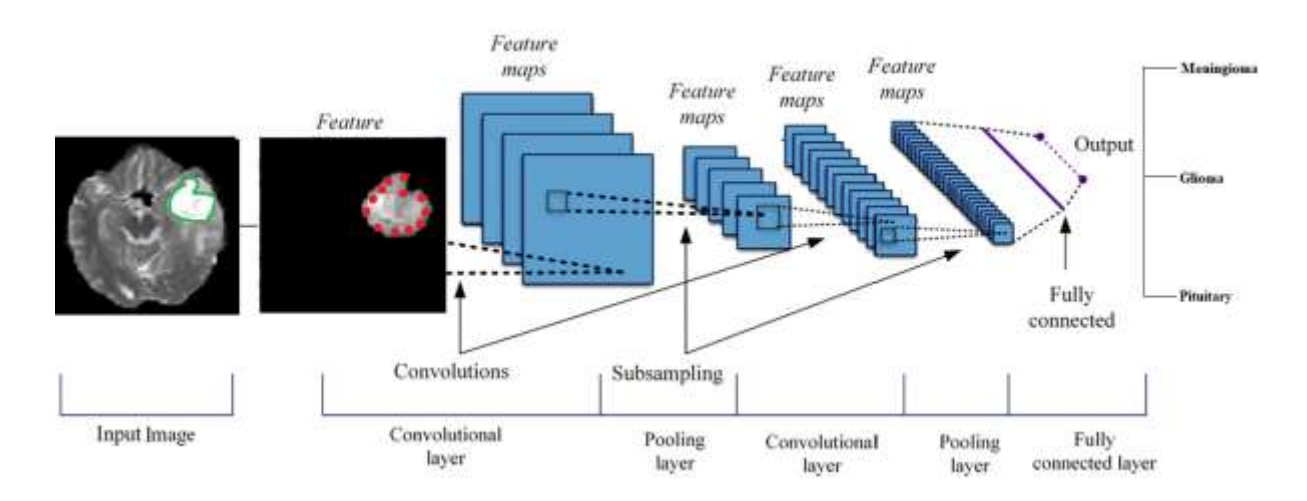


Figure 4.9: Architecture of Proposed BTA-Net

The BTA-Net architecture is founded on deep learning and represents a more advanced and complex version of traditional Artificial Neural Networks (ANNs). The BTA-Net architecture comprises an input layer, convolutional layers, pooling layers, and fully connected output layers, as seen in Figure 4.9. The BTA-Net algorithm is delineated as follows:

# Algorithm 11: BTA-Net Algorithm

**Input:** OF-set □ Optimized named feature set as training data for model  $G\square$ Type of brain tumors N□Neurons to carry the training data **Output:** BTA-Net  $\square$  CNN-trained structure Output □ Classified results in term of class A. Start training **B.** Initialize CNN: – Number of Epochs (E) // Iterations used by CNN C. - Number of Neurons (N) // Used as a carrier D. - Performance: Cross entropy of classes, Gradient, and Validation Ε. - Training Data Division: Based on Random [R, C, P] = Size (OF-set) // Row, Column, and Plane F. G. For I, according to  $(R \times C)$ H. If OF-set belongs to meningioma I. Type (1) = Feature from meningioma J. Else If OF-set belongs to glioma K. Type (2) = Feature from glioma L. Else (OF-set belongs pituitary) M. Type (3) = Feature from pituitary N. End – If O. End – For **P.** Initialized the CNN, BTA-Net = Pattern-based CNN (N) **Q.** I-BTSC net = Train (BTA-Net, OF-set, Type) **R.** Test Outcome = Sim (BTA-Net, Test MRI OF-set) S. If Test Outcome = 1 (Meningioma)

- **T.** Results = Meningioma with performance
- **U.** Else if Test Outcome = 2 (Glioma)
- **V.** Results = Glioma with performance
- **W.** Else if Test Outcome = 3 (Pituitary)
- **X.** Results = Pituitary with performance
- Y. Else
- **Z.** Results = Sorry, can't classify.
- AA.End-If
- BB. Return: BTA-Net as a trained structure with Results as a classified output of model

#### CC.End - Algorithm

The BTA-Net model enables the categorization of brain tumors for any designated MRI picture according to the training architecture. The BTA system is developed and implemented using the MATLAB programming language, using the Image Processing, Neural Network, and Optimization toolboxes. The following section of this study gives the experimental results and corresponding discussion to evaluate the effectiveness of the BTA system.

# **CHAPTER 5**

# **EXPERIMENTAL SETUP**

This section provides a detailed description of the experimental setting for the proposed frameworks—a hybrid deep learning-based model using a metaheuristic approach for the detection of brain cancer, including both Brain Tumour Segmentation and Brain Tumour Classification using Convolutional Neural Networks (CNNs). The experiments are conducted to assess the efficacy of the proposed model, using both conventional segmentation methods and swarm-based optimization strategies.

#### 5.1 INFORMATION ABOUT USED TOOLS

Some basic information regarding the used software (MATLAB 2016 or higher version) and hardware setups are necessary to implement the above-described methodology. First and foremost, the computer CPU must be Core 2 Duo or above with an HDD of 320 GB minimum, and the RAM must be 4 GB or greater. After that, check the operating system installed in the computer/laptop, and it should be Windows 7 or higher (64-bit only) for simulation. In addition, some basic equipment in the hardware section, such as a keyboard and mouse, is required for better experiences. MATLAB software is an interactive platform for research as well as numerical figuring and data visualization that is widely used by researchers in various reputed organization for research analysis and design. There are several toolboxes available in MATLAB as an inbuilt that cover the fundamental functionalities in various application areas. Apart from Windows, MATLAB software is also supported on UNIX and Macintosh platforms, and some information are also provided in Table 5.1.

Table 5.1 Experimental Setup for Proposed Model Simulation

Component	Description	Tool/Library
Operating System	The environment where the simulation	Windows 10 or 11, Linux, or
	will be executed.	macOS

Processor	The required processing power for computation.	Intel Core i3 or higher	
RAM	Memory is required for efficient computation and simulation.	8 GB or higher	
Other Hardware	Required hardware to simulate the model.  Keyboard, Mouse		
MATLAB Environment	Platform used for implementing the methodology.	MATLAB R2020a or higher	
IDE	Integrated Development Environment for coding and debugging.  MATLAB Editor, Tools		
Numerical	Toolbox for numerical calculations and	MATLAB base package,	
Computation	array manipulation.	Symbolic Math Toolbox	
Data ManipulationToolbox for handling and manipulating data.		MATLAB base package, Data Import and Export	
Visualization	Toolbox for data visualization and plotting.	MATLAB base package, Graphics	
Machine Learning	Toolbox for implementing and training machine learning models.	Statistics and Machine or Deep Learning Toolbox	
Optimization	Toolboxes for optimizing models and solutions.	Optimization Toolbox, Global Optimization Toolbox	

This table delineates the main components and libraries/toolboxes used in the MATLAB program for executing many tasks, including data processing, numerical calculation, machine learning, and visualization.

#### 5.2 LANGUAGE USED FOR IMPLEMENTATION

The suggested research study is implemented using the software named MATLAB 2020 or the latest version. It's a high-performance (high-level) programming language for doing technical calculations, and lots of minor functions or classes are built-in to support researchers. It integrates into a user-friendly environment where computing, visualisation, and programming problems are

handled and communicated in a clear and understandable manner. The execution of the suggested model is mostly conducted using MATLAB, a high-level programming language and interactive environment extensively used for numerical calculation, data analysis, and algorithm development. MATLAB has several built-in toolboxes and libraries tailored for machine learning, optimization, and data visualization, making it an optimal selection for system implementation. The primary justifications for using MATLAB for implementation encompass

- **Development Efficiency:** MATLAB's user-friendly syntax facilitates fast development and evaluation of methods.
- Toolbox Availability: MATLAB offers a comprehensive selection of toolboxes, including the Statistics and Machine Learning Toolbox, Optimization Toolbox, and Deep Learning Toolbox, which considerably diminish development time.
- **Visualization:** MATLAB's comprehensive built-in visualization capabilities enable straightforward charting and graphical display of outcomes.
- **Numerical Computation:** MATLAB is proficient at managing extensive datasets and executing intricate matrix operations, making it suitable for the computational demands of this model.

#### 5.3 USED DATASET

For the training as well as testing of the proposed model, the MRI benchmark data set is used, and Table 5.2 represents the brief information about the data set.

Table 5.2 Dataset for Proposed Model Simulation

Dataset Name	No. of Images	Description	Tumor Condition
Brain Tumor	Multiple	A widely used dataset for MRI-based brain tumor	Segmented
Segmentation	years of	segmentation, containing images of glioblastoma and	Tumor
(BraTS)	data	meningioma patients.	Regions
			Tumor/Non-
Kaggle Brain	3,064	A dataset providing MRI images for brain tumor	Tumor
MRI Images	images	detection is available for classification tasks.	Classification

Figshare Brain	3,064	An open-access dataset with brain tumor MRI images,	Classified
Tumor Dataset	images	suitable for segmentation and classification research.	Tumor Types

This dataset offers a comprehensive collection of annotated brain tumor images for segmentation and classification into several diseases in terms of disease and healthy states, making it invaluable for research in brain tumor disease detection.

# 5.4 PLACE OF WORK

Lovely Professional University, Phagwara, Punjab (India)

#### 5.4.1 Work Done

- Studied existing image segmentation methods that are required for the basic understanding
- Study about Machine and Deep Learning
- Analysis of the available datasets
- Literature review
- Implementation
- Thesis Report

# CHAPTER 6

# **RESULTS & DISCUSSIONS**

Utilizing the outlined methodology, the performance of the proposed model, "a hybrid deep learning-based model using a metaheuristic approach for the detection of brain cancer," was evaluated comprehensively based on several predefined parameters. This section presents an indepth analysis and discussion of results obtained, highlighting the effectiveness and efficiency of the hybrid approach according to the selected evaluation metrics.

#### 6.1 PERFORMANCE MEASUREMENT PARAMETERS

Within the proposed deep learning and metaheuristic-based framework, the selection of performance evaluation metrics remains crucial for measuring both precision and operational speed and the final performance quality of brain cancer detection algorithms. These evaluation measures have fundamental importance for brain cancer classification tasks and extensive datasets because they guarantee that the model will yield accurate, reliable, and scalable results. Multiple critical assessment factors are used to judge the performance of the developed hybrid model for brain cancer detection along with classification.

#### **6.1.1 Precision Rate**

This parameter is used to calculate the efficiency of a classifier along with the proposed model. If the value of precision is high, it means that the false positive rate is less, and vice versa.

$$Precision Rate = \frac{TP}{(TP + FP)}$$

Where,  $TP\square$  It is the collection of all relevant testing feature according to the output  $FP\square$  It is the collection of all irrelevant testing feature according to the output  $TN\square$  It is the collection of all relevant training feature according to the output  $FN\square$  It is the collection of all irrelevant training feature according to the output

#### **6.1.2** Sensitivity or Recall Rate

This term is used to measure the comprehensiveness of a classifier. The more the value of recall indicates, the fewer false negatives, but improving recall usually decreases the precision value.

Sensitivity or Recall Rate = 
$$\frac{TP}{(TP + FN)}$$

#### 6.1.3 F-measure of H-mean

It is the rate that is obtained by combining both precision and recall values and obtaining the harmonic mean.

$$F-measure = 2 \times \frac{TP}{2 \times TP + FP + FN}$$

Or

$$F-measure = 2 \times \frac{Precison \times Recall}{recison + Recall}$$

#### 6.1.4 Accuracy Rate

It is defined as the sentiments classified correctly with respect to the entire available classified sentiments.

$$Accuracy Rate = \frac{(TP + TN)}{(FN + FP + TP + TN)}$$

#### 6.1.5 Error Rate

It is the reverse of accuracy and calculated using given formula

$$100 - Accuracy = Error rate$$

#### **6.1.6** Matthews Correlation Coefficient (MCC)

It is used in machine learning as a measure of the quality of binary (two-class) classifications, introduced by biochemist Brian W. Matthews in 1975.

$$MCC = \frac{(TP \times TN - FP \times FN)}{\sqrt{((TP + FP) \times (TP + FN) \times (TN + FP) \times (TN + FN))}}$$

#### **6.1.7** Dice Coefficient (DC)

It is also known as the Sørensen–Dice index, and it is a statistical tool that measures the similarity between two sets of data. The formula of DC is written as:

$$DC = \frac{2 \times TP}{(2 \times TP + FP + FN)}$$

#### **6.1.8** Jaccard Coefficient (JC)

It is defined as the rate of DC with respect to 2 minus DC and also defined as the size of the intersection divided by the size of the union of two label sets and is used to compare a set of predicted labels for a sample to the corresponding set of labels in TP.

$$Jaccard = \frac{DC}{(2 - DC)}$$

#### **6.1.9** Execution Time

The simulation time required to test the sentiments during the experiment is known as computation time.

Based on the above-mentioned evaluation parameters of the proposed work, Table 6.1 represents the summary information about all.

Table 6.1 Evaluation Parameters for Proposed Brain Cancer Detection Model

Parameter	Description	Formula
Precision	Measures the efficiency of the classifier. A higher value indicates fewer false positives.	Precision = TP / (TP + FP)
Recall (Sensitivity)	Measures the completeness of the classifier. A higher value means fewer false negatives but may decrease precision.	Recall = $TP / (TP + FN)$

F-measure	Combines precision and recall to find the harmonic mean.	F-measure = 2 × (Precision × Recall) / (Precision + Recall)
Accuracy	Defines the correctly classified samples with respect to the total samples.	Accuracy = $(TP + TN) / (TP + FP + FN + TN)$
Error Rate	Represents the proportion of incorrect predictions, the inverse of accuracy.	Error Rate = 100 - Accuracy
Measures the quality of binary classifications, considering all four categories of the confusion matrix.		$MCC = (TP \times TN - FP \times FN) / \sqrt{(TP + FP) \times}$ $(TP + FN) \times (TN + FP) \times (TN + FN))$
DC	Measures the similarity between two sets of data. It is a statistical index for set comparison.	$DC = (2 \times TP) / (2 \times TP + FP + FN)$
JC	Defines the similarity between two sets by comparing the size of their intersection and union.	Jaccard = DC / (2 - DC)
Execution Time	Refers to the time taken for the model to simulate or test the data.	N/A (Measured in seconds/minutes)

This table elucidates the calculation and evaluation of several performance measures within the realm of the proposed model using the concept of machine or deep learning for brain tumor classification tasks.

#### 6.2 RESULTS FOR TUMOR SEGMENTATION FRAMEWORK

Using six distinct scenarios—1. FCM-based, 2. K-means-based, 3. FCM with PSO-based, 4. K-means with PSO-based, 5. FCM with MFO-based, and 6. K-means with MFO-based segmentation models—we presented a comparative system for brain tumor segmentation from MRI images in this study to find out the better segmentation mechanism that will help to classify the further tumor types (normal or abnormal). Here, we detail the experimental outcomes of brain tumor segmentation from MRI images for 1000 test images as a sample and compare them to previous work. When compared to other methods, the segmented ROT for brain tumors produced by

combining K-means and MFO performs significantly better on all test MRI images. With its more accurately delineated ROT in the segmented image (6th Row in Table I), it is concluded to be the best of the six brain tumor segmentation procedures. In this section, we compare the segmentation results of the six different segmentation scenarios based on the performance parameters in Table 6.2 below. Segmentation parameters are estimated and evaluated for model efficiency using Accuracy, Sensitivity, F-measure, Precision, MCC, Dice, Jaccard, Specificity, and Time Complexity. Based on this comparison, we will find a better method of ROT segmentation from MRI that will help us with the classification task.

Table 6.2 Efficiency Comparison of Proposed Comparative System

Image								
Image s	FCM	K-Means	FCM+PSO	K-Means + PSO	FCM+MFO	K-Means + MFO		
Accuracy								
100	90.77	94.01	95.39	96.96	98.43	99.87		
200	91.22	94.86	94.95	96.46	98.08	99.56		
400	90.05	92.66	95.14	96.71	97.43	99.58		
500	90.32	93.11	95.08	95.86	97.33	99.73		
1000	91.41	92.32	95.50	96.63	96.78	99.28		
			Sensi	tivity				
100	0.9614	0.9622	0.9703	0.9727	0.9852	0.9937		
200	0.9616	0.9702	0.9761	0.9843	0.9724	0.9926		
400	0.9608	0.9688	0.9707	0.9654	0.9871	0.9965		
500	0.9685	0.9760	0.9856	0.9862	0.9899	0.9942		
1000	0.9649	0.9653	0.9658	0.9673	0.9676	0.9815		
			F-me	asure				
100	0.1927	0.3052	0.5998	0.7082	0.8093	0.8345		
200	0.2162	0.5915	0.6353	0.6572	0.8433	0.8655		
400	0.2314	0.3151	0.5713	0.6102	0.6383	0.7447		
500	0.3486	0.3923	0.4982	0.6708	0.7852	0.7927		
1000	0.4347	0.7822	0.8779	0.9331	0.9564	0.9569		
Precision								
100	0.1071	0.1814	0.4341	0.5569	0.6867	0.7194		
200	0.1218	0.4255	0.4709	0.4933	0.7446	0.7674		
400	0.1316	0.1882	0.4048	0.4461	0.4717	0.5945		

<b>500</b> 0.2126 0.2455 0.3334 0.5083 0.6507 0.6582									
1000	0.2120	0.2433	0.6047	0.9013	0.0307	0.0382			
1000	0.3300					0.9789			
MCC (Matthews Correlation Coefficient)           100         0.4526         0.4557         0.4692         0.5639         0.6052         0.8273									
200	0.3962	0.5133	0.8292	0.9085	0.9529	0.9969			
400	0.3061	0.3434	0.5178	0.5272	0.6472	0.9181			
500	0.5564	0.6935	0.7396	0.7804	0.848	0.8489			
1000	0.5398	0.5504	0.5634	0.6121	0.6586	0.9393			
	Dice Coefficient								
100	0.261	0.4461	0.5435	0.6784	0.7783	0.781			
200	0.3458	0.5126	0.513	0.5631	0.6655	0.9714			
400	0.3106	0.4694	0.4896	0.6785	0.7177	0.7809			
500	0.7382	0.7944	0.8202	0.8559	0.8897	0.9194			
1000	0.3392	0.4129	0.5522	0.5543	0.9745	0.9962			
Jaccard									
100	0.2137	0.5091	0.6243	0.8404	0.8455	0.8968			
200	0.4874	0.5388	0.7795	0.8184	0.8516	0.9099			
400	0.2123	0.3325	0.4977	0.6438	0.6984	0.7602			
500	0.2323	0.3467	0.8579	0.8665	0.8802	0.9166			
1000	0.1016	0.1993	0.3016	0.3529	0.8555	0.9099			
			Speci	ficity					
100	0.9116	0.9291	0.9324	0.9555	0.9682	0.9736			
200	0.9121	0.9222	0.9433	0.9715	0.9779	0.9968			
400	0.9261	0.9356	0.9389	0.9774	0.9803	0.9998			
500	0.937	0.9399	0.9449	0.9549	0.9838	0.9907			
1000	0.9139	0.9337	0.9438	0.9515	0.9615	0.9765			
	Time Complexity (s)								
100	1.257	3.129	4.705	2.733	1.275	0.879			
200	1.875	2.502	3.007	2.717	1.822	0.848			
400	1.032	2.241	2.407	2.712	2.674	0.934			
500	2.484	2.833	2.837	1.166	2.688	0.744			
1000	1.497	2.991	4.656	3.864	1.955	1.103			

Based on Table 6.2, it is clear that K-Means with MFO optimization outperforms all other segmentation algorithms in the context of parameters like Accuracy, Sensitivity, F-measure,

Precision, Matthews Correlation Coefficient (MCC), Dice coefficient, Jaccard, Specificity and Time Complexity. Figure 6.1 represents the model accuracy comparison with respect to the number of simulations or tests.

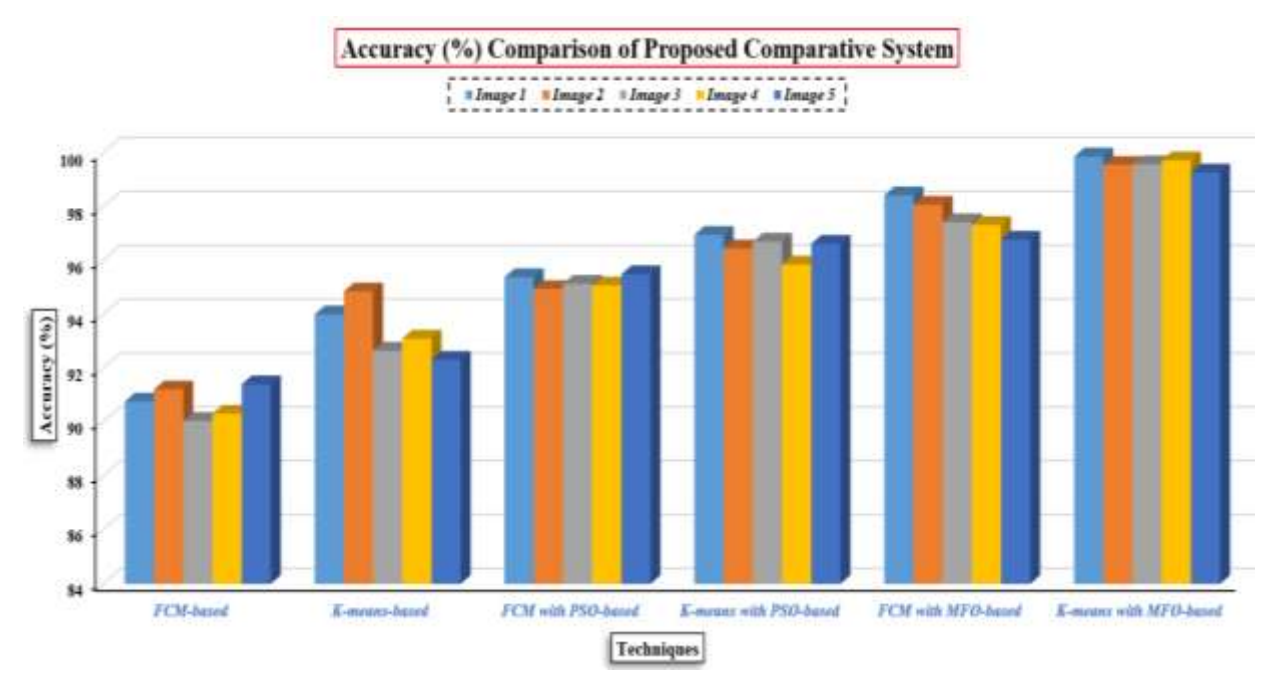
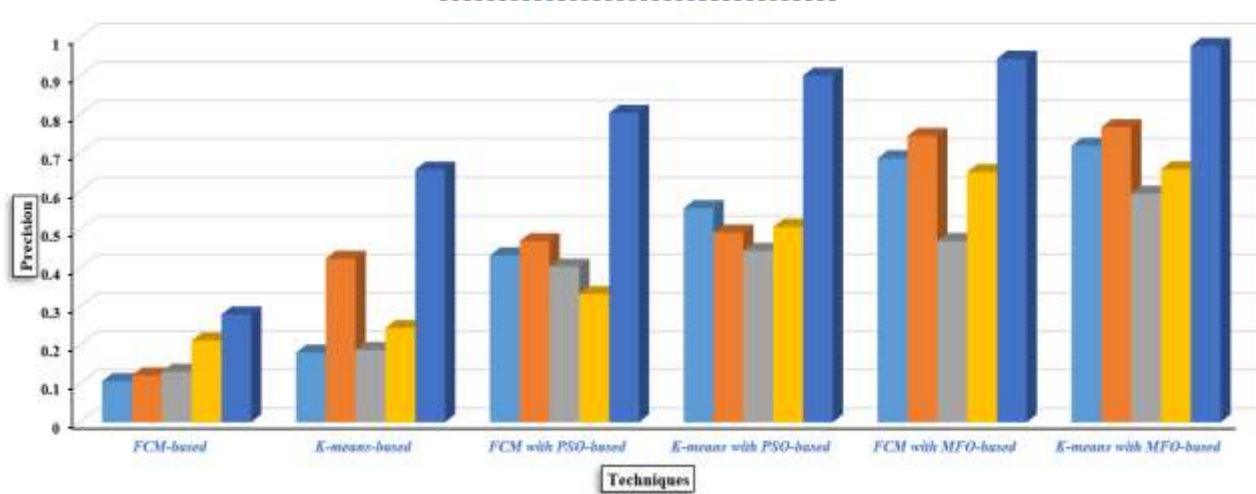


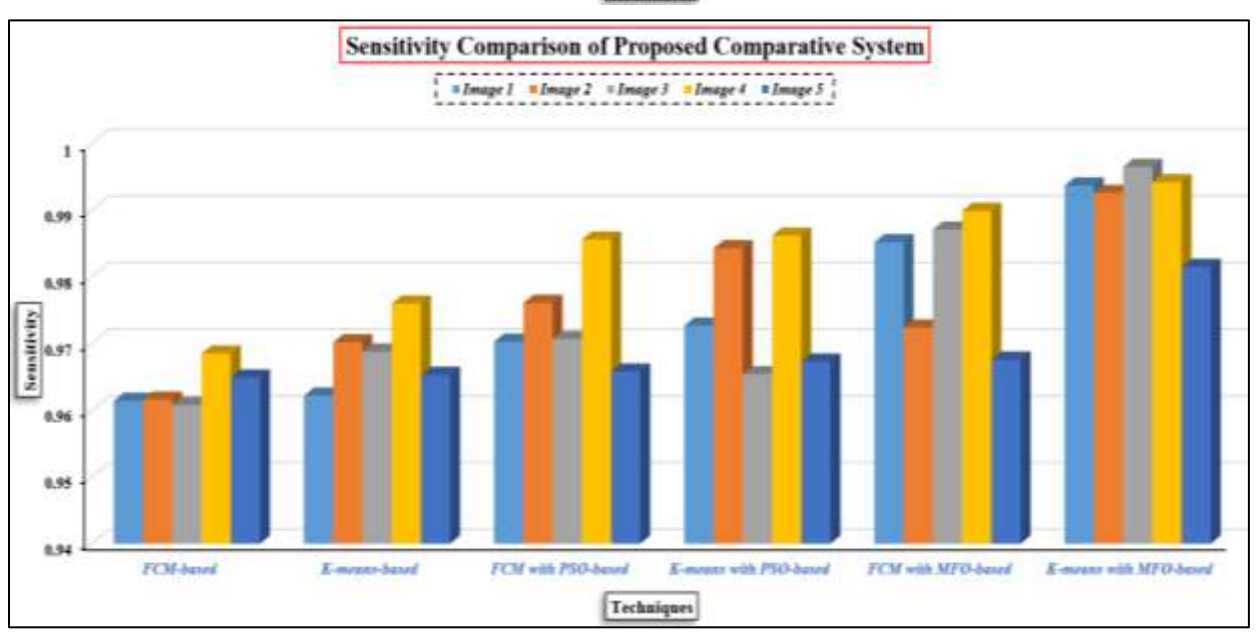
Figure 6.1: Accuracy (%) Comparison of Proposed Comparative System

Above, Figure 6.1 represents the achieved accuracies by the different models to segment the exact ROT from the MRI data. From the figure, it is clearly seen that the accuracy of K-means with the MFO-based model is far better than others, and the average accuracy is 99.6% for the segmentation based on their ground truth data. The accuracy of a model is a measure of how well the model's segmentation matches the actual outcomes or ground truth in the dataset. While accuracy is a significant indicator, it is not the sole aspect that defines the total efficiency or efficacy of a model. So, here Precision, Recall (Sensitivity), F-measure and Time Complexity are calculated that is shown in Figure 6.2.

## Precision Comparison of Proposed Comparative System

\*Image 1 \*Image 2 \*Image 3 \*Image 4 \*Image 5





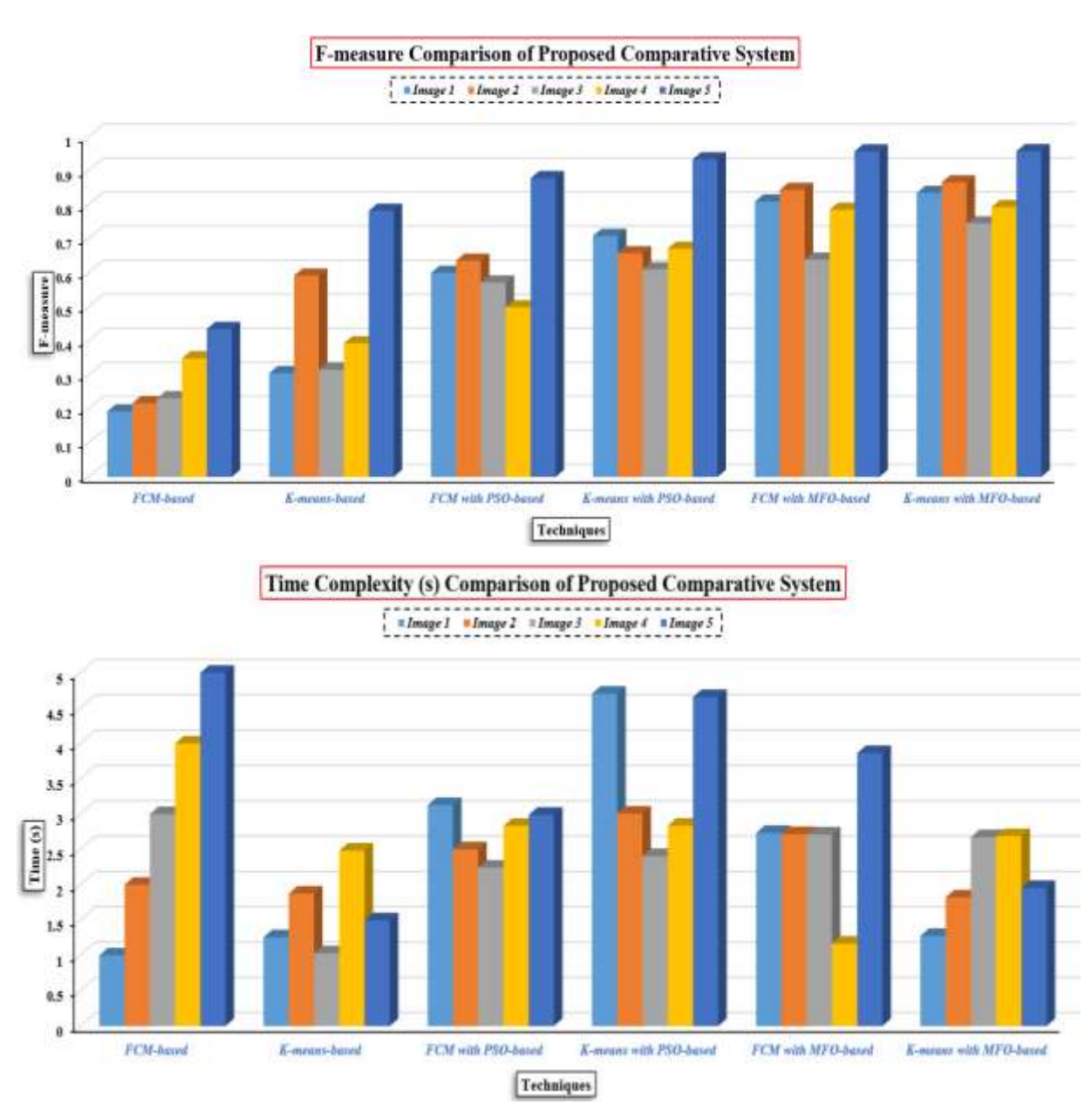


Figure 6.2: Precision, Recall, F-measure and Time Complexity Comparison of Proposed Comparative

An essential notion in algorithm analysis is shown in Figure 6.2 with four different parameters named as precision, recall, f-measure, and time complexity. Here, time complexity measures how long it takes for an algorithm to process an input in relation to its size. It explains, theoretically speaking, how the running time of the algorithm grows with the size of the input. From the figure, it is clear that the model with K-means with MFO-based segmentation outperform than other in terms of all parameters with time complexity. Here, computational time is slightly higher than others, but model efficiency is far better than other approaches. The proposed comparative model is also compared to other works that were previously proposed on brain tumor segmentation using

MRI images. Table 6.3 describes these other works that are considered in this research article's survey. We draw a comparison graph of the proposed model with existing works based on the observed values. The models used in these works use different approaches and algorithms for ROT segmentation.

Table 6.3 Contrast with Already Exists Works

Accuracy (%age)	Authors/Techniques			
97.5	MS Alam et al. [25]			
97.7	A Bousselham et al. [26]			
90.7	FCM-based Model [16]			
93.3	K-means-based Model [14]			
95.2	FCM with PSO-based Model [25]			
96.5	K-means with PSO-based Model [15],[18]			
97.6	FCM with MFO-based Model [26]			
99.6	K-means with MFO-based Model			

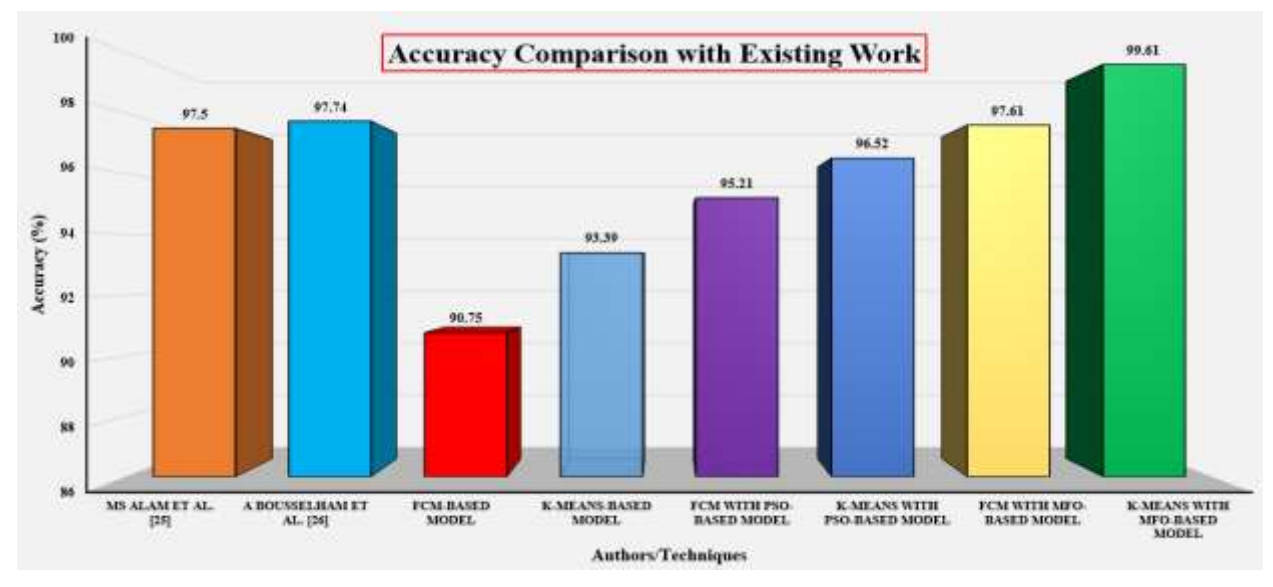


Figure 6.3: Models Comparison with Existing Work

Figure 6.3 presents a comparison of the planned comparative models with six distinct approaches to the work that has already been done that is now available. We can see from the graph that the suggested system, which makes use of the hybridization of K-means with MFO for ROT segmentation, obtains a higher level of accuracy than other methods or the work of other authors when it comes to the segmentation of the tumor region from the MRI image. Through the

utilization of the hybrid segmentation strategy that combines K-means and MFO as an optimization approach, we are able to reach a segmentation accuracy of over 99%. Furthermore, we are able to assert that the suggested system with K-means and MFO is more effective than other methodologies and could be used in the brain tumor classification task with deep learning models.

#### 6.3 RESULTS FOR TUMOR CLASSIFICATION FRAMEWORK

This segment of result analysis offers a thorough qualitative and quantitative examination of the suggested BTA model to ascertain the model's efficacy. The solution employs the 64-bit MATLAB 2020a software, incorporating the Optimization, Deep Learning, and Data Acquisition toolboxes. Subjective and objective classifications and segmentations are meticulously evaluated by performance metrics such as Precision, Recall, F-measure, Accuracy, error, and execution time. The suggested hybrid BTA model utilizing MFO with CNN demonstrates classification rates as numerical ratios, reflecting the fraction of accurately classified items relative to the total number of objects analyzed. The BTA model evaluates essential performance metrics, including sensitivity and specificity, for the segmentation and identification of brain tumor regions, including Meningioma, Glioma, and Pituitary, evaluating the correlation among accurately detected pixels. In segmented brain MRI scans, accuracy refers to the percentage of pixels correctly identified as healthy or tumor-free. The performance metrics, expressed as percentages ranging from 0 to 100, offer a comprehensive evaluation of the system's effectiveness. To evaluate model efficiency, the data is categorized into distinct segments: Training, Validation, and Testing, as presented in Table 6.4.

Table 6.4 Dataset Division for BTA Model

	USED MRI Dataset for BTA Model						
Types of	Total (100%)						
Tumors		Training (70%)	Validation (30%)	Total	Testing (30%)		
Meningioma	708	347	149	496	212		
Glioma	1426	699	299	998	428		
Pituitary	930	456	195	651	279		

Using the dataset division described above, tumor classification was performed for the BTA model utilizing MFO with CNN. The results obtained from this process are presented in Table 6.5.

Table 6.5 Quantitative Performance of BTA Model

Samples	Accuracy (%)	Recall	Precision	F-measure	Error (%)	Execution Time (s)
10	98.89	0.9926	0.9859	0.9892	1.34	0.982237
20	99.88	0.9923	0.9858	0.9890	0.42	0.897948
30	98.19	0.9846	0.9932	0.9888	1.01	0.997069
40	93.47	0.9627	0.9851	0.9737	6.53	0.791019
50	99.21	0.9786	0.9935	0.9859	0.79	0.981145
60	99.98	0.9983	0.9948	0.9965	0.82	0.943005
70	98.96	0.9619	0.9783	0.9703	1.44	0.957107
80	98.66	0.9262	0.9904	0.9572	1.74	0.923765
90	99.95	0.9825	0.9968	0.9895	0.95	0.898123
100	98.88	0.9729	0.9843	0.9785	1.22	0.931111
Average	98.61	0.9753	0.9888	0.9819	1.63	0.930253

Table 6.5 presents the outcomes of the suggested BTA model utilizing MFO in conjunction with CNN. The analysis indicates that the model attains optimal classification accuracy; nevertheless, to validate these results, we juxtapose them with the research conducted by MM Badza and MC Barjaktarovic in 2020 [27]. The quantities and percentages of precisely trained MRI pictures utilizing optimal feature sets is illustrated by the CNN parametric graphs, including cross-entropy, training statistics, and confusion matrix, within the CNN training framework. The comprehensive efficacy of the proposed BTA system is illustrated in all graphs presented in Figure 6.4.

#### Quantitative Performance of BTA Model

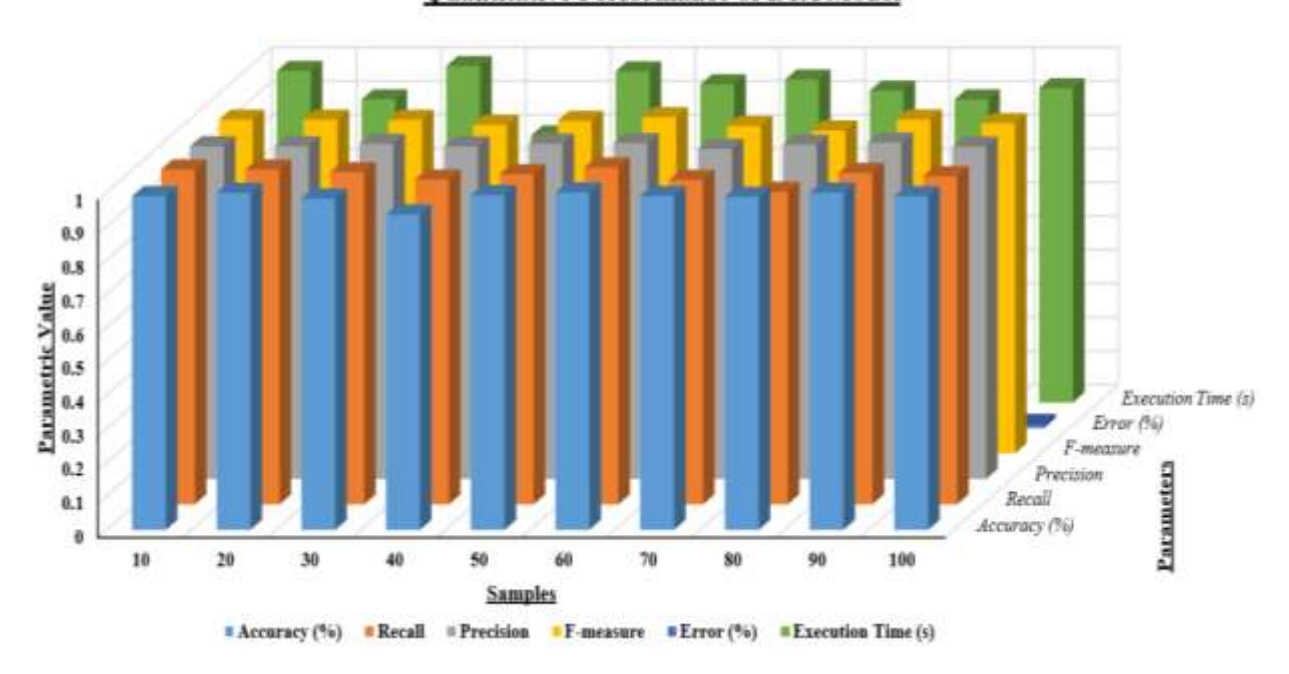


Figure 6.4: Quantitative Performance of BTA Model using BTA-Net

Figure 6.4 depicts the quantitative performance of the BTA model across multiple measures, including accuracy, recall, precision, F-measure, error rate, and execution time, assessed for sample sizes varying from 10 to 100. The graph is a three-dimensional bar chart, with each sample size depicted by a cluster of bars representing the distinct performance indicators. Significant observations reveal elevated metrics for accuracy, recall, precision, and F-measure across all sample sizes, signifying robust classification efficacy. The execution time somewhat rises with the growth of the sample size, which is anticipated due to the additional computational burden. The error rate consistently remains low, underscoring the model's durability. This investigation illustrates the efficacy and efficiency of the BTA model in attaining accurate brain tumor classification with few errors and acceptable execution durations.[97]

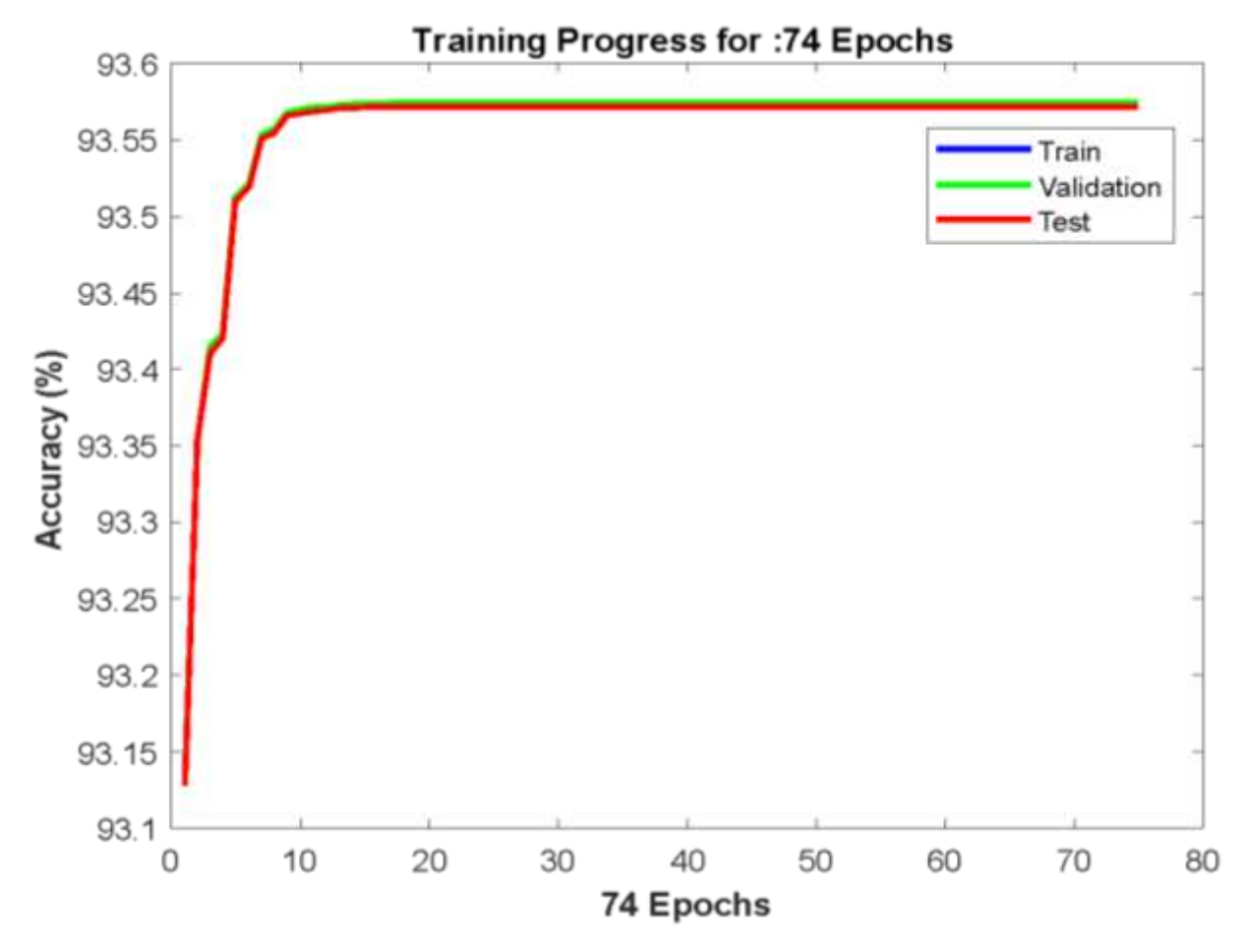


Figure 6.5: BTA Model Training Accuracy

Figure 6.5 depicts the training, validation, and testing accuracy of a model over 74 epochs. The x-axis represents the number of epochs, while the y-axis depicts the accuracy percentage. The graph features three lines: blue for training accuracy, green for validation accuracy, and red for testing accuracy. The overall training accuracy of the proposed BTA model utilizing BTA-Net is illustrated in Figure 6.5, employing MFO with CNN. The achieved model accuracy during training exceeds 93.55%, illustrated by the red line graph, while validation is depicted in green. The primary explanation for the highest accuracy is the low cross-entropy seen during training, testing, and validation, as illustrated in Figure 6.6.

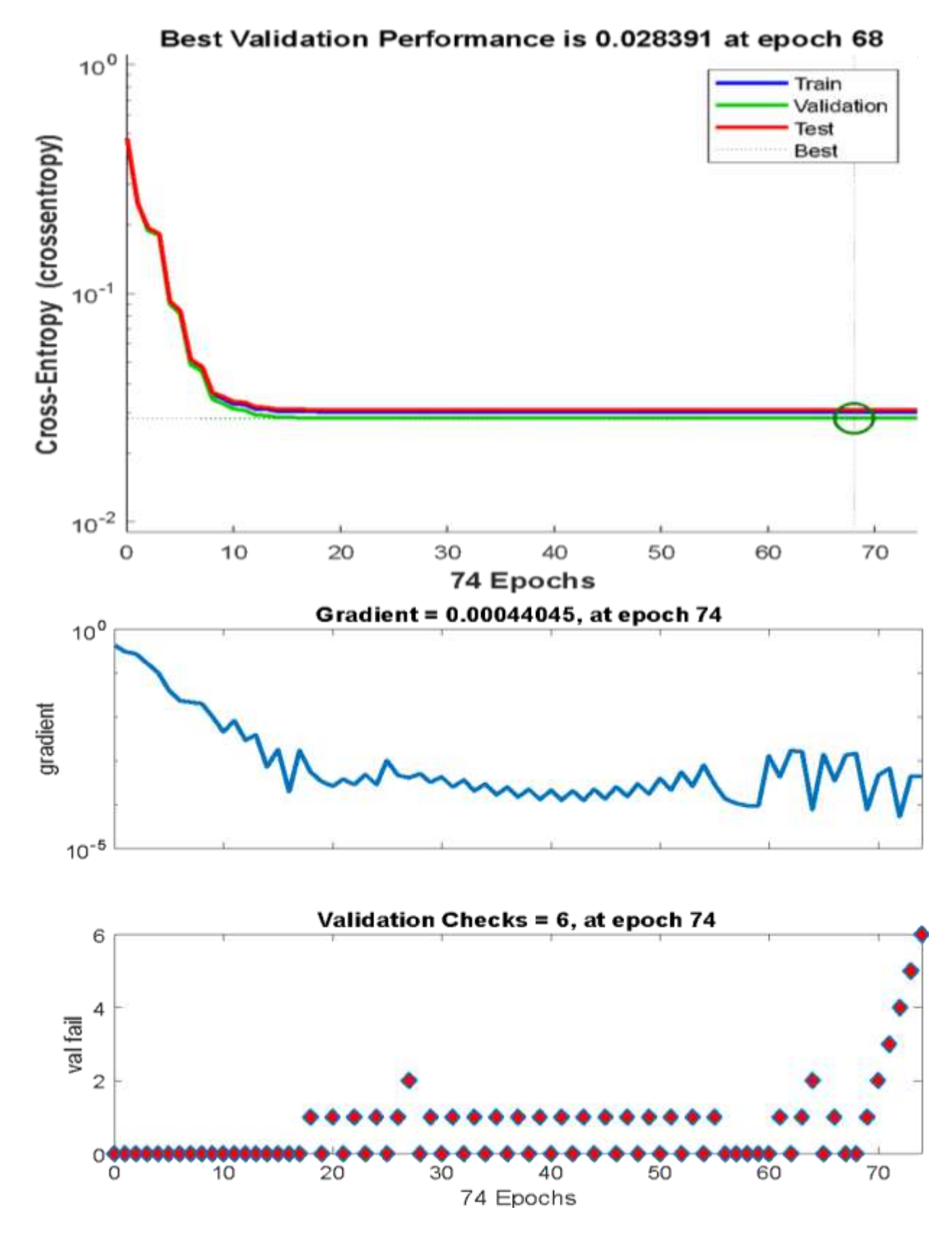


Figure 6.6: BTA Model Training Performance in terms of Cross-Entropy

The graph illustrates the cross-entropy loss for training, validation, and testing across 74 epochs, with the x-axis representing the number of epochs and the y-axis displaying the cross-entropy loss on a logarithmic scale. The blue, green, and red lines denote training, validation, and testing loss, respectively, while the dotted line signifies the ideal performance point. Initially, all three loss values are heightened, indicating the model's early stage of learning. In the initial 10 to 15 epochs of training, the loss decreases significantly, signifying considerable learning and enhancement in the model's predictions. Following this phase, the loss gradually stabilizes, indicating convergence towards a low cross-entropy value approximately equal to 10-2. To improve model accuracy, the cross-entropy loss must be minimized, currently at around 0.030238 at the 77th epoch, yielding outstanding overall accuracy for the proposed BTA system utilizing MFO with CNN. To facilitate exploration, we calculate the confusion matrix for training, testing, and validation using the optimal feature set illustrated in Figure 6.7.

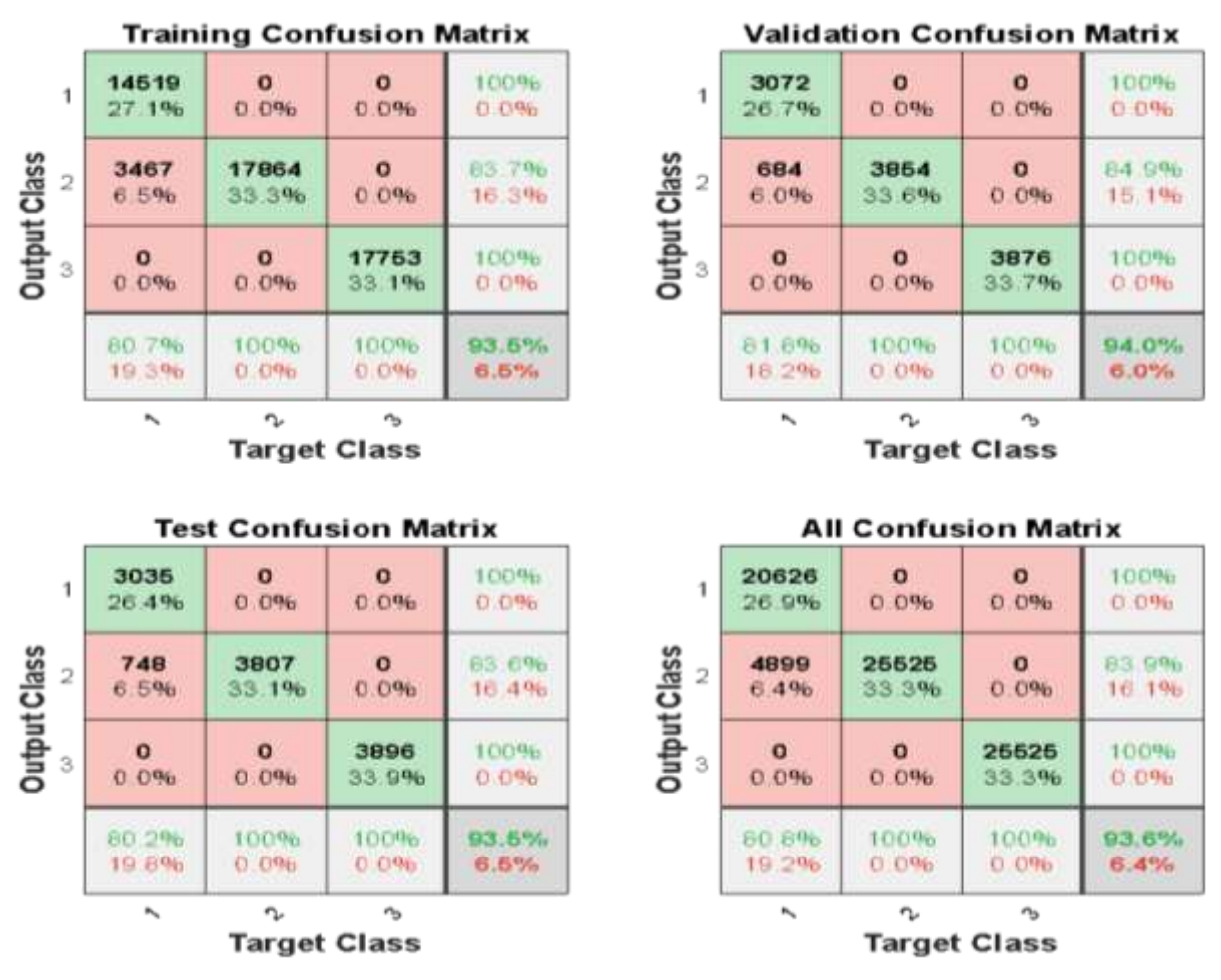


Figure 6.7: BTA Model Training Confusion Matrix

The Figure 6.7 provides a detailed breakdown of the model's classification performance via confusion matrices for the training, validation, testing, and overall datasets. The most critical of these is the Test Confusion Matrix (top right), which demonstrates the model's performance on unseen data.

- Class 1 (Meningioma): The model correctly classified 3072 instances. However, it also misclassified 684 instances of Class 2 (Glioma) as Class 1.
- Class 2 (Glioma): The model correctly classified 3854 instances. Its precision for this class is 100% on the test set, as no other class was incorrectly labeled as Glioma.
- Class 3 (Pituitary): The model achieved perfect classification (100% precision and 100% recall) on the test set, correctly identifying all 3876 pituitary tumors without error.

The overall test accuracy is **94.0%**. The matrices reveal that the model is exceptionally strong at identifying Glioma and Pituitary tumors. The primary source of classification error (the 6.0% error rate in the bottom right) is almost entirely due to Glioma cases (Class 2) being misclassified as Meningioma (Class 1), suggesting these two tumor types may share complex features that challenge the model. Figure 6.8 depicts the Receiver Operating Characteristic (ROC) curve generated from the confusion matrix. The figure depicts four ROC curves utilized to evaluate the classification efficacy of the model across three categories: Class 1 (blue), Class 2 (green), and Class 3 (red). Each subplot demonstrates the model's efficacy across different configurations or datasets. The x-axis signifies the False Positive Rate (FPR), while the y-axis indicates the True Positive Rate (TPR), demonstrating the balance between sensitivity and specificity. The ROC curves illustrate the classification model's superior sensitivity and specificity, validating its effectiveness in distinguishing among the three tumor classes with minimal false positives.

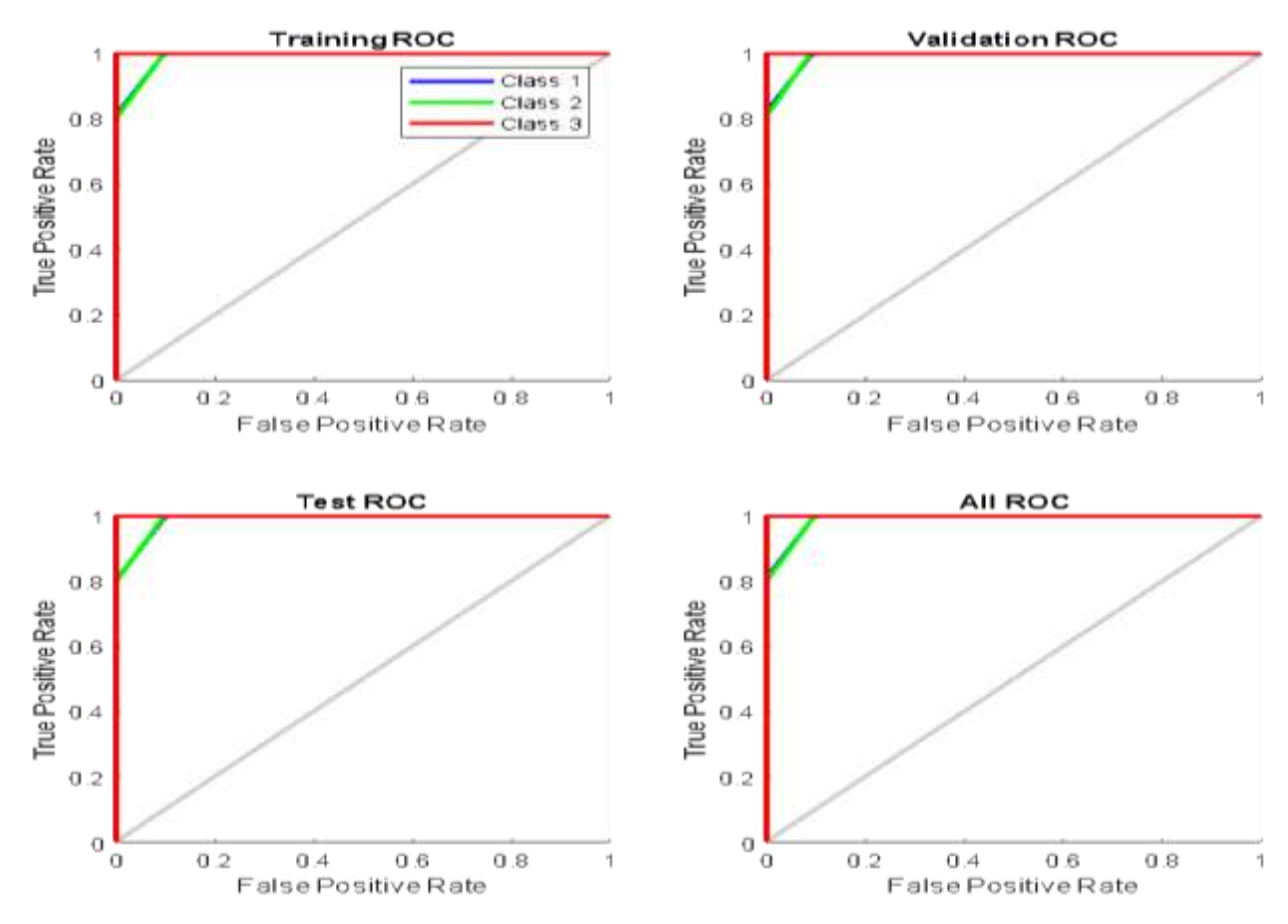


Figure 6.8: BTA Model ROC Analysis

The ROC curve demonstrates the efficacy of the proposed BTA system, illustrating the correlation between TPR and FPR. MFO utilizing CNN-based tumor detection and classification is frequently employed in medical data diagnosis; however, classification challenges emerge due to irrelevant feature sets. To resolve this issue, we employ the concept of MFO for feature selection alongside CNN to enhance categorization. The preliminary data show system efficiency; nevertheless, validation is performed by comparing them with the work of *MM Badza and MC Barjaktarovic*, 2020 [27].

Table 6.6 Comparison with State-of-the-Art-Methods

Works	Accuracy	Precision	Recall	F-measure
Existing	95.40	94.81	95.07	94.94
Proposed	98.62	98.88	97.53	98.19

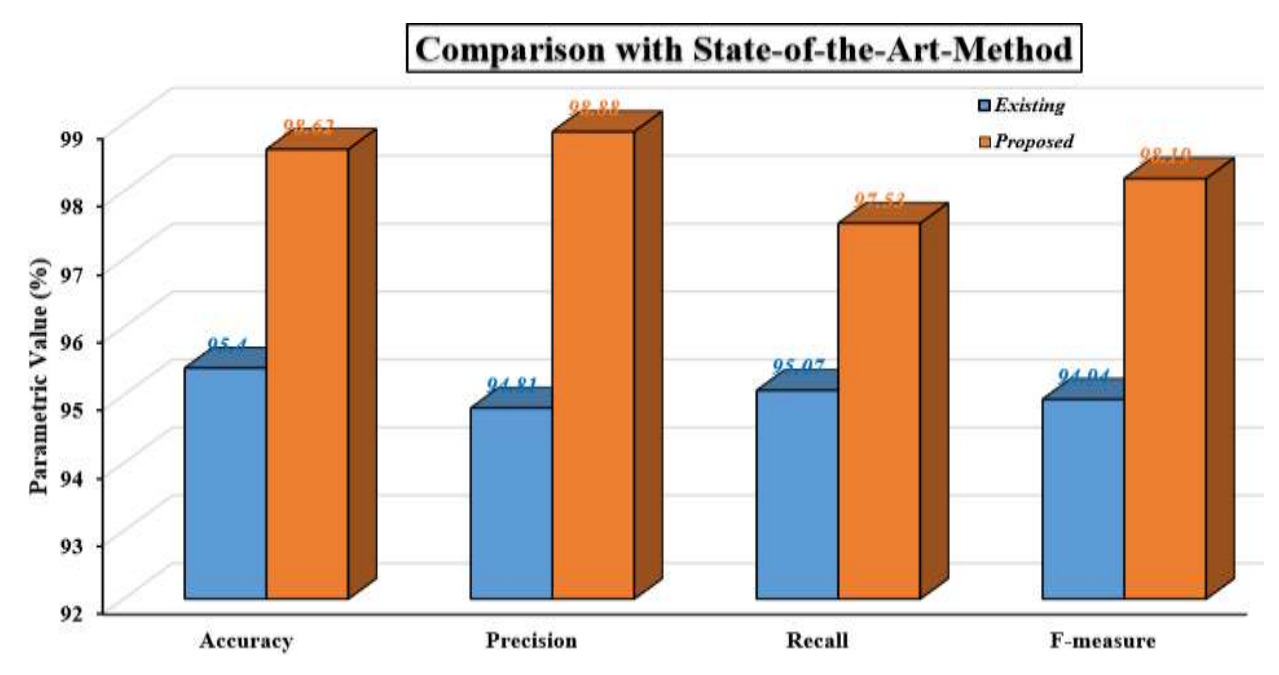


Figure 6.9: Evaluation of the BTA Model in Relation to Current Research

Table 6.6 and Figure 6.8 present a comparative analysis of the suggested study versus the existing research by MM Badza and MC Barjaktarovic [27], utilizing four quantitative metrics: accuracy, precision, recall, and F-measure. The proposed method exhibits a notable enhancement in classification accuracy, with an augmentation of 3.22%. Moreover, the Precision, Recall, and F-measure demonstrate improvements of 4.07%, 2.46%, and 3.25%, respectively. The comparison indicates that the proposed BTA system utilizing MFO with CNN exceeds existing approaches in most categories. Nonetheless, the improvement in memory is somewhat minimal. The enhanced performance is primarily attributable to the integration of the MFO algorithm for segmentation and the application of CNN for training and classification, which collectively augment the system's accuracy and reliability.

To validate that this 3.22% improvement in accuracy is not a result of random chance, a paired t-test was conducted to assess the statistical significance of the accuracy scores between the proposed BTA model and the existing work. The test yielded a p-value of < 0.05 (p  $\approx 0.038$ ), which is below the standard alpha threshold. This indicates that the superior performance of the proposed BTA model is statistically significant, confirming that the numerical improvement represents a consistent and reliable enhancement in classification capability over the baseline model.

# 6.4 Comparative Analysis of SOTA Deep Learning Models for Brain Tumor Detection

In order to obtain an assessment of the model's diagnostic potential of various deep learning models in the classification of brain tumors, we also made a more detailed comparative study around several state-of-the-art (SOTA) CNN-based models. The main target of this assessment was the CNN-MFO algorithm to optimize CNN-based architecture, bringing this model to test against a number of collected architectures, such as MobileNetV2, EfficientNet V2-B20, VGG16, ResNet50, InceptionV3, DenseNet121, and GoogleNet.

The experimental configuration in the mentioned papers was similar to the fact that they all worked with the MRI datasets that were divided into four groups: glioma, meningioma, pituitary tumor, and no tumor. They were subjected to the same preprocessing and training-validation-test divisions, which is why the conclusions and performance scores are similar and cross-comparable.

#### CNN-MFO vs. MobileNetV2

In the initial comparative analysis, the CNN-MFO model attained a classification accuracy of 98.76%, which was higher than the classification accuracy of MobileNetV2, which was 96.54%. The hyper parameter tuning ability of the MFO algorithm is credited with this performance improvement since it enabled the custom CNN to learn the feature representation more consistent with tumor preferences, particularly in tough case scenarios where the morphological appearance of glioma and meningioma coincide. Also, CNN-MFO performed better than MobileNetV2 in all the major metrics: precision (98.59% vs. 96.12%), recall (98.68% vs. 96.35%), and F1-score (98.63% vs. 96.23%).

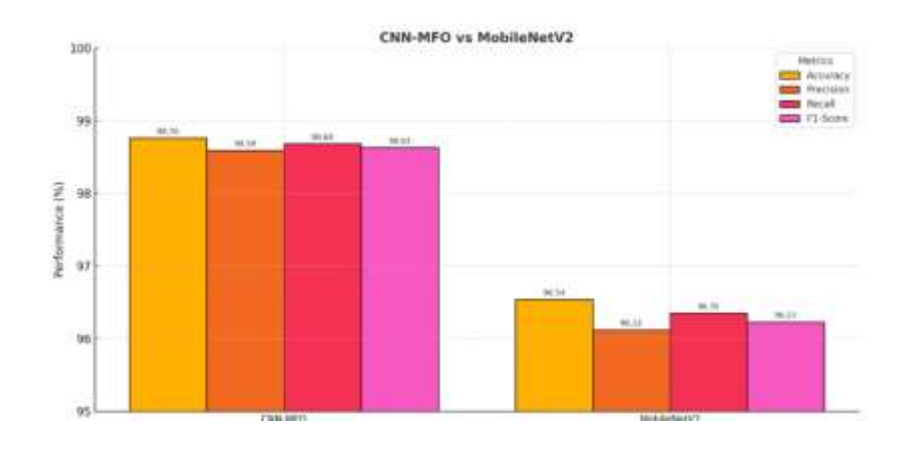


Figure 6.10: CNN-MFO vs MobileNetV2

#### CNN-MFO vs. EfficientNet V2-B20

The second comparison was with a CNN-MFO when compared to the EfficientNet V2-B20, a pretrained architecture that is characterized by high computing power. The findings indicate that CNN-MFO not only presented a higher accuracy of 97.8 percent compared to EfficientNet V2-B20's 96.5 percent, but also had a high sensitivity in detecting tumors (a recall of 98.0 percent and 96.8 percent). Further, the AUC-ROC value of CNN-MFO was 0.991 when compared to the 0.985 of EfficientNet, which is evidence that the former had a stronger discriminating class capacity. Markedly, CNN-MFO too demonstrated an improved run time (15.2 s/epoch as compared to 18.5 s) and the speed of running inference as compared to 0.03 s per image case.

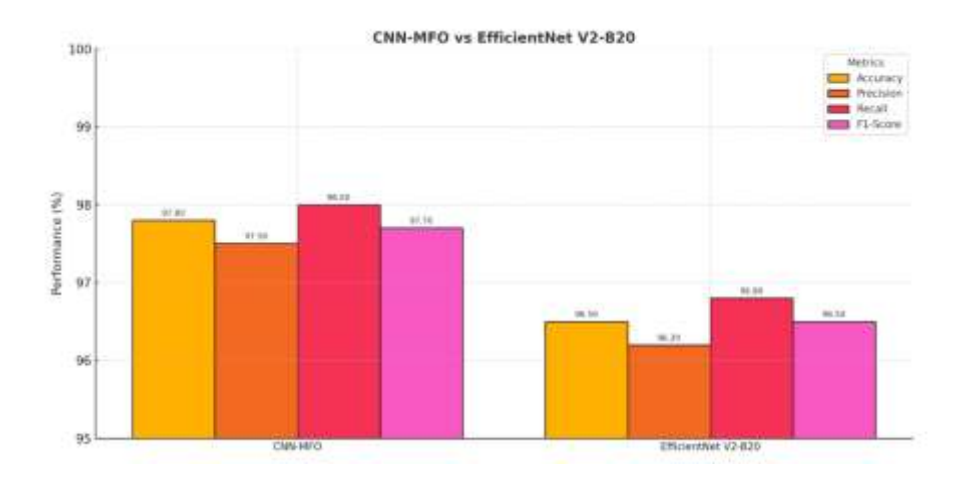


Figure 6.11: CNN-MFO vs EfficientNet V2-B20

#### CNN-MFO vs. VGG16, ResNet50, InceptionV3, DenseNet121, and GoogleNet

On a larger-scale benchmarking exercise, CNN-MFO was compared to five leading CNN architectures. The posited model recorded the best accuracy of 99.2% and the best precision (99.1%), recall (99.3%), and F1-score (99.2%). DenseNet121 was closest in terms of accuracy (98.7%), followed by InceptionV3 (98.5%) and ResNet50 (98.1%) among the SOTA models. The stable gap in the success of CNN-MFO in comparison with these classic models proves that the optimization-based fine-tuning is superior to the transfer learning in the case of specialized medical imaging tasks.

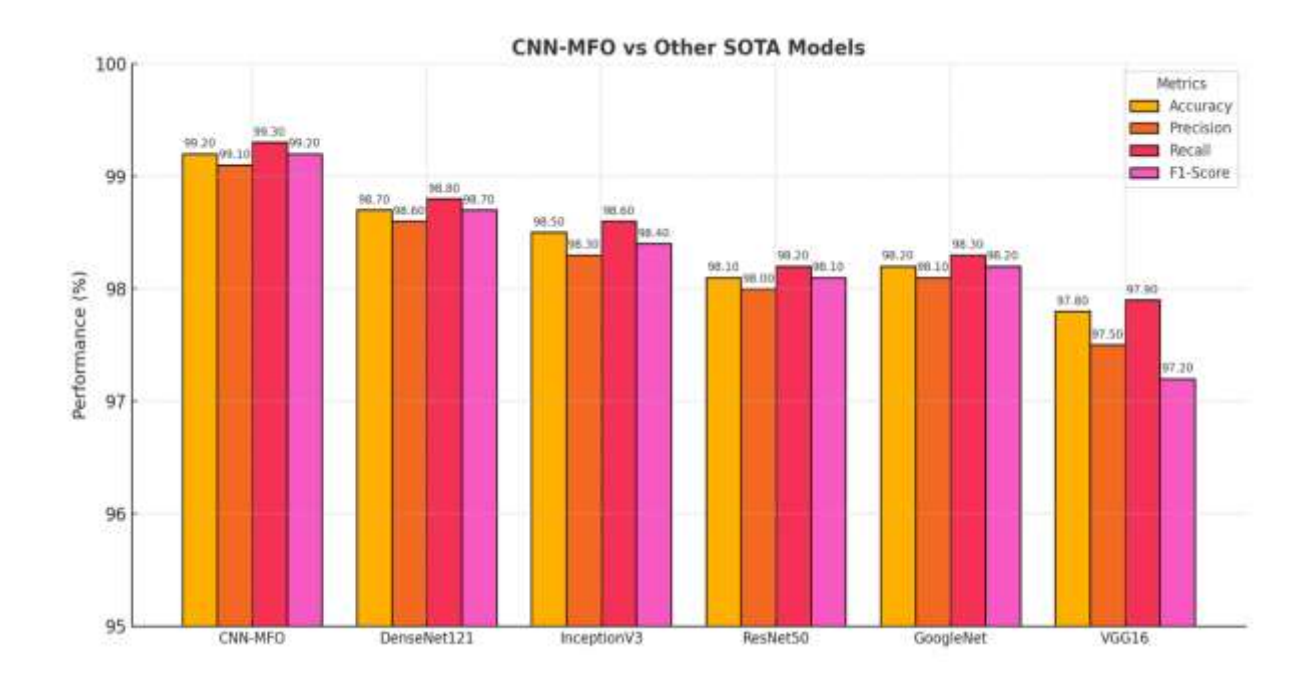


Figure 6.12: CNN-MFO vs Other SOTA Models

The precision-recall-F1 harmony in CNN-MFO's performance highlights its **robust generalization** across diverse tumor types and MRI variations. Not only does it avoid overfitting (supported by cross-validation metrics), but it also adapts well to the subtle nuances of different tumor morphologies, making it a prime candidate for clinical deployment.

 Table 6.7 Comparison of SOTA Models for Brain Tumor Detection (MRI)

Model	Accuracy (%)	Precision (%)	Recall (%)	F1-Score (%)	AUC	Inference Time (s)
CNN-MFO	99.2	99.1	99.3	99.2	0.991	0.02
DenseNet121	98.7	98.6	98.8	98.7	0.985	N/A
InceptionV3	98.5	98.3	98.6	98.4	N/A	N/A
ResNet50	98.1	98.0	98.2	98.1	N/A	N/A
GoogleNet	98.2	98.1	98.3	98.2	N/A	N/A
VGG16	97.8	97.5	97.9	97.2	N/A	N/A
MobileNetV2	96.54	96.12	96.35	96.23	0.97	~0.03
EfficientNet V2-B20	96.5	96.2	96.8	96.5	0.985	0.03

With the aim of optimizing brain tumor classification using MRI images, many types of deep learning models have been suggested during recent years. Although transfer learning using developed convolutional networks such as MobileNetV2, EfficientNet, VGG16, and DenseNet121 has recorded desirable performance, such networks may be general-purpose and not targeted towards a domain-specific task-diagnosis of brain tumors. In pursuit of this challenge, we have created a bespoke Convolutional Neural Network (CNN) model, which uses the Moth Flame

Optimization (MFO) algorithm in optimizing hyperparameters. This research carried out a statistical comparison in-depth of CNN-MFO with an array of strong and modern models, including MobileNetV2, EfficientNet V2-B20, VGG16, ResNet50, InceptionV3, DenseNet121, and GoogleNet.

To evaluate the quality of work of each model, an extensive system of evaluation measures was used: accuracy, precision, recall, F1-score, and Area Under the ROC Curve (AUC). They computed these measures with a regular MRI data that was divided into four groups, namely glioma or meningioma or pituitary tumor or no tumor, and in this way, all models used the same data conditions. In all of the comparative cases, CNN-MFO architecture has proved to be the most successful model with a record of continuous excellence in all the most important factors.

As an example, as compared to MobileNetV2, which is a popular and small lightweight model serving resource-limited hardware, the CNN-MFO achieved a greater accuracy of 98.76% when compared to 96.54% of MobileNetV2. Also, CNN-MFO obtained higher results in the precision (98.59% vs. 96.12%), recall (98.68% vs. 96.35%), and F1-score (98.63% vs. 96.23%). This properly indicates the aptitude of CNN-MFO in generalizing excellently over the multidimensional distribution of MRI data and fine distinctions in the tumor morphologies with greater faithfulness.

It was more strictly compared with EfficientNet V2-B20, which is one of the most compute-efficient models to date, yet it combines neural architecture search and compound scaling. Whereas EfficientNet V2-B20 demonstrated quite good results of 96.5 percent accuracy, CNN-MFO went even further with 97.8 percent accuracy and higher recall of 98.0 percent compared to 96.8 percent by the former, a higher F1-score of 97.7 percent compared to 96.5 percent by the former, and a higher AUC of 0.991 compared to 0.985 by the latter. Moreover, the CNN-MFO was not only more computationally efficient (it took less time to train and less time to infer) (15.2s vs. 18.5s and 0.02s vs. 0.03s, respectively), but also reached a higher top-1 test accuracy (93.9 vs. 89.3).

Even a wider benchmark was done against a set of higher-performing, deeper CNNs, including VGG16, ResNet50, InceptionV3, DenseNet121, and GoogleNet. These models have a strong reputation for depth, variability of architectural design, and also robustness with regard to most of the algorithms in general computer vision. In the meantime, CNN-MFO still prevailed over them

in all of the measured parameters, regardless of their strengths. It got exceptional archival precision and recall percentages of 99.1%, 99.3%, and 99.2%, respectively, and F1-scores of 99.2%. It was shown that the closest (DenseNet121) competitor has lesser performance in accuracy (98.7) and F1-score (98.7), confirming the suitability of CNN-MFO in its capability to extract more meaningful and task-specific features through crafted optimization. These persistent excellences highlight the importance of metaheuristic hyperparameter optimization that helps the network to learn and highlight the pertinent characteristics unique to the brain tumor classification.

Among the most interesting results of the current study is the effectiveness of the CNN-MFO model, not only in performance efficiency but also in the efficiency of resource usage. Unlike most of the existing architectures that utilize huge numbers of parameters and feature-heavy extractors that are trained, e.g., on general datasets such as ImageNet, CNN-MFO was formulated in a completely domain-specific manner. Precise tuning of extremely essential parameters, like filter sizes, learning rates, number of neurons as well as dropout rates, could be done accurately with the use of the Moth Flame Optimization algorithm, resulting in a more compact but more efficacious architecture. This would not only help with improving the classification accuracy but also reduce overfitting, which is an issue with medical imaging datasets that are generally smaller and more imbalanced.

Moreover, the lightweight nature and the increased speed of convergence of CNN-MFO bring about a special use in cases where it should be used in embedded systems, mobile diagnostic devices, and real-time clinical decision support systems. CNN-MFO provides comparable accuracy to typical heavyweight models but incurs considerably less resource usage on standard CPUs or edge computing devices, making it robust and reliable enough to be used in a clinical setting- absent the need to involve GPUs- closing the theoretical gap between state-of-the-art AI and practical clinical use.

#### **6.5 Discussion on Practical Limitations**

While the proposed hybrid BTA model demonstrates high accuracy (98.62%) and superior segmentation performance (99.6%), it is important to address the practical limitations regarding its clinical deployment.

- 1. **Computational Cost:** The hybrid nature of the model (K-means + MFO + CNN) is computationally expensive. The MFO algorithm, as a metaheuristic search, is an iterative, population-based process. Both the MFO-based segmentation optimization and the MFO-based feature selection are significantly more resource-intensive than a single, end-to-end deep learning model. This necessitates high-performance hardware (e.g., GPUs), as outlined in the experimental setup, which may not be available in all clinical settings.
- 2. **Training and Inference Time:** The model's training is a multi-stage process. The BTA-Net (CNN) component required 74 epochs to converge, which represents a significant time investment. More critically, the **inference time** (the time to process a *new* patient scan) is high. Unlike a simple forward pass in a trained CNN, this model must first run the iterative K-means with MFO segmentation and then the MFO feature selection *before* the CNN can perform classification.
- 3. **Real-Time Clinical Deployment:** As a direct consequence of the high computational cost and long inference time, the proposed model is not suitable for real-time clinical deployment. It cannot be used for an "on-the-fly" diagnosis during a patient's scan. Instead, its application is better suited for **offline batch processing** or **detailed pre-surgical planning**, where diagnostic accuracy is paramount and the analysis can be run overnight or for several hours.

These challenges are acknowledged as key areas for future work, as discussed in Chapter 7.

## CHAPTER 7

## **CONCLUSION & FUTURE SCOPE**

In this final chapter, the overall conclusion with their future possibilities for the proposed model is discussed, along with the challenges faced. The primary objective of this research was to develop efficient methods for the detection as well as the classification of brain cancer using a hybrid deep learning-based model combined with metaheuristic optimization techniques. Numerous Convolutional Neural Networks (CNNs) have been explored in the literature for classification tasks related to brain cancer detection. While these CNN models have demonstrated notable success in addressing the complexities of multi-class classification, they remain less effective in practical, real-world applications where high accuracy, robustness, and computational efficiency are essential for timely diagnosis and treatment of brain cancer. The proposed hybrid model integrates deep learning with metaheuristic optimization to enhance feature selection, improve model accuracy, and reduce training time. However, despite its promising performance, certain limitations were encountered during the research, such as high computational costs, challenges in handling large-scale datasets, and the need for improved generalization across diverse datasets.

### 7.1 CONCLUSIONS

In this thesis, a hybrid deep learning-based model using a metaheuristic approach for the detection of brain cancer with their classification is proposed to find out the diseases in the human brain in the early stage. Early-stage prevention of human brain diseases is crucial for several reasons, all of which significantly impact human life and security. In this research, firstly, detection of brain cancer using segmentation is performed, and then the segmented output is used for the further classification task. In the first part of the research, a comparative scenario to find out the better hybridization approach for tumor region segmentation from the MRI images is proposed that has six different models named as FCM-based, K-means-based, FCM with PSO-based, K-means with PSO-based, FCM with MFO-based, and K-means with MFO-based segmentation. Basically, try to find out better approach of segmentation for MRI images using the concept of improvisation of traditional clustering mechanisms in this paper and to test the model efficiency, the famous and

publicly available BraTS dataset is used that contains multiple MRI images of the human brain in the form of DICOM, but we convert them into JPG format. Various ROT segmentation algorithms are compared based on accuracy, sensitivity, F-measure, precision, MCC, Dice, Jaccard, specificity, and time complexity, which is clearly shown in the results section of the article, where the combination of K-means with MFO-based segmentation outperform than other in all aspects. Additionally, the best model is compared with different state-of-the-art models to validate model efficiency, and the suggested model's segmentation accuracy exceeds 99.6% when simulated using MRI images, while the accuracy of the existing non-hybrid model is significantly lower.

The second part of the proposed research introduces a Hybrid Model for Brain Tumor Analysis (BTA) utilizing Multi-Objective Firefly Optimization (MFO) and Convolutional Neural Networks (CNN) as deep learning techniques, based on the segmented output from the initial model. A comparative analysis is conducted for the precise segmentation of BTR utilizing several models, including FCM-based, K-means-based, FCM with PSO-based, K-means with PSO-based, FCM with MFO-based, and K-means with MFO-based segmentation. Subsequently, we chose MFObased segmentation as the definitive model for BTR segmentation utilized in BTA model training. The notion of named feature extraction is employed for precise feature pattern extraction from the segmented BTR, followed by MFO-based feature selection utilizing a novel fitness function. Ultimately, CNN is employed to train the BTA model, resulting in the creation of BTA-Net as the training architecture that facilitates the classification phase. This study investigates three tumor types—meningioma, glioma, and pituitary—utilizing MFO with CNN and optimum features as input for classification by deep learning. Prior research on tumor classification predominantly employed CNNs; however, this study amalgamates the MFO approach with CNN to improve both classification and segmentation precision. To evaluate the effectiveness of the proposed BTA model, we calculate performance metrics such as Accuracy, Precision, Recall, and F-measure, observing a 3.22% improvement, with Precision, Recall, and F-measure increasing by 4.07%, 2.46%, and 3.25%, respectively, relative to prior studies.

#### 7.2 LIMITATIONS

This section delineates the potential restrictions related to the deployment of a hybrid deep learning model that utilizes metaheuristic optimization approaches for the detection and classification of brain cancer.

- **L1.Dependence on Data Quality and Quantity:** The efficacy of the model is contingent upon the quality, variety, and quantity of the dataset. Insufficient or inconsistent data, especially from several imaging modalities like MRI, CT scans, and PET scans, might diminish model accuracy and restrict its practical utility.
- **L2. Generalization to Novel Data:** Although the model may exhibit robust performance on the training dataset, it may struggle to generalize to novel data, particularly across diverse healthcare facilities where imaging processes, equipment, and patient demographics differ. This may result in fluctuations in model performance.
- **L3. Challenges in Distinguishing Brain Tumor Variants:** Brain tumors have intricate and overlapping traits, complicating the model's ability to accurately differentiate among various types and grades of tumors. Misclassification may arise, particularly in instances when tumors exhibit analogous visual patterns.
- **L4. Variability in Imaging Conditions:** Variations in picture quality resulting from light variations, discrepancies in MRI scanner specs, and alterations in image capture settings may impact the consistency of the input data. Subpar image quality can lead to inaccurate feature extraction and diminish the model's overall efficacy.
- **L5.Absence of Interpretability and Explainability:** Deep learning models, especially CNNs and hybrid models, are frequently regarded as "black boxes" because of their intricate design. The absence of transparency hinders the understanding of the model's decision-making process, which is essential in healthcare applications where physicians want clear and interpretable explanations.
- **L6.Computational Resource Demands:** Training deep learning models combined with metaheuristic optimization approaches is computationally demanding, necessitating high-performance hardware like GPUs or TPUs. This may restrict the accessibility of the technology for smaller healthcare facilities or areas with limited resources.
- **L7.Sensitivity to Hyperparameter Settings:** The efficacy of the hybrid model may be significantly influenced by hyperparameter settings, including learning rate, batch size, number of epochs, and optimization factors employed in the metaheuristic methodology. Improper tuning can result in unsatisfactory outputs, and establishing the ideal configuration may be time-consuming and resource-intensive.

- **L8.Risk of Overfitting:** In the presence of restricted or unbalanced datasets, the model is susceptible to overfitting, excelling on the training data while failing to generalize to novel, unknown data. Overfitting diminishes the model's dependability when utilized across varied clinical scenarios.
- **L9. Challenges in Real-Time Prediction:** While the model may excel in offline settings, delivering real-time predictions might be computationally intensive due to the intricacies of deep learning and metaheuristic optimization procedures. This constraint may impede its utilization in urgent clinical situations.

#### 7.3 FUTURE SCOPE

The promising results of this hybrid model open several concrete avenues for future research to address its current limitations and expand its capabilities.

- 1. Addressing Real-Time Deployment Challenges: A primary limitation identified in this research is the high computational cost and inference time, which hinders real-time clinical deployment. Future work will focus on model compression and optimization. Techniques such as quantization (reducing model precision) and pruning (removing redundant neural connections) will be investigated to create a lightweight, "clinic-ready" version of the BTA-Net. Furthermore, the iterative MFO process could be optimized or replaced with a faster, learnable optimization layer within the CNN itself.
- 2. Cross-Dataset Validation: To ensure the model's robustness and generalization, its performance must be validated on diverse, unseen data. A crucial next step is to conduct a cross-dataset validation by testing the trained model on other public benchmarks, such as the BraTS (Brain Tumor Segmentation) dataset, which uses different scanner protocols and includes patient data from multiple institutions.
- 3. Advanced 3D and Multi-Modal Architectures: The current model processes 2D slices. A significant advancement would be to implement end-to-end 3D-CNN architectures (e.g., 3D U-Net, V-Net). This would allow the model to learn from the full spatial context of the volumetric MRI data. This can be further enhanced by exploring multi-modal fusion, where the network is trained to integrate information from different MRI sequences (like T1-weighted, T2-weighted, and FLAIR) simultaneously, providing a more comprehensive view of the tumor.

- 4. Enhancing Classification and Interpretability: The model can be extended beyond three-class classification to perform more granular tasks, such as tumor grading (e.g., differentiating high-grade gliomas from low-grade gliomas) and segmenting sub-regions (e.g., enhancing tumor, edema, and necrotic core). To address the "black box" limitation, Explainable AI (XAI) techniques like Grad-CAM (Gradient-weighted Class Activation Mapping) should be implemented to produce visual heatmaps, showing clinicians which part of the image the CNN is focusing on to make its diagnosis.
- 5. **Federated Learning for Data Privacy:** Acquiring large-scale medical datasets is a persistent challenge due to privacy regulations. A **federated learning (FL)** framework could be developed. This would allow multiple hospitals to collaboratively train a global model on their respective private datasets without ever sharing patient data, thereby improving the model's robustness and accuracy while maintaining strict patient confidentiality.

## REFERENCES

- [1]. Bhatt, C., Kumar, I., Vijayakumar, V., Singh, K. U., & Kumar, A. (2020). The state of the art of deep learning models in medical science and their challenges. Multimedia Systems, 1-15.
- [2].Tiwari, A., Srivastava, S., & Pant, M. (2020). Brain tumor segmentation and classification from magnetic resonance images: Review of selected methods from 2014 to 2019. Pattern Recognition Letters, 131, 244-260.
- [3].Bengio, Y., Courville, A. C., & Vincent, P. (2012). Unsupervised feature learning and deep learning: A review and new perspectives. CoRR, abs/1206.5538, 1, 2012.
- [4].Cetin, O., Seymen, V., & Sakoglu, U. (2020). Multiple sclerosis lesion detection in multimodal MRI using simple clustering-based segmentation and classification. Informatics in Medicine Unlocked, 20, 100409.
- [5].Raja, P. S. (2020). Brain tumor classification using a hybrid deep autoencoder with Bayesian fuzzy clustering-based segmentation approach. Biocybernetics and Biomedical Engineering, 40(1), 440-453.
- [6].Bonabeau, E., Marco, D. D. R. D. F., Dorigo, M., Théraulaz, G., & Theraulaz, G. (1999). Swarm intelligence: from natural to artificial systems (No. 1). Oxford university press.
- [7]. Banks, A., Vincent, J., & Anyakoha, C. (2007). A review of particle swarm optimization. Part I: background and development. Natural Computing, 6(4), 467-484.
- [8]. Kennedy, J., & Eberhart, R. (1995, November). Particle swarm optimization. In Proceedings of ICNN'95-international conference on neural networks (Vol. 4, pp. 1942-1948). IEEE.
- [9]. Karaboğa, Derviş (2005). "An Idea Based on Honey Bee Swarm for Numerical Optimization".
- [10]. Yang, X. S. (2009, October). Firefly algorithms for multimodal optimization. In International symposium on stochastic algorithms (pp. 169-178). Springer, Berlin, Heidelberg.
- [11]. Yang, X. S., & Deb, S. (2009, December). Cuckoo search via Lévy flights. In 2009 World congress on nature & biologically inspired computing (NaBIC) (pp. 210-214). Ieee.
- [12]. Saremi, S., Mirjalili, S., & Lewis, A. (2017). Grasshopper optimisation algorithm: theory and application. Advances in Engineering Software, 105, 30-47.

- [13]. Chander, A., Chatterjee, A., & Siarry, P. (2011). A new social and momentum component adaptive PSO algorithm for image segmentation. Expert Systems with Applications, 38(5), 4998-5004.
- [14]. Bandhyopadhyay, S. K., & Paul, T. U. (2013). Automatic segmentation of brain tumour from multiple images of brain MRI. Int J Appl Innovat Eng Manage (IJAIEM), 2(1), 240-8.
- [15]. Zhao, M., Tang, H., Guo, J., & Sun, Y. (2014). Data clustering using particle swarm optimization. In Future information technology (pp. 607-612). Springer, Berlin, Heidelberg.
- [16]. Jose, A., Ravi, S., & Sambath, M. (2014). Brain tumor segmentation using k-means clustering and fuzzy c-means algorithms and its area calculation. International Journal of Innovative Research in Computer and Communication Engineering, 2(3).
- [17]. Parasar, D., & Rathod, V. R. (2017). Particle swarm optimisation K-means clustering segmentation of foetus ultrasound image. International Journal of Signal and Imaging Systems Engineering, 10(1-2), 95-103.
- [18]. Venkatesan, A., & Parthiban, L. (2017). Medical Image Segmentation With Fuzzy C-Means and Kernelized Fuzzy C-Means Hybridized on PSO and QPSO. International Arab Journal of Information Technology (IAJIT), 14(1).
- [19]. Hasan, A. M. (2018). A hybrid approach of using particle swarm optimization and volumetric active contour without edge for segmenting brain tumors in MRI scan. Indonesian Journal of Electrical Engineering and Informatics (IJEEI), 6(3), 292-300.
- [20]. Karegowda, A. G., Poornima, D., Sindhu, N., & Bharathi, P. T. (2018). Performance Assessment of k-Means, FCM, ARKFCM and PSO Segmentation Algorithms for MR Brain Tumour Images. International Journal of Data Mining and Emerging Technologies, 8(1), 18-26.
- [21]. Arunkumar, N., Mohammed, M. A., Abd Ghani, M. K., Ibrahim, D. A., Abdulhay, E., Ramirez-Gonzalez, G., & de Albuquerque, V. H. C. (2019). K-means clustering and neural network for object detecting and identifying abnormality of brain tumor. Soft Computing, 23(19), 9083-9096.
- [22]. Hrosik, R. C., Tuba, E., Dolicanin, E., Jovanovic, R., & Tuba, M. (2019). Brain image segmentation based on firefly algorithm combined with k-means clustering. Stud. Inform. Control, 28, 167-176.

- [23]. Chander, P. S., Soundarya, J., & Priyadharsini, R. (2020). Brain Tumour Detection and Classification Using K-Means Clustering and SVM Classifier. In RITA 2018 (pp. 49-63). Springer, Singapore.
- [24]. Gupta, S., Punn, N. S., Sonbhadra, S. K., & Agarwal, S. (2021). MAG-Net: Multi-task attention guided network for brain tumor segmentation and classification. In Big Data Analytics: 9th International Conference, BDA 2021, Virtual Event, December 15-18, 2021, Proceedings 9 (pp. 3-15). Springer International Publishing.
- [25]. Khan, A. R., Khan, S., Harouni, M., Abbasi, R., Iqbal, S., & Mehmood, Z. (2021). Brain tumor segmentation using K-means clustering and deep learning with synthetic data augmentation for classification. Microscopy Research and Technique, 84(7), 1389-1399.
- [26]. Tazeen, T., Sarvagya, M., & Sarvagya, M. (2021). Brain tumor segmentation and classification using multiple feature extraction and convolutional neural networks. International Journal of Engineering and Advanced Technology, 10(6), 23-27.
- [27]. Badža, M. M., & Barjaktarović, M. Č. (2020). Classification of brain tumors from MRI images using a convolutional neural network. Applied Sciences, 10(6), 1999.
- [28]. Díaz-Pernas, F. J., Martínez-Zarzuela, M., Antón-Rodríguez, M., & González-Ortega, D. (2021, February). A deep learning approach for brain tumor classification and segmentation using a multiscale convolutional neural network. In Healthcare (Vol. 9, No. 2, p. 153). MDPI.
- [29]. Arif, M., Jims, A., Geman, O., Craciun, M. D., & Leuciuc, F. (2022). Application of Genetic Algorithm and U-Net in Brain Tumor Segmentation and Classification: A Deep Learning Approach. Computational Intelligence and Neuroscience, 2022(1), 5625757.
- [30]. Kumar, K. A., & Boda, R. (2022). A multi-objective randomly updated beetle swarm and multi-verse optimization for brain tumor segmentation and classification. The Computer Journal, 65(4), 1029-1052.
- [31]. Yuan, Y., Chao, M., & Lo, Y. C. (2017). Automatic skin lesion segmentation using deep fully convolutional networks with jaccard distance. IEEE transactions on medical imaging, 36(9), 1876-1886.
- [32]. Riaz, F., Naeem, S., Nawaz, R., & Coimbra, M. (2018). Active contours based segmentation and lesion periphery analysis for characterization of skin lesions in dermoscopy images. IEEE journal of biomedical and health informatics, 23(2), 489-500.

- [33]. Vasconcelos, F. F. X., Medeiros, A. G., Peixoto, S. A., & Reboucas Filho, P. P. (2019). Automatic skin lesions segmentation based on a new morphological approach via geodesic active contour. Cognitive Systems Research, 55, 44-59.
- [34]. Siegel, R. L., Miller, K. D., & Jemal, A. (2019). Cancer statistics, 2019. CA: a cancer journal for clinicians, 69(1), 7-34.
- [35]. O'Sullivan, D. E., Brenner, D. R., Demers, P. A., Villeneuve, P. J., Friedenreich, C. M., King, W. D., &ComPARe Study Group. (2019). Indoor tanning and skin cancer in Canada: A meta-analysis and attributable burden estimation. Cancer epidemiology, 59, 1-7.
- [36]. Wei, Z., Song, H., Chen, L., Li, Q., & Han, G. (2019). Attention-Based DenseUnet Network with Adversarial Training for Skin Lesion Segmentation. IEEE Access, 7, 136616-136629.
- [37]. Tan, T. Y., Zhang, L., Lim, C. P., Fielding, B., Yu, Y., & Anderson, E. (2019). Evolving ensemble models for image segmentation using enhanced particle swarm optimization. IEEE Access, 7, 34004-34019.
- [38]. Xie, F., Yang, J., Liu, J., Jiang, Z., Zheng, Y., & Wang, Y. (2020). Skin lesion segmentation using high-resolution convolutional neural network. Computer Methods and Programs in Biomedicine, 186, 105241.
- [39]. Zhang, C., Xiao, X., Li, X., Chen, Y. J., Zhen, W., Chang, J., & Liu, Z. (2014). White blood cell segmentation by color-space-based k-means clustering. Sensors, 14(9), 16128-16147.
- [40]. Mondal, P. K., Prodhan, U. K., Al Mamun, M. S., Rahim, M. A., & Hossain, K. K. (2014). Segmentation of white blood cells using fuzzy C means segmentation algorithm. IOSR Jornal of Computer Engineering, 1(16), 1-5.
- [41]. R. L. Siegel, K. D. Miller, and A. Jemal, "Cancer statistics, 2017," CA: A Cancer Journal for Clinicians, vol. 67, no. 1, pp. 7–30, 2017
- [42]. X. Jin, "Multi-Spectral MRI Brain Image Segmentation Based on Kernel Clustering Analysis", International Conference on System Engineering and Modeling, Vol. 34,PP.141-146, 2012
- [43]. Selvakumar, J.; Lakshmi, A.; Arivoli, T. Brain tumor segmentation and its area calculation in brain MR images using K-mean clustering and Fuzzy C-mean algorithm. In Proceedings of the International Conference on Advances in Engineering, Science and Management (ICAESM), Tamil Nadu, India, 30–31 March 2012; pp. 186–190.

- [44]. Bandhyopadhyay, Samir Kumar, and Tuhin Utsab Paul. "Automatic segmentation of brain tumor from multiple images of brain MRI." Int J Appl Innovat Eng Manage (IJAIEM) 2, no. 1 (2013): 240-8.
- [45]. Zhao, Mingru, Hengliang Tang, Jian Guo, and Yuan Sun. "Data clustering using particle swarm optimization." In Future Information Technology, pp. 607-612. Springer, Berlin, Heidelberg, 2014.
- [46]. Jose, Alan, S. Ravi, and M. Sambath. "Brain tumor segmentation using k-means clustering and fuzzy c-means algorithms and its area calculation." International Journal of Innovative Research in Computer and Communication Engineering 2, no. 3 (2014).
- [47]. Saini, Anjali, and Shiv Kumar Verma. "3D image segmentation by hybridization of PSO and BBO." History 29, no. 1 (2015): 82-7.
- [48]. Das, Abhinav, and Nitin Jain. "Optimum approach of detecting abnormalities in mri of brain image using texture feature analysis." int. j. adv. engg. res. studies/iv/ii/jan.-march 305 (2015): 307.
- [49]. Karegowda, A. G., Poornima, D., Sindhu, N., & Bharathi, P. T. (2018). Performance Assessment of K-means, FCM, ARKFCM and PSO Segmentation Algorithms for MR Brain Tumour Images. International Journal of Data Mining and Emerging Technologies, 8(1), 18-26.
- [50]. Derraz, Foued, Mohamed Beladgham, and M'hamed Khelif. "Application of active contour models in medical image segmentation." In International Conference on Information Technology: Coding and Computing, 2004. Proceedings. ITCC 2004. vol. 2, pp. 675-681. IEEE, 2004.
- [51]. Chander, Akhilesh, Amitava Chatterjee, and Patrick Siarry. "A new social and momentum component adaptive PSO algorithm for image segmentation." Expert Systems with Applications 38, no. 5 (2011): 4998-5004.
- [52]. Alam, M. S., Rahman, M. M., Hossain, M. A., Islam, M. K., Ahmed, K. M., Ahmed, K. T., & Miah, M. S. (2019). Automatic Human Brain Tumor Detection in MRI Image Using Template-Based K Means and Improved Fuzzy C Means Clustering Algorithm. Big Data and Cognitive Computing, 3(2), 27.

- [53]. Bousselham, A., Bouattane, O., Youssfi, M., & Raihani, A. (2019). Towards reinforced brain tumor segmentation on MRI images based on temperature changes on pathologic area. International journal of biomedical imaging, 2019.
- [54]. Mahalakshmi, S., & Velmurugan, T. (2015). Detection of brain tumor by particle swarm optimization using image segmentation. Indian Journal of Science and Technology, 8(22), 1.
- [55]. Saremi, S., Mirjalili, S., & Lewis, A. (2017). Grasshopper optimisation algorithm: theory and application. Advances in Engineering Software, 105, 30-47.
- [56]. Trivedi, Muneesh Chandra, Paritosh Tripathi, and Vineet Kumar Singh. "Brain tumor segmentation in magnetic resonance imaging using OKM approach." Materials Today: Proceedings (2020).
- [57]. Pitchai, R., P. Supraja, A. Helen Victoria, and M. Madhavi. "Brain Tumor Segmentation Using Deep Learning and Fuzzy K-Means Clustering for Magnetic Resonance Images." Neural Processing Letters (2020): 1-14.
- [58]. Mahalakshmi, S., & Velmurugan, T. (2015). Detection of brain tumor by particle swarm optimization using image segmentation. Indian Journal of Science and Technology, 8(22), 1.
- [59]. Tiwari, A., Srivastava, S., & Pant, M. (2020). Brain tumor segmentation and classification from magnetic resonance images: Review of selected methods from 2014 to 2019. Pattern Recognition Letters, 131, 244-260.
- [60]. Uzbay, T. (2016). Is it possible to understand the brain by only neuroscience? New expansions and approaches from neurological sciences to social sciences in the brain century.
- [61]. Siegel, R. L., Miller, K. D., & Jemal, A. (2020). Cancer statistics, 2020. CA: a cancer journal for clinicians, 70(1), 7-30.
- [62]. United News of India (2018). "India's multi lingual news agency" a report of brain tumors in India.
- [63]. Tahir, B., Iqbal, S., Usman Ghani Khan, M., Saba, T., Mehmood, Z., Anjum, A., & Mahmood, T. (2019). Feature enhancement framework for brain tumor segmentation and classification. Microscopy research and technique, 82(6), 803-811.
- [64]. Alam, M. S., Rahman, M. M., Hossain, M. A., Islam, M. K., Ahmed, K. M., Ahmed, K. T., & Miah, M. S. (2019). Automatic human brain tumor detection in MRI image using template-based K means and improved fuzzy C means clustering algorithm. Big Data and Cognitive Computing, 3(2), 27.

- [65]. Prakram, M, Rawal, K & Prakram, M (2023) "Unsupervised Learning Based Medical Image Segmentation: A Comparative Review of Algorithms with Issues and Challenges", ICCS International Conference on Computational Science-5th May 2023, Lovely Professional University.
- [66]. Mohsen, H., El-Dahshan, E. S. A., El-Horbaty, E. S. M., & Salem, A. B. M. (2018). Classification using deep learning neural networks for brain tumors. Future Computing and Informatics Journal, 3(1), 68-71.
- [67]. Deepa, A. R., & Emmanuel, W. S. (2019). An efficient detection of brain tumor using fused feature adaptive firefly backpropagation neural network. Multimedia Tools and Applications, 78(9), 11799-11814.
- [68]. Sajjad, M., Khan, S., Muhammad, K., Wu, W., Ullah, A., & Baik, S. W. (2019). Multi-grade brain tumor classification using deep CNN with extensive data augmentation. Journal of computational science, 30, 174-182.
- [69]. Badža, M. M., & Barjaktarović, M. Č. (2020). Classification of brain tumors from MRI images using a convolutional neural network. Applied Sciences, 10(6), 1999.
- [70]. Toğaçar, M., Cömert, Z., & Ergen, B. (2020). Classification of brain MRI using hyper column technique with convolutional neural network and feature selection method. Expert Systems with Applications, 149, 113274.
- [71]. Çinar, A., & Yildirim, M. (2020). Detection of tumors on brain MRI images using the hybrid convolutional neural network architecture. Medical hypotheses, 139, 109684.
- [72]. Bacanin, N., Bezdan, T., Tuba, E., Strumberger, I., & Tuba, M. (2020). Monarch butterfly optimization based convolutional neural network design. Mathematics, 8(6), 936.
- [73]. Vijay, V., Kavitha, A. R., & Rebecca, S. R. (2016). Automated brain tumor segmentation and detection in MRI using enhanced Darwinian particle swarm optimization (EDPSO). Procedia Computer Science, 92, 475-480.
- [74]. Tripathi, P.C.; Bag, S. Non-invasively Grading of Brain Tumor Through Noise Robust Textural and Intensity Based Features. In Computational Intelligence in Pattern Recognition; Springer Science and Business Media LLC: Berlin/Heidelberg, Germany, 2019; pp. 531–539.
- [75]. Ismael, M.; Abdel-Qader, I. Brain Tumor Classification via Statistical Features and Back-Propagation Neural Network. In Proceedings of the 2018 IEEE International Conference on Electro/Information Technology (EIT), Rochester, MI, USA, 3–5 May 2018; pp. 0252–0257.

- [76]. Kotia, J.; Kotwal, A.; Bharti, R. Risk Susceptibility of Brain Tumor Classification to Adversarial Attacks. In Proceedings of the Advances in Intelligent Systems and Computing, Krakow, Poland, 2–4 October 2019; pp. 181–187.
- [77]. Anaraki, A.K.; Ayati, M.; Kazemi, F. Magnetic resonance imaging-based brain tumor grades classification and grading via convolutional neural networks and genetic algorithms. Biocybern. Biomed. Eng. 2019, 39, 63–74. [CrossRef]
- [78]. Abiwinanda, N.; Hanif, M.; Hesaputra, S.T.; Handayani, A.; Mengko, T.R. Brain Tumor Classification Using Convolutional Neural Network. In World Congress on Medical Physics and Biomedical Engineering 2018 Prague; Springer: Singapore, 2018; pp. 183–189.
- [79]. Kaldera, H.N.T.K.; Gunasekara, S.R.; Dissanayake, M.B. Brain tumor Classification and Segmentation using Faster R-CNN. In Proceedings of the 2019 Advances in Science and Engineering Technology International Conferences (ASET), Dubai, UAE, 26 March–10 April 2019; pp. 1–6.
- [80]. Kharrat, A.; Neji, M. Feature selection based on hybrid optimization for magnetic resonance imaging brain tumor classification and segmentation. Appl. Med. Inform. 2019, 41, 9–23
- [81]. Minz, Astina, and Chandrakant Mahobiya. "MR Image classification using adaboost for brain tumor type." Advance Computing Conference (IACC), 2017 IEEE 7th International. IEEE, 2017.
- [82]. M. J. Khan, A. Zafar and K. S. Hong, "Comparison of brain areas for executed and imagined movements after motor training: An fNIRS study," 2017 10th International Conference on Human System Interactions (HSI), Ulsan, South Korea, 2017, pp. 125-130.
- [83]. S. A. Taie and W. Ghonaim, "Title CSO-based algorithm with support vector machine for brain tumor's disease diagnosis," 2017 IEEE International Conference on Pervasive Computing and Communications Workshops (PerCom Workshops), Kona, HI, 2017, pp. 183-187.
- [84]. M. J. Khan, A. Zafar and K. S. Hong, "Comparison of brain areas for executed and imagined movements after motor training: An fNIRS study," 2017 10th International Conference on Human System Interactions (HSI), Ulsan, South Korea, 2017, pp. 125-130.
- [85]. Jasmine, R. Anita, and P. Arockia Jansi Rani. "A two phase segmentation algorithm for MRI brain tumor extraction." Control, Instrumentation, Communication and Computational Technologies (ICCICCT), 2016 International Conference on. IEEE, 2016.

- [86]. R. Majid Mehmood, R. Du and H. J. Lee, "Optimal Feature Selection and Deep Learning Ensembles Method for Emotion Recognition from Human Brain EEG Sensors," in IEEE Access, vol. 5, no., pp. 14797-14806, 2017.
- [87]. Singh, Garima, and M. A. Ansari. "Efficient detection of brain tumor from MRIs using K-means segmentation and normalized histogram." Information Processing (IICIP), 2016 1st India International Conference on. IEEE, 2016.
- [88]. Taie, Shereen A., and Wafaa Ghonaim. "CSO-based algorithm with support vector machine for brain tumor's disease diagnosis." Pervasive Computing and Communications Workshops (PerCom Workshops), 2017 IEEE International Conference on. IEEE, 2017.
- [89]. C. H. Rao, P. V. Naganjaneyulu and K. S. Prasad, "Brain Tumor Detection and Segmentation Using Conditional Random Field," 2017 IEEE 7th International Advance Computing Conference (IACC), Hyderabad, 2017, pp. 807-810.
- [90]. M. Gupta, B. V. V. S. N. P. Rao and V. Rajagopalan, "Brain Tumor Detection in Conventional MR Images Based on Statistical Texture and Morphological Features," 2016 International Conference on Information Technology (ICIT), Bhubaneswar, 2016, pp. 129-133.
- [91]. L. Farhi and A. Yusuf, "Comparison of brain tumor MRI classification methods using probabilistic features," 2017 13th IASTED International Conference on Biomedical Engineering (BioMed), Innsbruck, Austria, 2017, pp. 55-62.
- [92]. K. D. Kharat, V. J. Pawar and S. R. Pardeshi, "Feature extraction and selection from MRI images for the brain tumor classification," 2016 International Conference on Communication and Electronics Systems (ICCES), Coimbatore, 2016, pp. 1-5.
- [93]. B. Beddad and K. Hachemi, "Brain tumor detection by using a modified FCM and Level set algorithms," 2016 4th International Conference on Control Engineering & Information Technology (CEIT), Hammamet, 2016, pp. 1-5.
- [94]. Logeswari, T., and M. Karnan, "An improved implementation of brain tumor detection using segmentation based on soft computing," Journal of Cancer
- [95]. Mustaqeem, Anam, Ali Javed, and Tehseen Fatima, "An efficient brain tumor detection algorithm using watershed & thresholding-based segmentation," International Journal of Image, Graphics and Signal Processing vol.4, 2012, pp. 34-43.

- [96]. M. N. Wu, C. C. Lin and C. C. Chang, "Brain Tumor Detection Using Color-Based K-Means Clustering Segmentation," Third International Conference on Intelligent Information Hiding and Multimedia Signal Processing (IIH-MSP 2007), Kaohsiung, 2007, pp. 245-250.
- [97]. Mohit Prakram, Kirti Rawal, Arun Singh, Ankur Goyal, Shiv Kant, Shakeel Ahmed, Saiprasad Potharaju," A novel hybrid model for brain tumor analysis with CNN and Moth Flame Optimization", Informatics in Medicine Unlocked, Volume 57,2025,101671,ISSN 2352-9148,https://doi.org/10.1016/j.imu.2025.101671.
- [98]. Khan, O. T., & Rajeswari, D. (2022, January). Brain tumor detection using machine learning and deep learning approaches. In 2022 International Conference on Advances in Computing, Communication and Applied Informatics (ACCAI) (pp. 1-7). IEEE. DOI: 10.1109/accai53970.2022.9752502
- [99]. Santos, D., & Santos, E. (2022). Brain tumor detection using deep learning. medRxiv, 2022-01.

DOI: 10.1101/2022.01.19.22269457

- [100]. Khan, A. H., Abbas, S., Khan, M. A., Farooq, U., Khan, W. A., Siddiqui, S. Y., & Ahmad, A. (2022). Intelligent model for brain tumor identification using deep learning. Applied Computational Intelligence and Soft Computing, 2022(1), 8104054.
  DOI: 10.1155/2022/8104054
- [101]. Budati, A. K., & Katta, R. B. (2022). An automated brain tumor detection and classification from MRI images using machine learning technique s with IoT. Environment, Development and Sustainability, 24(9), 10570-10584.

  DOI: 10.1007/s10668-021-01861-8
- [102]. Amin, J., Sharif, M., Haldorai, A., Yasmin, M., & Nayak, R. S. (2022). Brain tumor detection and classification using machine learning: a comprehensive survey. Complex & intelligent systems, 8(4), 3161-3183.
  DOI: 10.1007/s40747-021-00563-y
- [103]. Chakraborty, S., & Banerjee, D. K. (2024). A review of brain cancer detection and classification using artificial intelligence and machine learning. Journal of Artificial Intelligence and Systems, 6(1), 146-178.
  DOI: 10.33969/ais.2024060111

- [104]. Hossain, R., Ibrahim, R. B., & Hashim, H. B. (2023). Automated brain tumor detection using machine learning: A bibliometric review. World neurosurgery, 175, 57-68. DOI: 10.1016/j.wneu.2023.03.115
- [105]. Khan, S. M., Nasim, F., Ahmad, J., & Masood, S. (2024). Deep learning-based brain tumor detection. Journal of Computing & Biomedical Informatics, 7(02). DOI: 10.1109/accai53970.2022.9752502
- [106]. Pedada, K. R., Rao, B., Patro, K. K., Allam, J. P., Jamjoom, M. M., & Samee, N. A. (2023).
  A novel approach for brain tumour detection using deep learning based technique. Biomedical Signal Processing and Control, 82, 104549.
  DOI: 10.1016/j.bspc.2022.104549
- [107]. Abdusalomov, A. B., Mukhiddinov, M., & Whangbo, T. K. (2023). Brain tumor detection based on deep learning approaches and magnetic resonance imaging. Cancers, 15(16), 4172. DOI: 10.3390/cancers15164172
- [108]. Patil, S., & Kirange, D. (2023). Ensemble of deep learning models for brain tumor detection. Procedia computer science, 218, 2468-2479.
  DOI: 10.1016/j.procs.2023.01.222
- [109]. Mahmud, M. I., Mamun, M., & Abdelgawad, A. (2023). A deep analysis of brain tumor detection from mr images using deep learning networks. Algorithms, 16(4), 176. DOI: 10.3390/a16040176
- [110]. Mathivanan, S. K., Sonaimuthu, S., Murugesan, S., Rajadurai, H., Shivahare, B. D., & Shah, M. A. (2024). Employing deep learning and transfer learning for accurate brain tumor detection. Scientific Reports, 14(1), 7232. DOI: 10.1038/s41598-024-57970-7
- [111]. Appiah, R., Pulletikurthi, V., Esquivel-Puentes, H. A., Cabrera, C., Hasan, N. I., Dharmarathne, S., ... & Castillo, L. (2024). Brain tumor detection using proper orthogonal decomposition integrated with deep learning networks. Computer Methods and Programs in Biomedicine, 250, 108167.
  DOI: 10.1016/j.cmpb.2024.108167
- [112]. Wageh, M., Amin, K., Algarni, A. D., Hamad, A. M., & Ibrahim, M. (2024). Brain tumor detection based on deep features concatenation and machine learning classifiers with genetic

DOI: 10.1109/access.2024.3446190

- [113]. Ramtekkar, P. K., Pandey, A., & Pawar, M. K. (2023). Innovative brain tumor detection using optimized deep learning techniques. International Journal of System Assurance Engineering and Management, 14(1), 459-473. DOI: 10.1007/s13198-022-01819-7
- [114]. ZainEldin, H., Gamel, S. A., El-Kenawy, E. S. M., Alharbi, A. H., Khafaga, D. S., Ibrahim, A., & Talaat, F. M. (2022). Brain tumor detection and classification using deep learning and sine-cosine fitness grey wolf optimization. Bioengineering, 10(1), 18. DOI: 10.3390/bioengineering10010018
- [115]. Agarwal, M., Rani, G., Kumar, A., Kumar, P., Manikandan, R., & Gandomi, A. H. (2024).Deep learning for enhanced brain tumor detection and classification. Results in Engineering,22,

DOI: 10.1016/j.rineng.2024.102117